

**Reliability-Based Performance Assessment and  
Optimum Maintenance of Corroded Reinforced  
Concrete Structures**

**Jaya Nepal**

A thesis submitted in partial fulfilment of the requirements  
of the University of Greenwich for the  
Degree of Doctor of Philosophy

**November 2015**

*Dedicated to my family*

## DECLARATION

I certify that this work has not been accepted in substance for any degree, and is not concurrently being submitted for any degree other than that of Doctor of Philosophy (PhD) being studied at the University of Greenwich. I also declare that this work is the result of my own investigations except where otherwise identified by references and that I have not plagiarised the work of others.

-----

PhD candidate: Jaya Nepal

-----

1<sup>st</sup> Supervisor: Prof. Hua-Peng Chen

-----

2<sup>nd</sup> Supervisor: Prof. Colin Hills

## SUMMARY

Reinforcement corrosion is one of the major causes of deterioration of reinforced concrete structures exposed to aggressive environments. Deterioration caused by reinforcement corrosion reduces the serviceability and load bearing capacity of the concrete structures to an extent of serious structural failure. Consequently, this increases the resources required for the maintenance and rehabilitation over time. Due to uncertainties associated with the performance deterioration, it is difficult to accurately assess the residual strength and remaining useful life of corrosion damaged concrete structure. Therefore, the reliability-based performance assessment techniques based on stochastic deterioration modelling has significant potential for assessing the present and future performance of these structures. This can be ultimately helpful in sustainable and cost-effective infrastructure management.

This research presents new analytical methods for evaluating concrete crack evolution, estimating rebar bond strength degradation and predicting residual flexural strength of concrete structures affected by reinforcement corrosion. At first, cracking in cover concrete due to reinforcement corrosion is investigated by using rebar-concrete model and realistic concrete properties. The bond strength evolution of the corroded rebar is then evaluated at different stages of cover cracking by considering adhesion, confinement and corrosion pressure acting at the bond interface. Furthermore, the residual flexural strength of concrete beams is predicted with consideration of bond failure between the rebar and concrete. The gamma process is adopted for stochastic modelling of concrete crack growth and strength deterioration with uncertainties. Then, a time-dependent reliability analysis is undertaken to

evaluate the probability of failure in serviceability and load carrying capacity of corrosion damaged concrete beams. Optimal repair planning during the service life is also determined by balancing the cost for maintenance and the risk of structural failure. Finally, the results evaluated from the proposed methods are examined by available experimental and field data and the applicability is demonstrated by numerical examples.

The results obtained show that the proposed methods are capable of evaluating the performance and can also provide risk-cost balanced repair strategy during the lifetime of corrosion damaged concrete structures. The knowledge gained from this research contributes to the better understanding of the mechanics of performance deterioration associated with reinforcement corrosion. Furthermore, the methods presented in this study could be helpful in assessing the actual state of performance deterioration and making decision regarding the optimal repair.

## ACKNOWLEDGEMENTS

Pursuing PhD has been a truly life-changing experience for me and it would not have been possible to do without the support, guidance and encouragement that I received from many people. I wish to express my sincere appreciation to all those who have contributed to the successful outcome of this research. I would like to thank to the University of Greenwich for giving me an opportunity and providing the resources to execute this research successfully.

My special thanks go to my supervisor, Professor Hua-Peng Chen who took time out of his busy schedule to provide expert advice and direction in every step during the research. I would like to express my profound gratitude to him for his constant inspiration and encouragement. My grateful thanks are also extended to Professor Colin Hills for his valuable advice and support.

I am grateful to all my colleagues and friends within the research unit who provided the laughs and social relief during those very busy, frustrated and stressful days. I would like to extend my sincere thanks and appreciation to my parents for their continuous support no matter what path I choose. Your love and continuous encouragement have always kept me motivated.

Finally, saving the most important for last, I wish to give my heartfelt thanks to my husband, Hari, whose unconditional love, patience, and continual support of my academic endeavours over the past several years enabled me to complete this thesis. This would not have been possible without him.

# TABLE OF CONTENTS

<b>Chapter 1 Introduction</b>	<b>1</b>
1.1 Background.....	1
1.2 Research significance and contribution .....	6
1.3 Aim and objectives .....	7
1.4 Scope of thesis .....	7
<b>Chapter 2 Literature Review</b>	<b>11</b>
2.1 Introduction.....	11
2.2 Reinforcement corrosion .....	11
2.2.1 <i>Mechanism of corrosion</i> .....	12
2.2.2 <i>Properties of corrosion products</i> .....	14
2.2.3 <i>Effect of reinforcement corrosion</i> .....	17
2.2.4 <i>Sectional loss of rebar due to corrosion</i> .....	18
2.3 Concrete cover cracking .....	21
2.3.1 <i>Mechanism of corrosion induced cover cracking</i> .....	22
2.3.2 <i>Review of existing investigations on cover cracking due to corrosion</i> .....	23
2.3.3 <i>Cohesive crack model and tension softening of cracked concrete</i> .....	30
2.4 Bond strength.....	34
2.4.1 <i>Bond strength mechanism</i> .....	35
2.4.2 <i>Existing investigations on bond strength degradation</i> .....	37
2.5 Flexural strength .....	44
2.5.1 <i>Flexural strength mechanism</i> .....	44
2.5.2 <i>Existing investigations on flexural strength degradation</i> .....	45
2.6 Lifecycle analysis and management of infrastructure .....	48

2.6.1	<i>Background of deterioration modelling</i>	49
2.6.2	<i>Definition of limit states</i>	53
2.6.3	<i>Theory of reliability analysis</i>	55
2.6.4	<i>Background on maintenance interventions</i>	59
2.6.5	<i>Existing investigations on lifecycle management</i>	61
2.7	Summary and conclusions	63
<b>Chapter 3 Development of Corrosion Induced Cracking Model</b>		<b>65</b>
3.1	Introduction	65
3.2	Structural deterioration	67
3.3	Determination of sectional loss of rebar and corrosion induced expansion	69
3.4	Modelling cover concrete as thick-walled cylinder model	71
3.5	Modelling cracked concrete as cohesive crack model	73
3.6	Mathematical formulations for isotropic thick-walled cylinder	75
3.7	Mathematical formulations for anisotropic thick-walled cylinder	76
3.7.1	<i>Crack initiation at bond interface</i>	79
3.7.2	<i>Crack propagation through concrete cover</i>	81
3.7.3	<i>Completely cracked concrete cover</i>	85
3.8	Numerical example 1	89
3.8.1	<i>Evolution of visible crack at the concrete cover surface</i>	89
3.9	Numerical example 2	90
3.9.1	<i>Evolution of cracking at the concrete cover surface</i>	90
3.9.2	<i>Comparison of cracking at the bond interface and cover surface</i>	92
3.9.3	<i>Effect of concrete geometry on corrosion induced cover cracking</i>	94
3.10	Summary and conclusions	95

## **Chapter 4 Development of Bond Strength Degradation Model 97**

4.1 Introduction.....	97
4.2 Mechanism of bond strength of corroded rebar.....	99
4.3 Evaluation of ultimate bond strength.....	101
4.4 Evaluation of adhesion stress .....	102
4.5 Evaluation of confinement stress.....	103
4.6 Evaluation of corrosion stress.....	106
4.7 Numerical example 1 .....	108
4.7.1 Comparison of corrosion pressure with existing models .....	109
4.7.2 Comparison of bond strength degradation with existing models.....	110
4.7.3 Role of each stresses in contribution of residual bond strength.....	112
4.8 Case-study of Ullasund Bridge.....	114
4.8.1 Effect of reinforcement corrosion on residual bond strength.....	115
4.8.2 Effect of cover surface defects on residual bond strength.....	117
4.8.3 Effect of concrete geometry on residual bond strength.....	117
4.9 Numerical example 2.....	120
4.9.1 Effect of reinforcement corrosion on residual bond strength.....	120
4.9.2 Effect of cover surface cracking on residual bond strength.....	123
4.10 Summary and conclusions .....	127

## **Chapter 5 Development of Flexural Strength Degradation Model 129**

5.1 Introduction.....	129
5.2 Mechanism of flexural strength of corroded RC beam .....	130
5.3 Evaluation of flexural strength of corroded RC beam at bond failure .....	134
5.4 Evaluation of strain compatibility of corroded RC beam.....	134
5.5 Evaluation of yielding of concrete and steel in corroded RC beam .....	135

5.6 Numerical example 1 .....	137
5.6.1 <i>Effect of reinforcement corrosion on residual strength</i> .....	137
5.6.2 <i>Effect of cover surface cracking on residual strength</i> .....	144
5.6.3 <i>Effect of concrete geometry on residual flexural strength</i> .....	146
5.7 Numerical example 2.....	148
5.7.1 <i>Effect of stirrups on residual flexural strength</i> .....	149
5.8 Summary and conclusions .....	151

## **Chapter 6 Time-dependent Reliability Analysis and Optimized**

### **Maintenance Strategy 153**

6.1 Introduction.....	153
6.2 Lifecycle performance assessment .....	154
6.3 Formulation of time-dependent reliability analysis.....	155
6.4 Stochastic deterioration modelling and probability of failure .....	157
6.5 Optimized maintenance strategy.....	160
6.6 Evaluation of cost of maintenance and optimal maintenance decision .....	162
6.7 Summary for structural reliability analysis and evaluation of optimal repair time	165
6.8 Numerical example 1 .....	166
6.8.1 <i>Effect of reinforcement corrosion on lifecycle performance</i> .....	168
6.8.2 <i>Effect of cover surface cracking on life cycle performance</i> .....	173
6.8.3 <i>Effect of stirrups on lifecycle performance</i> .....	177
6.9 Numerical example 2.....	179
6.9.1 <i>Evaluation of lifetime distribution of time to failure</i> .....	180
6.9.2 <i>Evaluation of optimal repair time</i> .....	182
6.9.3 <i>Effect of preventive maintenance cost on optimal repair time</i> .....	185
6.9.4 <i>Effect of cover depth on optimal repair time</i> .....	186

6.10 Summary and conclusions .....	188
<b>Chapter 7 Conclusions and Suggestions for Future Work</b>	<b>189</b>
7.1 Summary and conclusions .....	189
7.2 Suggestions for future work.....	192
<b>References</b>	<b>194</b>
<b>Appendices</b>	<b>214</b>
Appendix A: List of publications .....	214

## List of Figures

Figure 1.1 Partial collapse of Pipers Row multi-storey car park in Wolverhampton, UK in March 1997 ( <i>from Edwards 2012</i> ) .....	2
Figure 1.2 Collapse of Laval Bridge in Quebec in 2006 ( <i>from Usatoday 2006</i> ) .....	2
Figure 1.3 The exposed reinforcement on cross beams under the M4 elevated section due to de-icing salt leakage through the expansion joints onto the substructure ( <i>from FESI 2012</i> ).....	3
Figure 2.1 Schematic illustration of the reinforcement corrosion in concrete - as an electrochemical process.....	13
Figure 2.2 Relative volume of steel and its corrosion products .....	15
Figure 2.3 Phases and sub-phases in the service life of corrosion-affected RC structures .....	18
Figure 2.4 Residual reinforcing rebar section ( <i>from Rodriguez et al. 1996</i> ).....	19
Figure 2.5 Propagation of corrosion induced concrete cover cracking due to build-up of corrosion product.....	22
Figure 2.6 Corrosion induced damages in corroded RC Structures .....	22
Figure 2.7 Idealisation of thick-wall cylinder model of corroding rebar surrounded by cover concrete ( <i>from Lounis et al. 2006</i> ).....	27
Figure 2.8 Fictitious crack model by Hillerborg et al. (1976).....	31

Figure 2.9 Four stages of the cohesive crack model ( <i>from Roesler et al. 2007</i> ).....	32
Figure 2.10 Tensile softening law of cohesive crack model .....	33
Figure 2.11 Idealisation of bond force transfer mechanism in deformed rebar ( <i>from ACI 2003</i> ).....	36
Figure 2.12 Schematic representation of infrastructure management process .....	49
Figure 2.13 Schematic representation of time-dependent reliability problem ( <i>from Melchers 1999</i> ).....	58
Figure 2.14 Schematic representation of lifecycle cost and its components .....	60
Figure 3.1 Schematic representation of performance deterioration due to reinforcement corrosion in lifecycle of RC structures .....	67
Figure 3.2 Idealisation of cover concrete as thick-walled cylinder model for predicting concrete crack development and residual bond strength evolution (Note: figures not drawn to scale).....	72
Figure 3.3 Bilinear tension softening curve for cohesive cracking in the concrete around the rebar.....	74
Figure 3.4 Idealisation of completely cracked concrete cover (Note: figures not drawn to scale).....	86
Figure 3.5 Analytical prediction of equivalent cover surface crack width versus .....	92
Figure 3.6 Defects in concrete cover versus corrosion level.....	93

Figure 3.7 Corrosion level associated with formation of visible crack for various cover/rebar diameter ratios .....	94
Figure 3.8 Corrosion level at different stages of cracking at the cover surface for various concrete cover depths .....	95
Figure 4.1 Bond mechanisms for deformed rebar .....	100
Figure 4.2 Bond mechanisms for corroded deformed rebar.....	101
Figure 4.3 Predicted radial corrosion pressure at bond interface as a function of corrosion level, compared with other analytical results .....	109
Figure 4.4 Predicted ultimate bond strength as a function of corrosion level, compared with other analytical results and experimental data .....	111
Figure 4.5 Analytically predicted various contributions of ultimate bond strength as a function of corrosion level, compared with the experimental results of Auyeung et al. (2000) .....	113
Figure 4.6 Residual bond strength versus corrosion level, compared with available filed test data of the Ullasund Bridge and with the ultimate bond strength values given by EC2 (2004) and FIB (2010).....	116
Figure 4.7 Normalized residual bond strength versus cover surface defects of the Ullasund Bridge.....	117
Figure 4.8 Predicted residual bond strength versus corrosion level for various cover depth to rebar diameter ratios of the Ullasund Bridge .....	118

Figure 4.9 Predicted residual bond strength versus cover surface crack width for various cover depth to rebar diameter ratios of the Ullasund Bridge.....	119
Figure 4.10 Analytical prediction of normalized residual bond strength versus corrosion level for unconfined beam, compared with experimental test results available from various sources .....	121
Figure 4.11 Analytical prediction of normalized residual bond strength versus corrosion level for confined beam, compared with experimental test results available from various sources .....	123
Figure 4.12 Analytical prediction of normalized residual bond strength versus surface crack width for unconfined beam, compared with experimental test results available from various sources.....	124
Figure 4.13 Analytical prediction of normalized residual bond strength versus equivalent cover surface crack width for confined beam, compared with experimental test results available from various sources .....	125
Figure 4.14 Normalized residual bond strength versus cover surface defects for confined and unconfined beam.....	127
Figure 5.1 Flexural analysis of a RC beam section: (a) typical cross section of RC beam, (b) strain distribution, (c) equivalent stress distribution .....	131
Figure 5.2 A RC beam specimen and its cross section used in the experimental studies by Mangat and Elgarf (1999b) .....	138

Figure 5.3 Analytical prediction of normalized residual flexural strength versus corrosion level, compared with experimental test results of Mangat and Elgarf (1999b)	140
Figure 5.4 Analytical prediction of normalized residual flexural strength and bond strength versus corrosion level	141
Figure 5.5 Analytical prediction of normalized residual flexural strength versus corrosion level, compared with experimental test results available from various sources	143
Figure 5.6 Analytical prediction of normalized residual flexural strength and bond strength versus cover surface crack width	145
Figure 5.7 Normalized residual flexural strength versus cover surface defects	146
Figure 5.8 Normalized residual flexural strength versus corrosion level evaluated for various cover depths	147
Figure 5.9 Normalized residual flexural strength versus cover surface defects for different concrete cover depths	147
Figure 5.10 Normalized residual flexural strength as a function of corrosion level evaluated for confined and unconfined beam	149
Figure 5.11 Normalized residual flexural strength versus cover surface defects for confined and unconfined beam	150
Figure 6.1 Schematic presentation of time-dependent reliability problem in performance based assessment	156

Figure 6.2 Schematic presentation of lifecycle performance of corroded structures with different maintenance strategy .....	164
Figure 6.3 Probability of failure versus corrosion level for various allowable crack widths limits .....	168
Figure 6.4 Probability of failure and reliability versus corrosion level for allowable crack width limit of 0.3 mm .....	169
Figure 6.5 Probability of failure versus corrosion level for various allowable bond strength deterioration limits.....	170
Figure 6.6 Probability of failure and reliability versus corrosion level for allowable bond strength deterioration limit of 70%.....	170
Figure 6.7 Probability of failure versus corrosion level for various allowable flexural strength deterioration limits.....	172
Figure 6.8 Probability of failure and reliability of lifetime versus corrosion level for allowable flexural strength deterioration limit of 20%.....	172
Figure 6.9 Probability of failure versus cover surface cracking for various allowable bond strength deterioration limits.....	174
Figure 6.10 Structural reliability versus cover surface cracking for various allowable bond strength deterioration limits.....	175
Figure 6.11 Probability of failure versus cover surface cracking for various allowable flexural strength deterioration limits .....	176

Figure 6.12 Structural reliability versus cover surface cracking for various allowable flexural strength deterioration limits .....	177
Figure 6.13 Structural reliability versus cover surface cracking for various allowable bond strength deterioration limits of confined and confined beam .....	178
Figure 6.14 Structural reliability versus cover surface cracking for various allowable flexural strength deterioration limits of confined and unconfined concrete beam .....	179
Figure 6.15 Lifetime distribution of time to failure for various acceptable crack width limits .....	181
Figure 6.16 Lifetime distribution of time to failure for various allowable flexural strength deterioration limits .....	181
Figure 6.17 Expected relative costs over repair time interval with discounting of an annual rate of 5% as a function of repair time for for various acceptable crack width limits .....	183
Figure 6.18 Expected relative costs over repair time interval with discounting of an annual rate of 5% as a function of repair time for various allowable flexural strength deterioration limits of confined beam .....	183
Figure 6.19 Expected relative costs over repair time interval with discounting of an annual rate of 5% as a function of repair time for various allowable flexural strength deterioration limits of unconfined beam .....	184
Figure 6.20 Expected relative costs with discounting and $J_L = 0.3\text{mm}$ as a function of repair time for various preventive maintenance costs $C_P$ .....	185

Figure 6.21 Expected relative costs with discounting and $J_L = 25\%$ as a function of repair time for various preventive maintenance costs $C_P$ .....	186
Figure 6.22 Expected relative costs with discounting as a function of repair time, evaluated for various cover depths with $J_L = 0.3$ mm .....	187
Figure 6.23 Expected relative costs with discounting as a function of repair time, evaluated for various cover depths with $J_L = 25\%$ .....	187

## List of Tables

Table 2.1 Correlation between $\gamma_{mol}$ and $\gamma_{vol}$ of the corrosion products .....	16
Table 2.2 Empirical models.....	25
Table 3.1 Comparison of experimental and predicted corrosion level associated with visible cracking.....	90
Table 5.1 Concrete material properties .....	139

## List of Notations

$A_b$	= cross-sectional area of tension reinforcement
$A_{bx}$	= cross-sectional area of corroded tension reinforcement
$A_{rx}$	= reduced cross-sectional area of rib
$A_s$	= cross-sectional area of rebar
$A_{sc}$	= cross-sectional area of compression reinforcement
$A_{st}$	= cross-sectional area of stirrup leg
$A_{scx}$	= cross-sectional area of corroded compression reinforcement
$C$	= clear cover depth of concrete
$C_1, C_2$	= coefficients related with normalized crack width
$C_e(k)$	= expected cost of maintenance
$C_e(n)$	= expected cycle cost
$C_d(k)$	= expected discounted cost of maintenance
$D$	= overall depth of beam
$D_a$	= maximum aggregate size
$D_b, \phi_o$	= intact rebar diameter
$D_{bx}, \phi$	= reduced rebar diameter
$D_{sc}$	= diameter of compression reinforcement
$D_{st}$	= diameter of stirrup leg
$E$	= effective modulus of elasticity of concrete
$E_c$	= modulus of elasticity of concrete

$E_{st}$	= modulus of elasticity of steel
$F_e$	= iron
$G_F$	= fracture energy of concrete
$H$	= hydrogen
$H_2O$	= water
$J$	= random quantity with gamma distribution
$J_L$	= allowable deterioration limit
$J_x$	= average deterioration rate
$K_1, K_2$	= coefficients
$M_o$	= original mass of rebar
$M_r$	= mass of rust product formed per unit length
$M_{uo}$	= ultimate flexural strength
$M_{ux}$	= ultimate flexural strength of corroded beam
$O$	= oxygen
$OH$	= hydroxide
$P_f$	= probability of failure
$P_r$	= probability
$P_{cnfx}$	= confinement pressure
$P_{cnfx,c}$	= confinement pressure contributed by concrete
$P_{cnfx,st}$	= confinement pressure contributed by stirrups
$P_{corr}, \sigma_r$	= corrosion pressure
$P_s$	= probability of structural survivability or reliability

$R$	= resistance
$R_b$	= radius of un-corroded rebar
$R_c$	= radius of concrete cover surface
$S$	= load
$S_r$	= rib spacing
$S_{st}$	= spacing of stirrup
$T_{adx}$	= adhesion stress
$T_{cnfx,c}$	= confinement stress
$T_{corrx}$	= corrosion stress
$T_{ubo}$	= ultimate bond strength of un-corroded rebar
$T_{ubx}$	= ultimate bond strength of corroded rebar
$T_{ub,rqd}$	= ultimate bond strength required to prevent bond failure
$V_r$	= volume of corrosion product formed per unit length of rebar
$W(r), w(r)$	= normalized and actual crack width
$W_b, W_{bx}$	= normalized crack width at rebar surface
$W_c, W_{cx}$	= normalized crack width at cover surface
$W_{cr}, W_u$	= normalized critical and ultimate cohesive crack width
$X_p$	= corrosion level
$X_p^C$	= corrosion level at through cracking of concrete cover
$X_p^I$	= corrosion level at crack initiation
$X_p^U$	= corrosion level associated with ultimate cohesive crack width

$Y$	= neutral axis depth
$Y_x$	= neutral axis depth of corroded beam
$a, b$	= coefficients of bilinear tension softening law of cracked concrete
$a_2, a_1, a_o$	= coefficients related to the bond-slip law of stirrup
$b$	= width of beam
$d$	= effective depth
$d_x$	= effective depth of corroded beam
$d'$	= depth to compression reinforcement
$d'_x$	= depth to corroded compression reinforcement
$f(w)$	= function of cohesive cack opening
$f(\sigma)$	= function of stress associated with cohesive cack opening
$f_{cc}$	= resultant compressive force in concrete
$f_{cd}$	= design strength of concrete
$f_{ck}$	= characteristic compressive strength of concrete
$f_{ccx}$	= resultant compressive force in concrete of the corroded beam
$f_{cohx}$	= adhesion stress coefficient
$f_{J_x}$	= probability density function of performance deterioration
$f_R$	= probability density function of resistance
$f_S$	= probability density function of load
$f_{sc}$	= resultant compressive force in compression reinforcement
$f_{scx}$	= resultant compressive force in corroded compression reinforcement

$f_{st}$	= resultant tensile force in tension reinforcement
$f_{stx}$	= resultant tensile force in corroded tension reinforcement
$f_t$	= maximum tensile strength of concrete at onset of cracking
$f_{yd}$	= design strength of steel
$f_{ydx}$	= design strength of corroded steel
$f_{yk}$	= characteristic yield strength of steel
$g(X), G(t)$	= limit state function
$h_{rx}$	= reduced rib height
$i_{corr}$	= mean corrosion current per unit length
$k$	= number of age replacement interval
$k_c$	= constant
$k_{cnfx}$	= coefficient of confinement stress
$l_{ch}$	= characteristic length
$l_d$	= development length
$l_o$	= material constant
$m_c$	= empirical constant
$n$	= expected cycle length
$n_b$	= number of tension reinforcements
$n_c$	= number of cracks
$n_{st}$	= number of stirrups
$p_i$	= probability of renewal in unit time

$q_i$	= probability of failure in unit time
$r_1, r_2$	= radial distance between rebar and concrete cover surface
$r_{cr}$	= critical crack front
$r_y$	= crack front
$t$	= time
$t_L$	= service life of the structure
$u$	= radial displacement
$u_{bx}$	= radial displacement at rebar surface
$w$	= crack opening
$w_1$	= crack opening at stress $\sigma_1$
$w_b, w_{bx}$	= actual crack width at rebar surface
$w_c, w_{cx}$	= actual crack width at concrete cover surface
$w_f$	= final crack opening
$\alpha$	= discount factor
$\alpha_{bd}$	= coefficient of design bond strength
$\alpha_{bi}$	= coefficient of bilinear softening curve
$\alpha_{cc}$	= constant
$\alpha_p$	= attack penetration factor
$\alpha_{st}$	= shape factor of stirrup
$\beta$	= stiffness reduction factor
$\beta_b, \beta_{bx}$	= stiffness reduction factor at rebar surface

$\beta_p$	= coefficient related with position of rebar
$\delta_o$	= orientation of the rib
$\delta(r_1, r_2)$	= crack factor
$\varepsilon_r$	= radial strain
$\varepsilon_\theta$	= hoop strain
$\varepsilon_\theta^f$	= fracture strain
$\varepsilon_\theta^e$	= linear elastic strain
$\varepsilon_{cc}$	= ultimate strain of concrete
$\varepsilon_{ccx}$	= ultimate strain of concrete associated with corrosion
$\varepsilon_{sc}$	= strain of compression steel
$\varepsilon_{scx}$	= strain of compression steel associated with corrosion
$\varepsilon_{st}$	= strain of tensile steel
$\varepsilon_{stx}$	= strain of tensile steel associated with corrosion
$\theta_c$	= creep coefficient of concrete
$\mu_x$	= coefficient of the friction due to corrosion
$\sigma$	= stress corresponding to cohesive crack opening
$\sigma_\theta, \sigma_w$	= residual tensile stress acting across cohesive cracks
$\nu$	= Poisson's ratio of the concrete
$\rho_r$	= density of the rust product
$\rho_s$	= density of the steel
$\gamma_c$	= partial safety factor for concrete strength
$\gamma_s$	= partial safety factor for steel strength

$\gamma_{mol}$	= molecular weight of the corrosion product
$\gamma_{vol}$	= volume ratio of the corrosion product
$\eta, \lambda'$	= constants depends on concrete strength
$\eta_x$	= shape function of gamma distribution associated with corrosion
$\eta_x(R_c, R_b)$	= crack factor
$\varphi$	= angle of friction between steel and concrete
$\Gamma$	= gamma function
$\lambda$	= scale parameter of gamma distribution
$\Delta A_s, \Delta A_b$	= cross-sectional area loss of corroded rebar
$\Delta A_{so}$	= cross-sectional area loss of rebar associated with visible cracking
$\Delta M_s$	= mass loss of corroded rebar
$\Delta V$	= volume increase per unit length of the rebar
$\Delta V_s$	= volume of steel consumed per unit length of the rebar

# Chapter 1 Introduction

## 1.1 Background

Reinforced concrete (RC) is the most widely used construction material for civil engineering infrastructure such as buildings and bridges because of its durability, versatility and economic feasibility (Shi et al. 2012). However, the ability of the concrete structure to fulfil their intended functions are often compromised by reinforcement corrosion causing considerable costs and safety threats to civil engineering infrastructure systems (Mullard and Stewart 2012, Tilly and Jacobs 2007, Chen and Bicanic 2010). Reinforcement corrosion has been identified as the main cause of the deterioration of RC structures worldwide. The major source of reinforcement corrosion can be either due to the environment pollution (i.e. carbonation) or the ingress of chloride ions in RC structures exposed to de-icing salt or marine environment, but the latter is the dominant factor. Chloride induced reinforcement corrosion has caused major problems to the durability of RC structures in many countries including the UK (Broomfield 2007, Balafas and Burgoyne 2010).

Reduction in durability associated with reinforcement corrosion reduces the safety margin of concrete structure to an extent of serious structural failure. Some examples of the disaster caused by reinforcement corrosion are:

- \* Fall down of the Berlin Congress Hall, resulting in enormous casualties and damages (Borgard et al. 1990).

- \* Partial collapse of Pipers Row multi-storey car park in Wolverhampton, UK in March 1997 due to reinforcement corrosion caused by carbonation (Edwards 2012).
- \* Collapse of highway bridge in Laval, Quebec, 2006 killing 5 people (Usatoday 2006).



**Figure 1.1** Partial collapse of Pipers Row multi-storey car park in Wolverhampton, UK in March 1997 (*from Edwards 2012*)



**Figure 1.2** Collapse of Laval Bridge in Quebec in 2006 (*from Usatoday 2006*)

Recently temporary closure of the elevated section of the M4, Hammersmith flyover in December 2011, is another example which highlights the issue of structural deterioration caused by reinforcement corrosion. The motorway was partially reopened in January 2012 following further inspection which allowed reduced loads to use the motorway on a reduced carriageway. The repair works were completed fully in May 2012 at an estimated cost of £12 million (Edwards 2012).



**Figure 1.3** The exposed reinforcement on cross beams under the M4 elevated section due to de-icing salt leakage through the expansion joints onto the substructure (*from FESI 2012*)

The increasing number of deteriorating RC structures has caused great loss in infrastructure management industry due to increase in costs for repair, rehabilitation or replacement in short term in the highway networks of most European and North American countries (Neves and Frangopol 2005). The costs associated with managing these corrosion damaged RC structures are tremendous. In Europe, about 50% of its annual construction budget has been spent on refurbishment and repair of existing structures (Tilly and Jacobs 2007). In United States, over 160,000 bridges are

structurally deficient which represents 27.5% of the total inventory of highway bridges when bridges are weighed equally (FHWA 2004). Approximately \$3 billion per year is the estimated cost required for the repair of corrosion damaged structures in Canada. Reinforcement corrosion in RC structures cost the United States economy almost 1% of its gross domestic product (Whitmore and Ball 2004). Similar statistics were observed in Europe, Asia and Australia (EI Reedy 2008). In addition to these direct costs, there is significant portion of indirect costs such as traffic delay and loss of life and property. Hence the extent of the problem related to corrosion induced deterioration has resulted in a multimillion dollar expenses in both developed and developing countries. The maintenance cost is likely to increase year by year because of the increasing number of aging structures and continuous traffic demand and exposure to aggressive environment.

Despite the huge amount of cost associated with the management of deteriorating RC structures, safety is the primary issue. When the reinforcement corrodes, it damages the structures in the form of cracking, eventual spalling of concrete cover and reduction in cross-section of reinforcement bars (rebars). If the corrosion continues, it affects the bond mechanism between the reinforcement and concrete and thus the anchorage which ultimately affects on the performance of the RC structures. This leads to several safety issues such as sudden falling of loose concrete cover onto vehicles, general public etc. and sudden collapse of the structural elements. Therefore, deterioration of RC structures caused by reinforcement corrosion has significant influence on infrastructure management and is of greater challenge both technically and economically.

Structural performance deterioration caused by reinforcement corrosion is a complex phenomenon which in general is uncertain, hence for the effective condition assessment of the structure an effective evaluation of deterioration occurring in structure is required. Improving the understanding of the effects of corrosion on the structural behaviour of deteriorating RC structures would enhance in making effective and reliable decision related to the inspection, repair, strengthening, replacement and demolition of such structures. Timely maintenance activities which are well-planned and carried out with minimal disruption to users can present substantial savings in terms of both cost and time for both infrastructures owners and users. Hence it will ultimately help to achieve the goal of sustainable infrastructures management.

A comprehensive literature survey undertaken in this research show that the existing research mainly focuses on the causes and mechanisms of reinforcement regarding the prediction of corrosion initiation but the effects of steel rebar corrosion on structural performance, however, have received relatively little attention. Till now no analytical method has been proposed to evaluate the performance (load carrying and bond strength capacity) of the corroded RC structures based on crack evolution in concrete cover with specific reference to realistic concrete properties of cracked concrete. Moreover, the influence of bond strength loss on the residual flexural strength of corroded structures is not well understood. Furthermore, research on lifecycle performance analysis considering realistic damages caused by reinforcement corrosion is very limited. Therefore, there is a need to develop an approach for effective evaluation of deterioration and probability of failure associated with this deterioration, which can help to make decision of optimal repair during the service life of corrosion

damaged RC structures. In this regard this research is aimed at addressing such gaps in existing research.

## **1.2 Research significance and contribution**

The reliability-based performance assessment techniques based on stochastic deterioration modelling has tremendous potential in making cost effective decisions related to infrastructure management such as inspection, repair, strengthening, replacement and demolition. For the time-dependent reliability analysis of RC structures subject to reinforcement corrosion, an effective evaluation of performance deterioration associated with the propagation of the reinforcement corrosion during their service life is required. From a structural point of view, bond loss due to corrosion is particularly intriguing since it may lead to sudden, brittle or anchorage failure. Visualized surface cracks on the concrete cover surface is the first indicator of corrosion problem in the RC structure and is an important parameter of the most practical significance for assessment of deteriorating RC structures. Hence, it is always beneficial to have link between surface crack width and other hidden damages like bond strength and residual strength deterioration.

The analytical methods presented in this research are a significant contribution to more understanding of the structural behaviour. It also provides a novel method capable of evaluating the present and future condition of the corroded RC structures based on the corrosion induced cracking at the concrete cover and to effectively determine the optimal repair time by optimising the balance between the risk of a structural failure and the maintenance cost. This study could be a useful for researchers, engineers and

also for asset managers working in the field of management of corrosion affected RC infrastructures.

### **1.3 Aim and objectives**

The main aim of this research is to develop a theoretical model capable of evaluating the present and future performance of existing corrosion affected RC infrastructures like tunnels and bridges required for optimized maintenance strategy. The main objectives of the research are:

- \* To understand the mechanism of corrosion and its effect on the RC structures.
- \* To develop an analytical model for investigating the corrosion induced cover cracking process.
- \* To develop an analytical model for bond strength deterioration due to reinforcement corrosion.
- \* To investigate the effect of corrosion on load carrying capacity of the RC structures.
- \* To investigate the time-dependent failure probability and optimal repair planning of RC structures subject to reinforcement corrosion.

### **1.4 Scope of thesis**

This thesis is mainly based on the works of Chen and Nepal (2015a,b,c), Chen and Nepal (2014), Nepal and Chen (2015a,b,c), Nepal and Chen (2014a,b,c,d,e,f,g) and Nepal et al. (2013). This thesis consists of seven chapters (Chapter 1 to 7) and a brief outline of each chapter is as follows:

## **Chapter 1 Introduction**

This chapter describes the background and significance of the research and introduces the aim and objectives and scope of the thesis.

## **Chapter 2 Literature Review**

In this chapter, basic theories, methods and a state-of-the-art related to reinforcement corrosion and fracture mechanics are presented. Additionally basis of time-dependent reliability analysis and maintenance models are also discussed. This chapter also presents the relevant existing published research work related to: a) experimental and analytical investigation on the damages caused by reinforcement corrosion such as sectional loss of rebar, cover cracking, bond strength deterioration and flexural strength deterioration and b) lifecycle management of corrosion damaged RC structures which mainly focuses on time-dependent reliability analysis and lifecycle cost analysis.

## **Chapter 3 Development of Corrosion Induced Cracking Model**

In this chapter a new analytical model is developed to evaluate the corrosion induced cover cracking process corresponding to mass loss of the rebar. Cracked concrete is considered as anisotropic in nature and its realistic concrete properties such as residual tensile strength and reduced tensile stiffness are considered during the analysis. Numerical examples are presented to demonstrate the applicability of the developed model.

## **Chapter 4 Development of Bond Strength Degradation Model**

In this chapter a simple analytical model is presented to evaluate the bond strength

behaviour of corroded rebar associated with different phases of cover cracking. From the proposed analytical model of the crack width in the concrete cover presented in Chapter 3, the radial corrosion pressure, confinement stress and the adhesion stress acting at the bond interface are determined. The ultimate bond strength is then estimated by considering the contributions from adhesion, confinement and corrosion pressure related to corrosion level. The merit of the proposed method is that the bond strength degradation is directly related to crack growth in concrete cover. Finally, the effectiveness of the proposed method is demonstrated with experimental and field data available from various sources. Parametric studies on cover defects, concrete geometry and confinement conditions are also presented.

### **Chapter 5 Development of Flexural Strength Degradation Model**

This chapter presents a realistic method for evaluating load carrying capacity of corrosion damaged RC beams. During the analysis new compability condition existed by bond strength loss is considered together with different failure modes. The applicability of the proposed model is then demonstrated with the help of numerical examples. Effects of cover defects, concrete geometry and confinement conditions on residual flexural strength are also investigated.

### **Chapter 6 Time-dependent Reliability Analysis and Optimized Maintenance**

#### **Strategy**

This chapter presents an approach for time-dependent reliability analysis of corrosion affected RC structures together with the optimized maintenance strategy. The gamma process is adopted for stochastic modelling of deterioration caused by reinforcement corrosion. The time-dependent reliability analysis is then applied to evaluate the

probability of failure of the RC beam in predefined limit states. Then, optimal repair planning and maintenance strategies during the service life are determined by balancing the cost for maintenance and the risk of failure. Numerical examples are presented to demonstrate the applicability of the proposed approach. Furthermore, the effects of various factors such as concrete geometry, confinement condition and limit states on the lifecycle management of corrosion damaged RC structure are also investigated.

## **Chapter 7 Conclusions and Suggestions for Future Work**

This chapter presents the summary and main conclusions drawn from the present research work followed by some suggestions for future study.

## **Chapter 2 Literature Review**

### **2.1 Introduction**

In order to evaluate the effect of reinforcement corrosion on the performance of RC structures like tunnels, bridges and piers, it is necessary to understand how reinforcement corrosion occurs in RC structures and how the RC structures response to it. This chapter provides the critical review of all the aspects that are responsible for reinforcement corrosion and its effect on the performance of RC structures. At first, mechanism of reinforcement corrosion is discussed then its effect on the performance of the RC structures is presented. The second topic is divided into two parts: visible effect (concrete cover cracking) and hidden effects (bond and flexural strength deterioration). In order to analyse the corrosion induced cover cracking, knowledge of fracture mechanics is required which is then reviewed. To analyse the residual (bond and flexural) strength deterioration due to reinforcement corrosion, mechanisms of bond and flexural strength are discussed first and then critical overview of the existing investigations in the field of determining residual strength deterioration is presented. Furthermore, basic theory of reliability analysis and lifecycle cost analysis are presented. Overview of the existing investigations in the field of lifecycle management of corrosion damaged RC structures is finally presented.

### **2.2 Reinforcement corrosion**

Corrosion of reinforcing bars embedded in concrete has been identified as the most

common factor responsible for the deterioration of the RC structures worldwide costing billion dollars budget annually (Tilly and Jacobs 2007, Shi et al. 2012). As these structures continue to age and deteriorate, the costs of repair and maintenance will likely to increase each year. Many investigators (Ahmad 2003, Val et al. 2009, Cairns et al. 2008, Chen and Mahadevan 2008) have described about the corrosion of reinforcement and its significance in RC structures. Broomfield (2007) have provided good description about the corrosion in reinforced steel and assessment of existing structures.

### *2.2.1 Mechanism of corrosion*

The concrete surrounding the rebar is alkaline in nature and the pH of the concrete cover can be greater than 12.5. Steel rebar embedded in the concrete is normally protected by a passive layer created by the high alkalinity of the concrete. Once the passive layer is broken down, corrosion initiates (Broomfield 2007, Papakonstantinou and Shinozuka 2013, Ahmad 2003, Otieno et al. 2011). This protective layer can be broken down due to the carbonation or the chloride ingress from the environment.

Carbonation is more common in old and badly built structures (particularly buildings). It is comparatively rare on modern highway bridges and other civil engineering structures where low water cement ratio is utilized and proper compaction, curing, and adequate concrete cover are provided (Broomfield 2007). Chlorides can be found in concrete due to several sources. They can be cast into the concrete or they can diffuse in from the environment. Sea salt spray, seawater wetting and de-icing salts are some of the most frequent causes of chloride intrusion into the concrete. As soon as an amount

of chlorides accumulates to a critical level at the reinforcement, the passive layer of oxide on the steel breaks down and corrosion starts.

Reinforcement of corrosion in the RC structures is actually the electrochemical process as shown in Figure 2.1 (Ahmad 2003). It involves four basic parts: an anode, where electrochemical oxidation takes place; a cathode, where electrochemical reduction occurs; an electrical conductor, which is steel itself and an aqueous medium in the concrete, which serves as electrolyte (Ahmad 2003, Broomfield 2007).

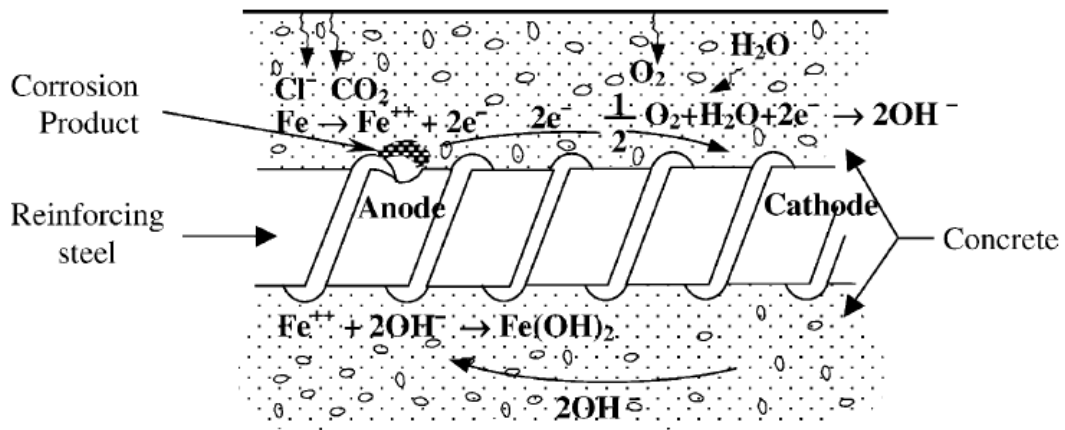
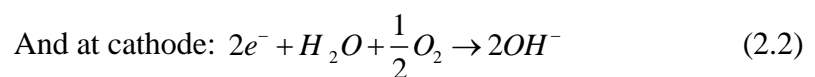
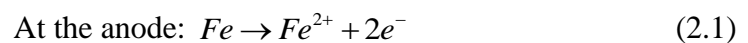
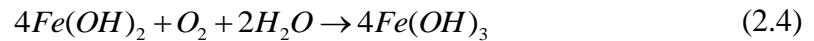


**Figure 2.1** Schematic illustration of the reinforcement corrosion in concrete - as an electrochemical process

The chemical reactions of steel corrosion can be presented by equations 2.1 to 2.5 (Broomfield 2007).



As shown in equations (2.1) and (2.2), the anode produces electrons which are transported through aqueous medium in the concrete to the cathode where they are consumed with oxygen and water. Ferrous and hydroxyl ions flow within the concrete and react with each other and with further involvement of oxygen and water result in the development of different form of rust products as shown in equations (2.3) to (2.5).



The rust ( $Fe_2O_3 \bullet nH_2O$ ) is the final product formed during the corrosion process, but the other iron oxides also exist.

### 2.2.2 *Properties of corrosion products*

The rust products formed are expansive in nature. The actual volume increase depends entirely on the composition of corrosion product formed which in turn depends on many factors such as oxygen supply, moisture content etc. Therefore properties of corrosion products cannot be credibly postulated (Liu and Weyers 1998, Pantazopoulou and Papoulia 2001, Papakonstantinou and Shinozuka 2013). However, existing research shows that depending on the level of oxidation, usually the volume of rust product formed increases of up to six to seven times of the volume of the original steel

(Jaffer and Hansson 2009, Bhargava et al. 2006, Liu and Weyers 1998), as shown in Figure 2.2 (Liu and Weyers 1998).

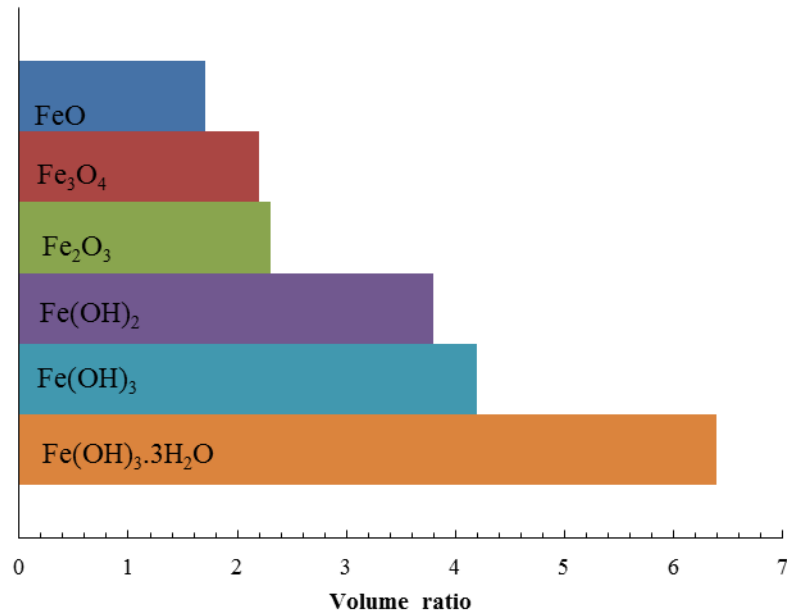


**Figure 2.2** Relative volume of steel and its corrosion products

Typical oxides formed during oxidation have different characteristics: relative volume ( $\gamma_{vol}$ ) and molecular weight ( $\gamma_{mol}$ ) as compared with the parent metal ( $Fe$ ), as shown in Table 2.1 (Liu and Weyers 1998, Pantazopoulou and Papoulia 2001).

The density of the rust product formed is still less understood. Therefore in modelling the mechanical effects of reinforcement corrosion, the general practice is to represent the density of the rust product  $\rho_r$  as a fixed fraction of the density of steel  $\rho_s$ . Pantazopoulou and Papoulia (2001) have defined the density of rust product as  $\rho_r = \rho_s / (\gamma_{mol}\gamma_{vol})$ . This formulation has been utilized in many numerical and theoretical studies such as Chernin et al. (2010), Bhargava et al. (2006), Papakonstantinou and Shinozuka (2013).

**Table 2.1** Correlation between  $\gamma_{mol}$  and  $\gamma_{vol}$  of the corrosion products

Corrosion products	Molecular weight ratio ( $\gamma_{mol}$ )	Volume weight ratio ( $\gamma_{vol}$ )
FeO	0.77	1.7
Fe <sub>3</sub> O <sub>4</sub>	0.724	2.2
Fe <sub>2</sub> O <sub>3</sub>	0.699	2.3
Fe(OH) <sub>2</sub>	0.622	3.8
Fe(OH) <sub>3</sub>	0.523	4.2
Fe(OH) <sub>3</sub> .3H <sub>2</sub> O	0.347	6.4

Due to the complex nature of formation and distribution of corrosion products, the identification of composition and properties of the corrosion products formed within concrete of RC structure is very challenging and highly debated topic in the field of reinforcement corrosion. For instance, in every anode position and in distinct times, a mix of different corrosion products can be developed in accordance with available local conditions, humidity and oxygen. Therefore, depending on the observations of the experimental investigations different view has been suggested. In the studies carried by Marcotte and Hansson (2007) and Jaffer and Hansson (2009) the volume ratio was typically in the range of 2-3 and 2-4 respectively. These results are in agreement with Vu et al. (2005), where the mean expansion ratio was equal to 2.94 and also with long-term (decades) corrosion cases (Poupard et al. 2006, Duffo et al. 2012), where the different corrosion compounds found had the volume expansion between 2.08 and 3.48. Similarly, in numerical and analytical studies different values of  $\gamma_{vol}$  have been used. However, in general the value of 2 to 4 is frequently used in numerical and theoretical models (Wang and Liu 2004, Lundgren 2002, Coronelli et al. 2013, Coronelli 2002, Molina et al. 1993, Bhargava et al. 2006, Balafas and Burgoyne 2011).

### 2.2.3 *Effect of reinforcement corrosion*

Reinforcement corrosion affects the overall performance of the corroded RC structures by affecting the initial properties of both reinforcement (rebar) and the concrete (Cairns et al. 2008, Bhargava et al. 2007). The process of resistance degradation and the maintenance strategy for extending the lifetime in RC structures affected by bar corrosion is described in Figure 2.3 (Chen and Alani 2013).

In Figure 2.3, there are three phases of deterioration. The corrosion initiation phase, during this phase no noticeable weakening of the material or reduction in the function of the structure occurs but some of the protective barrier is broken down due to ingress of chloride or carbon dioxide. Second stage is the corrosion propagation phase during which active deterioration develops and loss of function is observed. Third phase is the residual life phase, at which subsequent functional loss of the structure takes place and if repairing strategy is not considered the structure will finally collapse.

Therefore, in lifecycle modelling the direct effects of corrosion in reinforced concrete structures can be listed as below (Nepal and Chen 2014b, Chen and Nepal 2015b):

- a) Sectional loss of rebar
- b) Concrete cover cracking
- c) Change in the characteristics of bond strength at rebar-concrete interface
- d) Reduction in steel yield strength and load carrying capacity

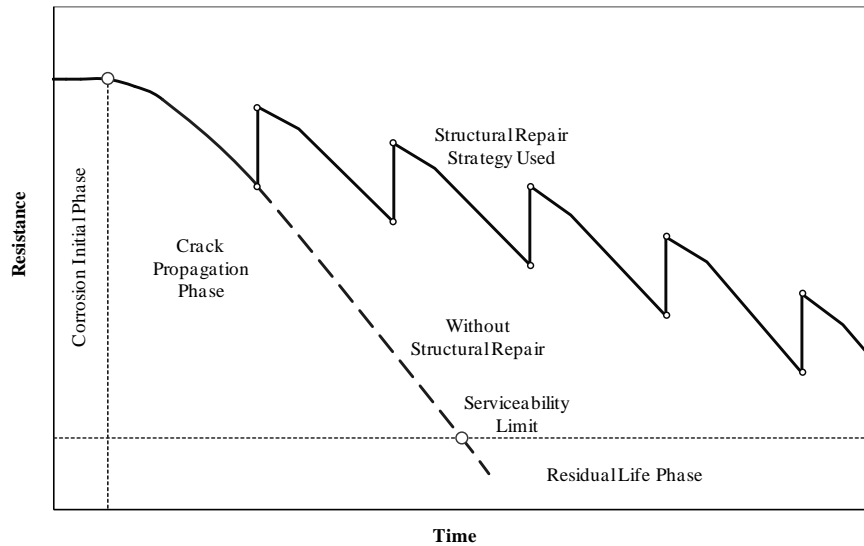


**Figure 2.3** Phases and sub-phases in the service life of corrosion-affected RC structures

The consequences of each of these direct effects mentioned earlier and their interrelationship ultimately change the performances of the RC structures at ultimate limit state (ULS) by reducing its load carrying capacity and more often effect on their serviceability limits by increasing deflection, cracking, spalling, rust staining, etc. (EI Maaddawy and Soudki 2007, Torres-Acosta et al. 2007, Cairns et al. 2008). This research will mainly focus on the aforementioned direct effects caused by reinforcement corrosion which will be discussed in detail in next sections.

#### 2.2.4 Sectional loss of rebar due to corrosion

In general, there are two form of reinforcement corrosion: a) uniform corrosion and b) pitting corrosion (Ahmad 2003, Vidal et al. 2004, Zhang et al. 2010). In an experimental investigation carried out by Zhang (2010), the initiation and propagation phases of steel corrosion in a natural corrosive environment were studied. Zhang (2010) observed that at the crack initiation stage, localized corrosion due to chloride ingress

was the predominant corrosion pattern. With the propagation of corrosion cracks, uniform corrosion rapidly developed and gradually became predominant in the second stage of crack propagation.

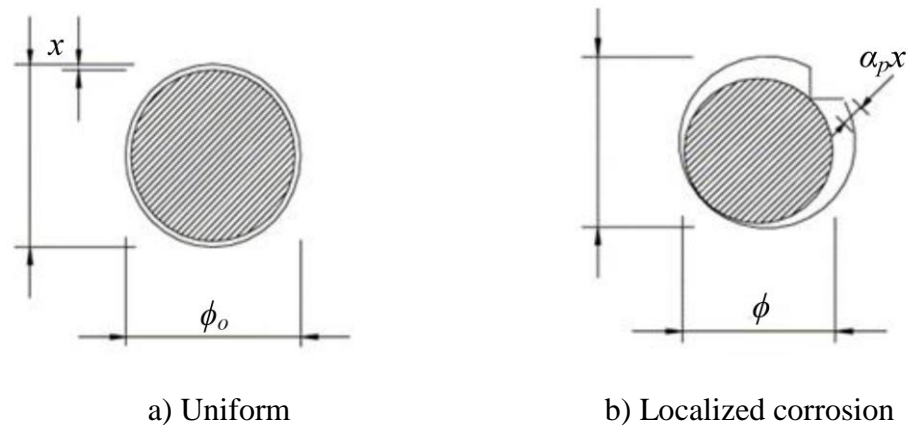


**Figure 2.4** Residual reinforcing rebar section (*from Rodriguez et al. 1996*)

General or uniform corrosion is the type of corrosion that proceeds at the same rate over the entire surface of a material as shown in Figure 2.4(a). This type of corrosion occurs due to carbonation or due to the presence of large amount of chlorides. Pitting is a form of localized corrosion that is confined to a small area and takes the form of cavities called pits as shown in Figure 2.4(b).

The reduction of reinforcement area or diameter is most accurately obtained by direct measurements. For corroded RC structures with cover spalling, the remaining rebar diameter can be measured on the exposed rebars after removal of the rust layer. For less corroded RC structures where the cover has not yet spalled off, small parts of the cover could be removed at non-critical locations and afterwards repaired. When there is uniform or pitting corrosion of a steel rebar, the effective reinforcement area is either evenly or locally reduced with the help of attack penetration depth or corrosion depth

(x). Depending on this theory, Rodriguez et al. (1996) has given the relation between attack penetration and reinforcing rebar, which has been frequently utilised in Vidal et al. (2004), Khan et al. (2014) and Zhang et al. (2010), expressed here as

$$\phi = \phi_o - \alpha_p x \quad (2.6)$$

where  $\phi$  is the residual rebar diameter,  $\phi_o$  is the initial rebar diameter,  $\alpha_p$  is the pit concentration factor. The value of  $\alpha_p$  is 2 for uniform corrosion and 4 to 8 for the pitting corrosion (Vidal et al. 2004, Rodriguez et al. 1996).

Sectional loss of rebar is often represented in terms of mass loss of the corroded rebar. The gravimetric loss method is the most widely adopted procedure to measure the loss in cross-section of the rebar in the laboratory where weight of the corroded rebar is compared with the weight of the intact (original) rebar and the associated mass loss is obtained. Another existing method used in laboratory to evaluate mass loss is by using Archimedes principle and Faraday's law. The electrochemical non-destructive techniques can be used both on-site and in the laboratory to assess the corrosion state (i.e. corrosion sites and corrosion rate). The measured corrosion rate is then transformed into the amount of metal loss by using the diffusion law related to growth of expansive corrosion products. However, the interpretation of the results must be performed carefully (Pantazopoulou and Papoulia 2001, Val et al. 1998). More information on the application of electrochemical techniques used in the condition monitoring of corroded RC structures are available in the literature such as Ahmed (2003), Bertolini et al. (2004) and RILEM TC-154-EMC (2004).

In theoretical model, rate of rust production is frequently estimated by two methods: a) constant rate model proposed by Andrade et al. (1993) and b) variable rate model proposed by Liu and Weyers (1998). According to Liu and Weyers (1998), the rate of rust production decreases with time because diffusion of iron ions is inversely proportional to the oxide layer. The model proposed by Liu and Weyers (1998) is frequently used in many studies (Pantazopoulou and Papoulia 2001, Balafas and Burgoyne 2011, Bhargava et al. 2006, Chen and Alani 2013). The governing equation for rate of rust production (i.e. mass of rust products (kg/m) per unit length) is given by Pantazopoulou and Papoulia (2001) expressed here as

$$M_r(t) = \sqrt{m_c \pi \phi_o i_{corr} t} \quad (2.7)$$

where  $m_c$  is an empirical constant taken as  $m_c = 2.1 \times 10^{-2}$ ,  $i_{corr}$  represents the mean annual corrosion current per unit length at the surface area of the rebar ( $A/m^2$ ) and  $t$  is the time in year.

### **2.3 Concrete cover cracking**

Corrosion induced concrete cover cracking is the most serious effect caused by corrosion of reinforcement. Appearance of corrosion induced cracks on the surface of RC structures is the main visual indicator of the corrosion presence in the structure and is frequently used as an important parameter in routine inspection of corroded RC structures (Chernin et al. 2012, Val et al. 2009, Saether 2011). In this section the mechanics behind the concrete cover cracking is discussed along with the critical review of the existing investigations in the field of corrosion induced cover cracking.

### 2.3.1 Mechanism of corrosion induced cover cracking

The volume of the rust products which is many times larger than the parent metal, exerts a tensile stresses on the surrounding concrete. As the corrosion progresses, this internal stress becomes greater than the tensile strength of the concrete and radial splitting cracks initiates at the rebar surface and propagates towards the cover surface. When the corrosion continues, it may lead towards the eventual spalling and delamination of the concrete cover as shown in Figure 2.5 (AGA 2015).

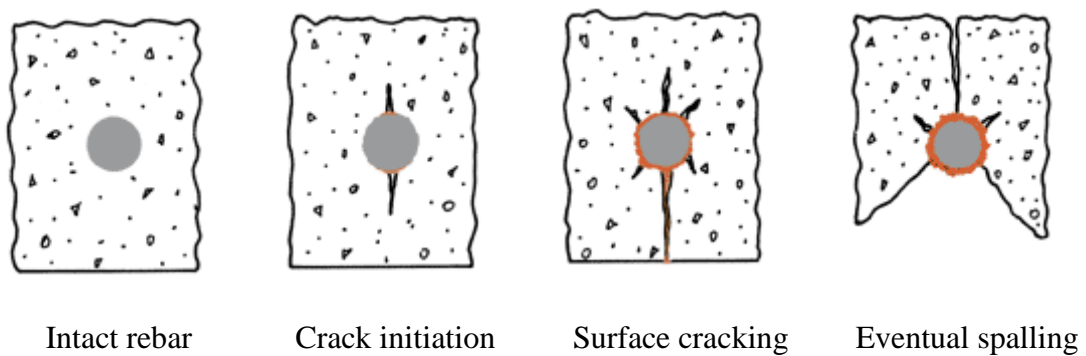


**Figure 2.5** Propagation of corrosion induced concrete cover cracking due to build-up of corrosion product

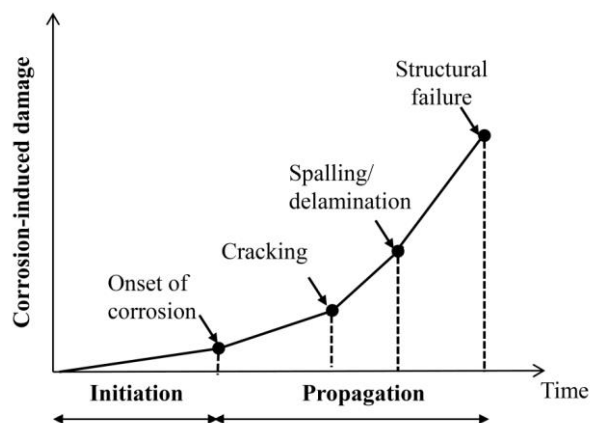


**Figure 2.6** Corrosion induced damages in corroded RC Structures

This ultimately reduces the stiffness of the concrete and bond strength between rebar and concrete causing the structure failure as shown in Figure 2.6 (Lounis et al. 2006).

### 2.3.2 *Review of existing investigations on cover cracking due to corrosion*

The existing investigations in the field of corrosion induced cover cracking are mainly focused on two aspects of the cracking process: a) crack initiation (i.e. formation) at cover surface and b) crack evolution on the cover surface.

Many experimental studies have been undertaken to determine the critical amount of corrosion needed for concrete cover cracking to find parameters having major influence on this amount, and to derive simple empirical models for its evaluation (Rodriguez et al. 1996, Rodriguez et al. 1994, Alonso et al. 1998). The critical amount in terms of the weight of corrosion products or the depth of corrosion penetration was expressed as a function of either only on cover to rebar diameter ratio  $C/D_b$  (Alonso et al. 1998), or the tensile strength of concrete  $f_t$  (Rodriguez et al. 1996). The model proposed by Rodriguez et al. (1996) has later adopted in Duracrete (2000).

Al-Sulaimani et al. (1990) demonstrated that cracks were initiated at the cover surface when corrosion penetrations reached approximately 0.1 mm. For the diameters used, this corresponds to reductions in cross-sectional area in the range 2.0 to 4.5%. Rodriguez et al. (1994 and 1996) revealed that cracking at the concrete cover surface first developed at attack penetrations (i.e. reduction in bar radius) of 15 to 40  $\mu\text{m}$ . For rebars with relatively small diameter, e.g. 12 mm, this corresponds to less than 2% reduction in cross-sectional area and even less for rebars of larger diameters. Similar

findings were reported by Webster and Clark (2000), Vu et al. (2005) and Coronelli et al. (2013). Thus in summary, although the relationship between section loss and formation of longitudinal cracks depends on number of parameters such as specimen conditioning, concrete cover, etc. It can be concluded that cover surface cracking develops before the reduction in rebar area becomes significant.

Crack evolution (growth) i.e. crack opening due to corrosion has also been investigated in a number of experimental studies. Most of these involved accelerated corrosion tests with impressed current that provide data on the crack growth depending on the amount of corrosion (Rodriguez et al. 1996, Alonso et al. 1998, Vu et al. 2005). Rodriguez et al. (1994) have observed different cracking trend for compression and tensile steel and introduced a factor  $\beta_p$  (=0.01 for top cast bars and 0.0125 for bottom cast bars) in their empirical model. Alonso et al. (1998) found that crack initiation at the concrete cover surface depends on cover to rebar diameter ratio and the amount of corrosion product required to initiate crack linearly increases with the increase in concrete cover depth while after the formation of cracks in concrete cover surface there is no influence of cover to rebar diameter ratio on crack growth.

All the above mentioned experimental investigations rely on accelerated corrosion tests using electrical fields that provide a poor substitute for real corrosion. Hence, Vidal et al. (2004) reported results linking the amount of corrosion with crack width which were obtained from two beams naturally corroded in a saline environment for 14 and 17 years. In order to incorporate the randomness of corrosion induced cracking in the concrete cover, concept of equivalent crack was introduced and defined as a sum of the cracks formed in concrete cover. The results revealed that the crack initiation

(formation) at the concrete cover surface depends on cover to rebar diameter ratio while after this stage cracks growth does not depends on it. For  $C/D_b = 1.33$  crack initiation occurs at about 30  $\mu m$  loss of rebar while for  $C/D_b = 3.0$  crack initiation occurs when radius loss of the rebar is about 40  $\mu m$ . This agrees with the results obtained by other researchers using accelerated corrosion in terms of influence of  $C/D_b$  ratio in crack evolution process. However, the influence of bar position as mentioned by Rodriguez et al. (1996) was not observed. Furthermore, Vidal et al. (2004) also concluded that cover depth does not have significant influence on crack growth after the cover concrete is completely cracked which is in agreement with the previous studies. Later, Zhang et al. (2010) also studied on beams naturally corroded in a saline environment. Vidal et al. (2004) and Zhang et al. (2010) have proposed empirical models to relate the crack growth with the loss of cross-section of the steel reinforcement.

**Table 2.2** Empirical models

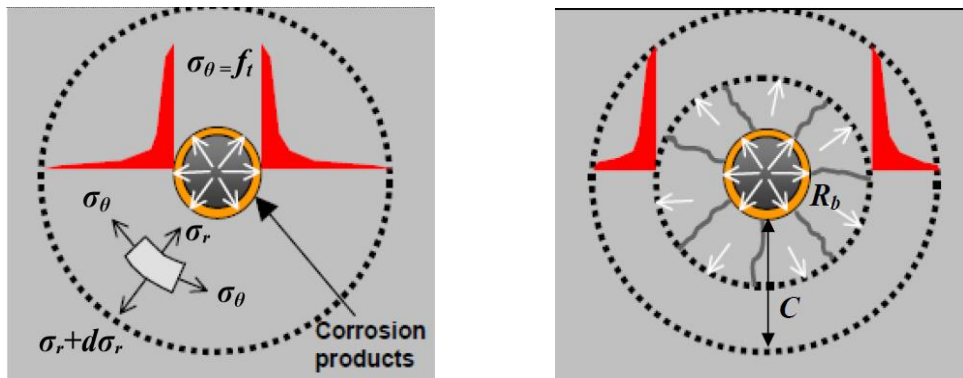
Reference	Empirical models	
	Crack formation at cover surface	Crack growth
Alonso et al. (1998)	$x_c (\mu m) = 7.53 + 9.3 \frac{C}{D_b}$	
Rodriguez et al. (1996)	$x_c (\mu m) = 83.8 + 7.4 \frac{C}{D_b} - 22.6 f_t (MPa)$	$w(mm) = 0.05 + \beta(x - x_o)$ for $w \leq 1.0mm$
Webster and Clark (2000)	$x_c (\mu m) = 1.25C(mm)$	
Vidal et al. (2004)	$\Delta A_{so} (mm^2) = A_s \left[ 1 - \left[ 1 - \frac{\alpha_p}{D_b} \left( 7.53 + 9.32 \frac{C}{D_b} \right) 10^{-3} \right]^2 \right]$	$w(mm) = 0.0575(\Delta A_s - \Delta A_{so})$
Zhang et al.2010		$w(mm) = 0.1916\Delta A_s + 0.164$

In most of the experiments a linear relationship between the amount of corrosion and the crack width has been observed. As mentioned earlier, based on the experimental observation a number of formulas relating the crack width with the amount of corrosion or sectional loss of rebar have been proposed. Some of the empirical models proposed by these experimental studies are summarized in Table 2.2.

In Table 2.2,  $x_c$  and  $A_{s0}$  are the corrosion depth and cross-section loss associated with visible crack development at the concrete cover surface,  $w$  is the crack width,  $A_s$  is the sectional area of original rebar and  $\Delta A_s$  is the sectional area loss of the corroded rebar. These empirical relationships were obtained from the regression analysis of the experimental results obtained and therefore these empirical models usually cannot take into account all of the relative parameters. Hence they cannot give the overall trend of crack evolution in concrete cover due to reinforcement corrosion. Therefore, analytical methods which are capable of considering more relevant parameters such as geometrical dimensions, concrete properties and corrosion etc. were undertaken to study corrosion-induced cracking process.

Although corrosion induced crack-width is the most important factor in service life modelling of corrosion affected RC structures, intensive research on developing theoretical model of corrosion induced cracking only began in 1970. One of the first analytical models predicting the time of cover cracking caused by the corrosion of the embedded reinforcing steel was proposed by Bazant (1979) and is the basis of most of the existing analytical models dealing with corrosion induced cracking. The model considers concrete around a corroding reinforcing bar as a thick-walled cylinder, which is subjected to internal pressure caused by the formation of corrosion products having

larger volume than that of the original steel creates stresses in radial ( $\sigma_r$ ) and hoop direction ( $\sigma_\theta$ ). The idealisation of thick-walled cylinder is shown in Figure 2.7 (Lounis et al. 2006), in which rebar of initial radius  $R_b$  is embedded in the thick walled cylinder of wall thickness  $C$  (clear cover depth). Stresses in the cylinder wall were calculated using the solution provided by isotropic linear elasticity theory. It is assumed that cracking occurs when the stresses reach the tensile strength of concrete and assumed that the cover fails with the first appearance of a crack on the inner surface of the cylinder



a) Tensile stresses developed at crack initiation

b) Propagation of internal cracks in thick-walled concrete cylinder

**Figure 2.7** Idealisation of thick-wall cylinder model of corroding rebar surrounded by cover concrete (from Lounis et al. 2006)

Unfortunately, Bazant (1979) did not provide comparison of his model with field or experimental data to validate his theory. However, experiments and field observations have showed that the model significantly underestimates the time of first cracking (Liu and Weyers 1998). In order to improve the agreement between analytical and experimental results Liu and Weyers (1998) suggested modifications to the Bazant's

model by introducing porous zone. Liu and Weyers (1998) also suggested that a corrosion rate was inversely proportional to the amount of corrosion products formed.

Martin-Perez (1999) extended the thick-walled model, but did not study the cracked part of concrete in detail. Later using similar approach EI Maaddawy and Soudki (2007) proposed a model for prediction of time from corrosion. The main drawback of above mentioned models is the inability of thick-walled cylinder model not considering the non-linear behaviour of cracked concrete, which takes place when radial cracks start to form at the rebar surface. But these limitations of anisotropic behaviour of cracked concrete was overcome by partition of the cylinder into two parts: a cracked inner cylinder and an intact outer one and considering tension softening behaviour of cracked concrete (Pantazopoulou and Papoulia 2001, Bhargava et al. 2006, Chernin et al. 2010, Balafas and Burgoyne 2011, Chen and Alani 2013).

At first Pantazopoulou and Papoulia (2001) treated cracks in the inner cylinder as smeared which was later adopted by many researchers (Wang and Liu 2004, Bhargava et al. 2006, Chen and Alani 2013). The build-up of the rust around the rebar was assumed as uniform and was estimated by using two alternative models: linear model that follows Faraday's law (Andrade et al. 1993) and a nonlinear model (Liu and Weyers 1998). They focussed on detailed modelling of cracked concrete and treated cracked concrete as anisotropic nonlinear elastic material with post-cracking softening. The residual strength of cracked concrete was defined by a bi-linear stress-strain relationship as given in CEB-FIP (1990). Due to the complexity, the unknown behaviour of the cracked cover was solved numerically by using finite difference instead of closed form solutions. Correlation with experimental evidence illustrated that

the Pantazopoulou and Papoulia (2001) model was capable of successfully reproducing the experimental trends and gives reasonable estimates for the time and critical mass of rust associated with cover cracking. They also conclude that of the two alternative methods used in representing the rate of the rust production, the nonlinear model proved far more successive in quantifying service life conditions. However, results were only provided till the stage of cover cracking and no results were provided in terms of crack evolution in concrete cover.

Furthermore, considering similar approaches of Pantazopoulou and Papoulia (2001), an improved analytical model was recently proposed by Chernin et al. (2010) and Balafas and Burgoyne (2011). All these above mentioned studies focuses only on surface cracking of the concrete cover rather than on the growth of crack width due to expansion of the corrosion products. To understand the behaviour of crack propagation in the concrete cover recently an improved analytical model was proposed by Chen and Alani (2013). They used the concept of equivalent crack width as defined by Vidal et al. (2004) and treated cracked concrete as an anisotropic material and its residual strength was determined by adopting linear softening cohesive crack model.

Therefore, from the review of existing studies on corrosion induced cover cracking, it can be concluded that although number of analytical studies have been carried out on time prediction for corrosion crack initiation at the concrete cover surface based on the change of volume of corrosion products but comparatively less research has been carried out concerning the prediction of crack growth during the progresses of corrosion.

### 2.3.3 *Cohesive crack model and tension softening of cracked concrete*

In analytical models of corrosion induced cover cracking, fracture mechanics in terms of cohesive crack model (CCM) and tension softening of cracked concrete is frequently applied in modelling the concrete cracking process (Pantazopoulou and Papoulia 2001, Bhargava et al. 2006, Chernin et al. 2010, Chen and Alani 2013). The main part of the research is to develop simple and effective analytical model, which can evaluate the present condition and predict the future performance of the corrosion affected RC structure. Therefore, this section provides fundamental theory of fracture mechanics applied in concrete cover cracking process.

Since concrete is a quasi-brittle material, the size of fracture process zone (FPZ) of concrete is not negligible (Bazant and Planas 1998, Elices et al. 2002). Classical linear elastic fracture mechanics (LEFM) is unable to predict the progressive failure of concrete specimens due to this large nonlinear process zone (Roesler et al. 2007, Elices et al. 2002). In order to overcome LEFM limitations for concrete fracture behaviour, Hillerborg et al. (1976) first proposed the fictitious crack model. This fictitious crack model has been widely used in modelling fracture in concrete (Elices et al. 2002). The fictitious crack model also known as cohesive crack model (CCM) assumes that the FPZ is long and narrow, and is characterized by a stress-crack opening displacement curve.

Hillerborg's cohesive crack model is characterized by cohesive stress-elongation relationship which is shown in Figure 2.8. The stress-elongation relationship is obtained from a uniaxial tensile test of a concrete plate. In Figure 2.8(a), the tensile stress starts from zero and increases simultaneously with the elongation of the concrete plate until it

reaches the tensile strength when the crack initiates. Then, the stress ahead of the crack tip decreases with continuous increase of the elongation, while unloading occurs outside the crack region. Hence the behaviour of the cohesive crack is defined by the relationship between the cohesive stress  $\sigma$  and the relative displacement  $w$  between the upper and lower face of the cohesive crack width or opening:  $\sigma = f(w)$ . In figure

2.8(b),  $G_F$  is the fracture energy defined as  $G_F = \int_0^{w_f} f(w)dw$ . Therefore, in the

cohesive crack model, there are three governing parameters: material tensile strength  $f_t$ , specific fracture energy  $G_F$  and the shape of the  $f(w)$  curve.

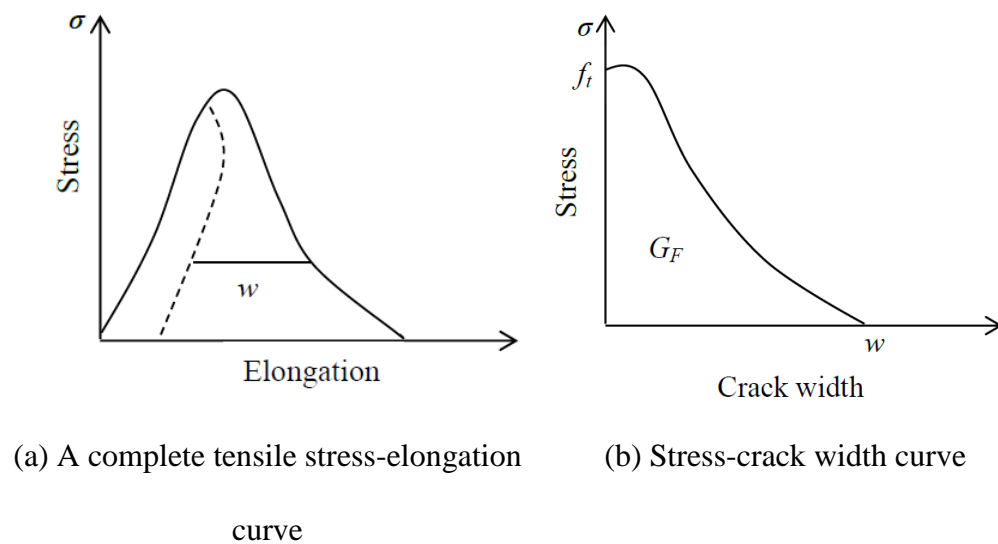


**Figure 2.8** Fictitious crack model by Hillerborg et al. (1976)

In cohesive crack model, the stresses are a function of the crack opening displacement (COD) (Hillerborg et al. 1976) or the tensile strain in the post-peak region (Bazant and Oh 1983). Since tensile strain measurement in the post-peak region is extremely difficult thereby crack opening displacement ( $w$ ) is measured in the experiments, and converted into equivalent strain measured over a gage length. At the tip of the FPZ,

tensile stress is equal to tensile strength ( $f_t$ ) of the material, corresponding crack opening is zero and equivalent strain is ultimate elastic tensile strain. The stress gradually reduces to zero at the tip of the true crack, which corresponds to ultimate crack opening ( $w_u$ ) or final crack opening ( $w_f$ ) with failure strain ( $\varepsilon_u$ ). Therefore, in general the CCM is characterized by four stages as shown in Figure 2.9.

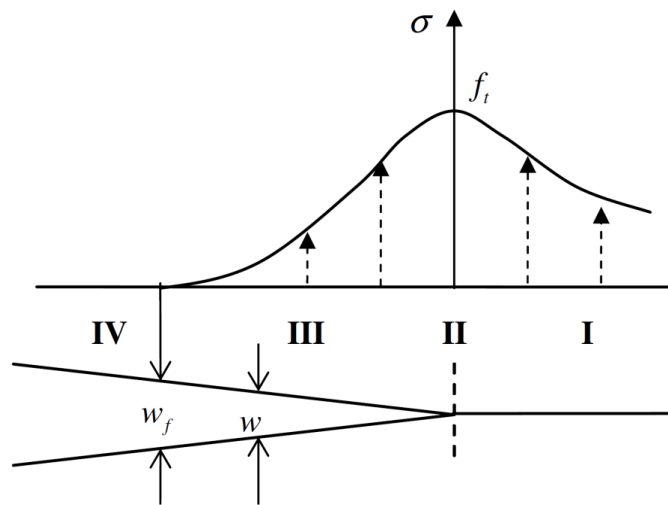


**Figure 2.9** Four stages of the cohesive crack model (from Roesler et al. 2007)

The first stage is characterized by general elastic material behaviour without separation (i.e. Stage I of Figure 2.9). The concrete material properties are assumed to be homogeneous and linear elastic in this stage. The next stage is the initiation of a crack when a certain criterion is met (i.e. Stage II of Figure 2.9). In corrosion induced cracking model, crack is assumed to occur when hoop tensile stress reaches the concrete tensile strength ( $f_t$ ). Stage III describes the evolution of the failure, which is governed by the cohesive law or the softening curve, i.e., the relation between the stress ( $\sigma$ ) and crack opening width ( $w$ ) across the fracture surface. Because the cohesive law defines the characteristic of the fracture process zone, the shape of the softening curve



FIP 1990). Bilinear softening expression can be written as (Roelfestra and Wittmann 1986).

$$\sigma = \begin{cases} f_t - (f_t - \sigma_1) \frac{w}{w_1} & \text{for } w \leq w_1 \\ \sigma_1 - \frac{\sigma_1(w - w_1)}{(w_f - w_1)} & \text{for } w_1 < w \leq w_f \end{cases} \quad (2.8)$$

where  $f_t$  is the tensile strength,  $w$  is the crack opening displacement and  $w_1$  is the critical crack opening displacement corresponding to stress  $\sigma_1$  and  $w_f$  is the crack opening displacement corresponding to  $\sigma = 0$ . As mentioned earlier one of the essential fracture parameter in a softening model is the total fracture energy  $G_F$  which corresponds to the area under the softening curve. The fracture energy  $G_F$  depends on the maximum size of aggregate and compressive strength of the concrete used. Another parameter required for the structural behaviour in tensile softening is the characteristic length  $l_{ch}$ , given by  $l_{ch} = EG_F / f_t^2$  (Bazant and Planas 1998). Actually the characteristic length is an inverse measure of the brittleness of the materials (i.e. the smaller  $l_{ch}$  the more brittle the materials).

## 2.4 Bond strength

Bond between concrete and reinforcing steel is required to transfer the forces between the two materials and therefore it significantly influences the behaviour of reinforced concrete structures. This section presents some basic information on the bond strength

mechanisms. An overview of the existing investigations in the field of bond strength deterioration caused by reinforcement corrosion is also presented with their limitations.

#### *2.4.1 Bond strength mechanism*

Bond strength acting at steel-concrete interface can be simply defined as the uniform shear stress over the nominal surface of a rebar (reinforcement). Actually, the bond mechanism is the interaction mechanism which maintains the composite action between steel and concrete and hence allows the force transfer between reinforcement and the surrounding concrete (Cairns and Abdullah 1996). Efficient and reliable force transfer between the reinforcement and concrete is the fundamental requirement for an effective performance of the RC structures. Insufficient bond can lead to a significant reduction in the load carrying capacity of the RC structures (FIB 2010, Tastani and Pantazopoulou 2010, Saether 2011).

Two common types of reinforcement, plain and deformed rebars, rely on different combinations of the bond mechanisms to carry load. Bond strength of plain rebars relies on friction and adhesion whilst deformed rebar rely on friction, adhesion and mechanical interlocking. In which mechanical interlocking plays the main role while adhesion and friction play the minor role (Cairns et al. 2006, ACI 2003, Cairns and Abdullah 1996). As deformed rebars are most commonly used in current practice, this thesis is focused on bond strength deterioration of corroded deformed rebars. Therefore in this section mechanism of bond strength in deformed rebar is considered and is discussed in detail.

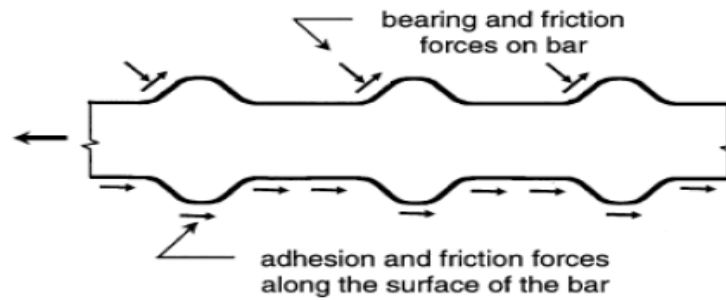


**Figure 2.11** Idealisation of bond force transfer mechanism in deformed rebar (from ACI 2003)

According to ACI (2003), an efficient and reliable force transfer between the reinforcement and the surrounding concrete depends on three mechanisms: adhesion, friction and mechanical interlocking as shown in Figure 2.11.

**Adhesion:**

Adhesion is the chemical bond between the rebar and the concrete which is related to the shear strength at the steel-concrete interface. For a small load, the basic resisting mechanism is the chemical adhesion, however when a deformed rebar moves with respect to the surrounding concrete, due to increase in the loads the chemical adhesion along the rebar surface is lost quickly. Therefore this is not considered as the reliable resisting effects in bond mechanisms.

**Friction:**

Friction is the force which resists the parallel displacement between rebar and concrete surfaces sliding against each other. It depends on the roughness of the rebar surface. Friction plays a significant role in force transfer between the concrete and the steel rebar. Based on the work of Treece and Jirsa (1989), the ACI Committee 408 ACI

(1992) suggested that friction can contribute up to 35% of the ultimate strength governed by the splitting of the concrete cover.

### **Mechanical interlocking:**

In deformed rebar, mechanical interlocking between the ribs and the concrete plays the primary role in providing bond strength. The mechanical interlocking of the deformed steel rebar depends on the surface profile of the rebar. When the cracks begin to form between the ribs and the concrete, the interlocking forces induce large bearing stresses around the ribs and slip occurs. Therefore, the rebar ribs restrain the slip movement by bearing against the concrete. The slip of a deformed rebar may occur in two ways, either through pushing the concrete away from the rebar by the ribs, i.e. wedging action, or through crushing of the concrete by the ribs.

#### *2.4.2 Existing investigations on bond strength degradation*

Bond strength behaviour of corroded reinforcement has been experimentally studied by many researchers in the past. These experimental studies have made use of a wide variety of specimens and rebar types. Furthermore, there have been considerable variations in the adopted procedures for conditioning of specimens for corrosion studies. Therefore reported bond strength values differ considerably between the various laboratory investigations. However, in summary they all agree that as the corrosion level increases, crack width increases and consequently causes the breakdown of adhesion, friction and mechanical interlocking at the steel–concrete interface. Hence the cracking in cover surface causes significant reduction in bond strength. Some of these tests are now discussed in detail.

Al-Sulaimani et al. (1990) conducted concentric pull-out tests on cubic concrete specimens of 150 mm per side. The specimens were reinforced with a centrally embedded rebar of 10, 14 and 20 mm diameter to give cover-to-bar diameter ratios of 7.50, 5.36 and 3.75, respectively. The average yield strength of the reinforcement was 450 MPa and average compressive strength of 30 MPa. A constant current density of  $2000 \mu\text{A}/\text{cm}^2$  was passed over the reinforcement. They found that at mass loss of about 1%, bond strength increase and after which bond strength decrease considerably. All these rebar with different sizes had a similar gradient of bond strength degradation. At similar level of corrosion, the 10 mm rebar always had highest bond strength followed by 14 mm rebar and with 20 mm rebar having the lowest bond strength.

Rodriguez et al. (1994) performed pull-out tests on the cubic concrete specimens of 300 mm per side. The specimens were reinforced with four rebars of 16 mm diameter in their corner with the cover of 24, 40 and 15 mm. Some of the specimens were provided with stirrups of 6 mm diameter at 70 mm and 100 mm. The yield strength of the reinforcement was 590 MPa and the compressive strength of the concrete was 40 MPa. Acceleration of corrosion process was achieved by applying a constant current of  $100 \mu\text{A}/\text{cm}^2$ . The results show that bond strength is better maintained in specimens with stirrups than those specimens without stirrups and the influence of rebar position on the bond strength of corroded rebar is negligible. They also concluded that the bond strength corresponding to specimen without corrosion shows higher bond strength value for larger cover depth and when concrete is cracked due to corrosion the influence of cover depth on bond strength degradation is negligible.

Auyeung et al. (2000) conducted a concentric pull-out tests on concrete prisms of size 175mm×175mm×350 mm with centrally placed rebar of 19 mm diameter. The average compressive strength of concrete was 28 MPa. The current density of 0.1 mA/cm<sup>2</sup> was used to induce the corrosion. They concluded that at <2% corrosion level bond strength increases and after which it decreases significantly. Based on the results reported in this paper, they concluded that when mass loss reaches 2%, concrete cracks along the rebar.

Lee et al. (2002) performed concentric pull-out tests on cubic concrete specimens of 8D per side where 'D' is the diameter of reinforcing bar. The clear cover to the reinforcing bar has been varied from 1.5D to 3.5D. The D13 (i.e. 13 mm diameter) type reinforcing bar was used for the experimental work that had yield strength of 315 MPa. The compressive strength of the concrete has been varied from 24.7 MPa to 42.1 MPa; which was achieved by varying water cement ratios (0.45–0.65) and mix proportions of cement, sand and gravel. Here again, impressed current was applied to induce corrosion and the result of bond strength degradation was presented in terms of mass loss in percentage. Maximum bond strengths have also been reported as a function of percentage corrosion for different water cement ratio. Based on the results of the experiment empirical formulae were also proposed to show the relationship between mass loss and bond strength degradation.

Fang et al. (2004) performed concentric pull-out tests on concrete specimens of size 140 mm×140 mm×180 mm. Specimens were reinforced with a centrally placed reinforcing bar of 20 mm diameter with embedded length of 40 mm. Some specimens were provided with stirrups of 6 mm at spacing of 40 mm. The yield strengths for deformed rebar was 289.6 MPa and 28-day average compressive strength for concrete

was 52.1 MPa. To induce corrosion specimen were subjected to a constant current density of 2 A. The amount of corrosion was measured as loss in weight of reinforcing bar. They concluded that for specimens without stirrups, bond strength was very sensitive to corrosion levels and generally decreases with the corrosion level while for specimens with stirrups, corrosion had no substantial influence on the bond strength.

Law et al. (2011) performed eccentric pull-out tests on concrete specimens of size 200 ×300 ×300 mm subject to current density of 200  $\mu\text{A}/\text{cm}^2$ . Specimens were reinforced with 12 mm and 16mm diameter rebar placed at the corners with cover of three times of rebar diameter. The confined specimens were provided with 6mm diameter stirrups at 75mm centre to centre. The 28-day average compressive strength of concrete was 40MPa and tensile strength of rebar was 500 MPa. Results of bond strength degradation with respect to mass loss (corrosion level) and cover surface crack width were presented. They concluded that 12mm rebar displayed higher bond strength values than 16 mm with similar crack width, and confined rebar displayed higher bond strength at the point of initial cracking while unconfined rebar displayed a decrease in bond strength and in both cases with increase in crack width bond strength decreases and relationship between surface crack width and bond strength has better correlation than that with corrosion level.

Chung et al. (2008a) performed concentric pull-out tests on the cubic concrete specimens of 150 mm per side with centrally placed rebar of diameter 13 mm and embedded length of 39 mm. A power supply of 24 VDC and 12 Amps were used to induce the corrosion. The average compressive strength of the specimen was 25 MPa

and the yield strength of the rebar was 384.7 MPa. They concluded that beyond 3% of corrosion, bond strength reduced significantly.

Zhao et al. (2013) carried out concentric pull-out tests on the cubic concrete specimens of 150 mm per side with normal and recycle aggregate. The diameter of the rebar centrally placed was 18 mm with embedded length of 100 mm and constant direct current was applied by a DC power supply. Some of the specimens were provided with 8 mm stirrups at 100 mm spacing. The average compressive strength of the specimen with normal aggregate was 41.9 MPa and specimen with recycled aggregate was 38.4 MPa. Results of bond strength degradation with respect to mass loss and cover surface crack width were presented. They concluded that specimens with stirrups have higher bond strength than those specimens without stirrups and the specimens with normal aggregate have slightly higher strength than specimen with recycle aggregate.

In comparison with experimental investigation of bond strength behaviour of corroded reinforcement, little research has been undertaken numerically and analytically. In past decades few studies have proposed on numerical models to predict the bond behaviour at the steel-concrete interface due to corrosion of reinforcing steel using finite element method (Lundgren 2002, Lee et al. 2002, Bertoa et al. 2008, Fischer 2010, Amleh and Ghosh 2006). Three dimensional finite element program DIANA was used to model the corrosion effect on bond strength by Lundgren (2002). Coronelli (2002) proposed a model to predict pressure around a corroded reinforcing bar and the bond strength. Wang and Liu (2004) proposed theoretical modelling of bond strength for corroded rebars before and after corrosion cracking by using nonlinear stress-strain relationship of cracked concrete. By using similar approach Bhargava et al. (2007) proposed new

theoretical model. Amleh and Ghosh (2006) developed a nonlinear finite element model to account for the effect of corrosion on the ultimate bond strength. For this purpose, the non-linear finite element program ABAQUS was used to model the bond stress at steel-concrete interfaces for different levels of corrosion with different concrete strengths and cover thicknesses. Since the present research concentrates on analytical modelling, only existing analytical models are reviewed in more detail.

Coronelli (2002) studied the interface pressure caused by the expansion of corrosion product and developed a model predicting the bond strength for corroded rebars in RC structures. Coronelli (2002) studied the role of the interface pressure caused by rebar expansion in different confinement situations. In order to determine the interface pressure, the total crack width with respect to corrosion depth  $x$ , proposed by Molina et al. (1993) was adopted. Coronelli (2002) modified a model proposed by Cairns and Abdullah (1996) for splitting bond failure by considering corroded rebars and formulated the bond strength as a sum of three stresses (i.e. adhesion, confinement and corrosion) acting at the steel-concrete interface. Although Coronelli (2002) proposed first analytical model for bond strength of corroded reinforcement, however the theoretical expression for corrosion pressure acting at bond interface was not suggested.

Later, Wang and Liu (2004) proposed theoretical bond strength model with the expression for corrosion pressure by using thick-walled cylindrical model and representing bilinear stress-strain relationship in cracked concrete. The drawback of Wang and Liu (2004) model is that the anisotropy of cracked concrete was not considered. Wang and Liu (2004) calculated the tangential stresses in the cracked

cylinder by using displacement obtained from the linear elastic solution applied for the intact cylinder.

Bhargava et al. (2007) modified the Coronelli (2002) model. They proposed a new theoretical expression of corrosion pressure in corroded bars caused by the expansive corrosion products before and after through cracking of the cover concrete. The cracking in the concrete cover thickness was modelled as a process of tension-softening according to nonlinear stress-strain relationship given by CEB-FIP (1990). The concrete was assumed to be linear-elastic before cracking and once the crack occurred, the residual strength of cracked concrete was considered using tension-softening.

Like Wang and Liu (2004), the main drawback of the Bhargava et al. (2007) was that the model did not consider the anisotropy of the cracked concrete. In the model, the concrete in the inner cracked cylinder was treated as material with reduced modulus of elasticity compared with outer intact cylinder while in reality stiffness of the cracked concrete in radial direction is significantly higher than in hoop direction (Chernin et al. 2010, Chen and Alani 2013). Another limitation of model proposed by Bhargava et al. (2007) is that the effect of confinement due to cracked concrete is evaluated by considering the tensile strength as given in CEB-FIP (1990) and no theoretical expression for crack width was provided to evaluate residual strength of cracked concrete and also the limited contribution of stirrups providing confinement was not mentioned.

## 2.5 Flexural strength

The consequences of corrosion process leads to several effects such as longitudinal cracking of concrete cover, steel cross section reduction, the steel-concrete bond reduction and steel yield strength reduction. As a result of these effects individually or in combination, the load-bearing capacity of reinforced concrete elements are considerably reduced which indeed affect the performance of whole structure (FIB 2010, Bhargava et al. 2007, Cairns et al. 2008). This section provides information on flexural strength mechanism together with the overview of the existing studies on the load carrying capacity of the corroded RC structures affected by reinforcement corrosion.

### 2.5.1 Flexural strength mechanism

The tensile strength of concrete is only about 10% of the compressive strength. Because of this, nearly all RC structures are designed on the assumption that the concrete does not resist any tensile force. In a RC member, the compressive force is resisted by concrete whereas the tensile force is resisted by steel rebar (reinforcement) which is transferred by bond between the interface of steel and concrete (Mosley et al. 2007). If this bond is not adequate, the reinforcing bars will just slip within the concrete and there will not be a composite action. The following assumptions are considered for the analysis and design of RC member (Mosley et al. 2007, EC2 2004):

1. Bernoulli's hypothesis: Plane sections before bending remain plane after bending. The assumption assures the absence of shear distortion and the consequent linear strain distribution across the cross section of the beam.

2. Strain-compatibility: The strain in concrete at a particular point on the cross section should be congruent to the strain in reinforcement at the same point.
3. The respective strain-strain curves of concrete and reinforcement are used to calculate the internal stresses developed.

### *2.5.2 Existing investigations on flexural strength degradation*

A number of experimental studies have been undertaken by different researchers to find the effect of corrosion on the flexural strength of corroded RC elements. Some of them are discussed below.

Almusallam et al. (1996) performed tests on 63 mm × 305 mm × 711 mm simply supported one-way slabs (centre to centre 610 mm span) reinforced with five 6 mm diameter rebars placed at 57 mm centres. The slab specimens were partially immersed in 5% NaCl solution and a constant current of 2 A was applied to the reinforcing bars. 25% and 60% reduction in ultimate strength was observed for corrosion level of 5% and 25% respectively.

Rodriguez et al. (1997) carried out experiments on six different types of reinforced concrete beams with a constant anodic current of 100  $\mu\text{A}/\text{cm}^2$  was applied for a period of time ranging between 100 and 200 days. The rate of reduction was linear. From the experiment they concluded that it is possible to predict a conservative value of the ultimate bending moment by means of using RC conventional models and considering the reduced section of rebars.

Mangat and Elgarf (1999b) investigated the effect of corrosion on the flexural strength of RC beams by examining a total of 111 simply supported beams. The beam specimens were tested using four-point loading and all beams were subjected to an accelerated corrosion technique in the laboratory. The results showed that up to corrosion degree of 3.75% there was very little effect of corrosion rate on flexural load capacity and at 5% and beyond, the flexural load capacity decreased significantly with increasing corrosion rate. The study observed a 75% decrease in load capacity for a 10% diameter reduction. They found that the reduction in reinforcing bar cross-section due to corrosion has an insignificant effect on the residual flexural strength of the beams. The reduction in residual strength was primarily attributed to the loss or breakdown of the steel/concrete interfacial bond. Similar finding was reported on study of 14 year beam carried out by Castel et al. (2000).

EI Maaddawy et al. (2005b) conducted tests on simply supported RC beams with two-point loading and partial length corrosion symmetrically arranged about the mid-span. The beam consisted of two deformed rebars of 16 mm diameter in the tension zone and two 8 mm diameter plain rebars in the compression zone. The rate of reduction was linear and only 45% reduction was observed at mass loss of 30%. EI Maaddawy et al. (2005b) concluded that at low corrosion levels, the effect of bond loss can be ignored and that the ultimate load carrying capacity of the beam is affected only by the loss on steel reinforcement. Recent investigations carried out by Zhang et al. (2012) and Xia et al. (2012) have also reported similar trend of flexural strength reduction.

Chung et al. (2008b) tested 70 simply supported slabs with 10 mm diameter rebar using a four-point load. The primary variables were bond length and corrosion level. They

found the load capacity of slabs decreases significantly after diameter loss of 2%. They concluded that the loss of flexural strength capacity due to bond deterioration is more critical than force loss due to decrease in cross-sectional area.

Azad et al. (2010) tested 48 simply supported beams with different dimensions and tension reinforcements. All beams were designed to fail in flexure by providing ample amount of shear reinforcement to exclude premature shear failure. They concluded that at low level of corrosion residual flexural strength of a corroded beam can be predicted with reasonable accuracy by considering only the reduced cross-section area of tension reinforcement. However, at a higher value of corrosion increasing adverse effect of bond cannot be ignored in determining the residual flexural capacity.

In comparison with experimental studies, very few studies have been devoted to the analytical modelling of the flexural strength behaviour of corroded RC member. An algebraic formulation was presented to predict the flexural strength of RC members by Eyre and Nokhasteh (1992). An iteration procedure was proposed to calculate the ultimate moment of the RC beams with exposed reinforcement on the basis of plane-section bending (Zhang and Raof 1995). Cairns and Zhao (1993) carried out analytical research work and developed a simplified numerical model by assuming the plane-section behaviour of the concrete section.

An analytical model that predicted the nonlinear flexural behaviour of corroded RC beam with partial length corrosion has been proposed by EI Maaddawy et al. (2005a), where the hypothesis of the plane sections remaining plane was still adopted. However, EI Maaddawy et al. (2005a) did not consider the effect of corrosion for bond

degradation. The results were presented in terms of deflection and verified with experimental data.

Later Bhargava et al. (2007) proposed a new analytical model with consideration of bond strength loss. However, the model did not consider the new compatibility condition cause by bond strength loss. Recently, Wang and Liu (2010) have proposed an improved analytical model using the concept of the equivalent plastic region length of the unbonded prestressed beam. Bond strength of corroded rebar was evaluated by using Wang and Liu (2004). The model has shown good agreement between the analytically predicted results and corresponding experimental results of EI Maaddawy et al. (2005b). They used the compatibility conditions of RC beam with partial length of complete loss of bond due to corrosion, and hence concluded that the ultimate flexural moment of corroded RC beam is not significantly influenced by bond characteristics over this partial length as long as the tensile steel of the beam can reach its yield strength before the bond failure. Recently, Yang et al. (2013) proposed a new model to predict the flexural deformation of a corroded RC beam by considering polynomial tension-stiffening model where the results were presented in terms of deflection. However the influence of bond strength loss on flexural strength of corroded rebar is still less understood.

## **2.6 Lifecycle analysis and management of infrastructure**

Lifecycle management of infrastructures generally consists of six stages: infrastructure system and elements hierarchy, condition rating method, data collection method, deterioration prediction method, cost forecasting, and decision-making as shown in

Figure 2.12 (Edirisinghe et al. 2013). The condition assessment of the structure reveals its current state in relation to the ongoing deterioration of the structure. As shown in Figure 2.12, in infrastructure management process decision related to effective repair and planning of the infrastructure actually depends on the effectiveness of deterioration prediction and hence is considered as the vital stage in infrastructure management. In this section basic background of deterioration modelling is discussed together with probabilistic time-dependent reliability analysis and its application in cost-effective maintenance. Additionally, a review on existing research in the field of lifecycle management of corrosion damaged RC structures is also discussed.

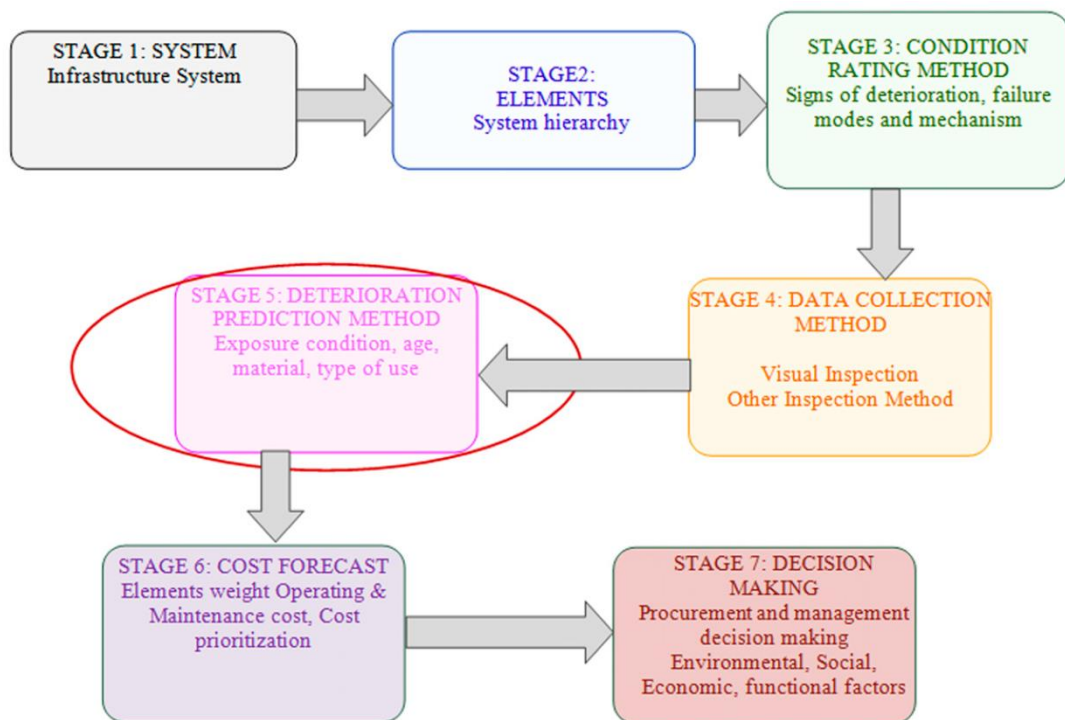


**Figure 2.12** Schematic representation of infrastructure management process

### 2.6.1 Background of deterioration modelling

Because of its importance in infrastructure management extensive research has been

undertaken in deterioration modelling. Various infrastructure deterioration prediction models have been put forward. Edirisidhe et al. (2013) has given a good review of existing deterioration models. According to their research all the existing deterioration models used in infrastructure management can be broadly classified into three categories:

- \* Deterministic models
- \* Stochastic models
- \* Artificial intelligence (AI)-based models

Deterministic deterioration prediction models can be of two types: linear or nonlinear. Deterministic models are often used for phenomenon where relationships between components are certain. Kleiner and Rajani (2001) and Lou et al. (2001) applied time linear and power law models for water mains and pavements, respectively. The deterministic models, where the relationship between input and output parameters are described by a mathematical relationship can be easily implemented in an asset management system. However, this approach often is not applicable to complex asset systems where a mathematical relationship with a good correlation cannot be derived from highly variable set of condition data. The deterministic models predict the condition of the structures deterministically by ignoring the possible random errors. They have several other limitations which have been well reviewed by Agrawal and Kawaguchi (2009).

Among the AI-based techniques, case-based reasoning (CBR), fuzzy set theory and neural networks (NNs) have also been used for modelling the deterioration of

infrastructure. Makropoulos et al. (2003) used fuzzy set theory to determine deterioration of buried pipes. NNs were used to model deterioration of various infrastructure assets such as deterioration of sewers (Al-Barqawi and Zayed 2006), bridge deterioration (Cattan and Mohammadi 1997), and concrete structures (Kim et al. 2005). Although these AI-based approaches can automatically detect nonlinear underlying models, they have a demand for large quantities of data and they are less likely to have an underlying model describing the process, which can lead to overfitting (Edirisinghe et al. 2013).

Stochastic model is based on statistical theory for modelling phenomenon where there is high level of uncertainties in forecasting. The likelihood that the condition of an infrastructure changes from one state to another is probabilistic in nature because the infrastructure deterioration cannot be predicted with certainty. These uncertainties arise from different sources such as: uncertainties in material properties, structural dimensions, loads, and environmental conditions. Representation of real infrastructure (or their component) by idealized analytical (or numerical models) is another source of uncertainty. Additionally, uncertainties can also arise from inspection data as a result of inaccuracy of inspection technique and limited numbers of observation and samples (Val et al. 2000). Hence, because of the uncertainties about deterioration process and pertinent causes and also due to the presence of measurement errors, decision related to deterioration of infrastructures is full of uncertainties. Therefore decision related to deterioration of infrastructure facilities should be based on stochastic modelling.

The existing stochastic models of deterioration can be divided into 1) state-based and 2) time-based models. Example of state-based stochastic deterioration model is the

Markov chains model. In this model the deterioration process is modelled through a probability of transition from one condition state to another in discrete time, given that the deterioration process is dependent on set of explanatory variables such as: exposure condition (Saydam et al. 2013). A Markovian process is considered to be the most used deterioration model, which has been extensively used in existing bridge management system such as PONTIS and RIDGIT. Although the Markov chain has been widely used to model the deterioration of various infrastructure assets, the process has been widely criticized because of its restrictive stationary assumptions about the time dependent deterioration rate (Frangopol et al. 2001) and time-dependent stochastic process is considered as more appropriate method for deterioration modelling of civil engineering infrastructures (Van Noortwijk 2009). In these time-dependent statistical models, the average rate of deterioration per unit time is defined as random variables under stochastic process such as gamma process.

As deterioration is generally uncertain and non-decreasing with time, it can best be regarded as a gamma process (Abdel-Hameed 1975), which gives an appropriate model for random deterioration with time. To the best of authors' knowledge, Abdel-Hameed (1975) was the first to propose the gamma process as a proper model for deterioration occurring random in time and called this stochastic process as "gamma wear process". The gamma process is a stochastic process with independent, non-negative increments having a gamma distribution with identical scale parameter and a time-dependent shape parameter. More details about the mathematical aspects of gamma processes and its application in deterioration modelling can be found in literatures such as Neves and Frangopol (2005), Van Noortwijk (2009).

A stochastic process model, such as gamma process, incorporates the temporal uncertainty associated with the evolution of deterioration (Chen and Alani 2013, Chen and Alani 2012, Van Noortwijk 2009). The gamma process is therefore, suitable to model gradual damage monotonically accumulating over time, such as corrosion, crack growth etc. An advantage of modelling deterioration processes through gamma processes is that the required mathematical calculations are relatively straightforward.

### *2.6.2 Definition of limit states*

In structural reliability analysis, the first step is to define the desired/required performance of the structure. The client or the owner of the structure is asked to define the required target service life and the event that identifies the end of service life. Performance of the structure is its combined short term and long term fulfilment of the functional requirements which includes safety, serviceability and appearance of the structure during the service life. In performance based design, these functional requirements are defined as the limit states.

According to DuraCrete (2000), a limit state can be defined as the border that separates desired states from the undesired or adverse states in situations, acceptable to the owner, which a structure may be subjected to during its lifetime. Hence a limit state is a boundary between desired and undesired performance of a structure. In the context of structural reliability analysis, the concept of a limit state is used to define failure state, expressed here as

$$\begin{aligned}
g(X) > 0 &: \text{Safe} \\
g(X) = 0 &: \text{Limit state} \\
g(X) < 0 &: \text{Failure}
\end{aligned}
\tag{2.9}$$

where  $g(X)$  is the limit state function. The undesired performance could occur by many modes of failure. Therefore, acceptable target limits or desired performance levels have to be set for the reliability assessment of the structures. In reliability analysis, two types of limit states are commonly defined as:

- \* Serviceability limit states (SLS), defined as the limit between the state where the performance of the structure is acceptable and the state where the structure is no longer serviceable. Examples of SLS are the onset of corrosion, deflection, crack widths, spalling, vibrations, aesthetics, etc.
- \* Ultimate limit state (ULS), defined as the limit between the state where the structure is no longer serviceable and the state where the structure has collapsed. Examples of ULS are collapse, buckling, and loss of stability of the structure.

The effects of corrosion mentioned in earlier sections shows that it ultimately changes the performances of the structure at ultimate limit state (ULS) by reducing its load carrying capacity and more often effect on the serviceability limit by cracking, spalling, rust staining. A number of limit states have been proposed to define critical points (limit states) in the deterioration of a structure (Val 2005, Liu and Frangopol 2005). Those proposed limit states include initiation of corrosion, initiation of longitudinal cracking, a limiting longitudinal crack width, loss of steel section to a defined level, and loss of structural strength. Clearly, different acceptance criteria will result in different times for the structure to be unserviceable and unsafe. Definition of limit states of

degradation for corrosion is hence a complex procedure and is the risk involved in decision making.

### *2.6.3 Theory of reliability analysis*

Over the past decades, reliability theory is extensively researched topic in the field of lifecycle management of civil engineering infrastructures. It is considered as the effective tool in service life modelling of the deteriorating concrete structure. Furthermore, reliability methods are also regarded as the noble tools in repair and maintenance of these deteriorating structures. Reliability analysis of a structure or a system can also be used at the conceptual design stage to evaluate various design choices and to determine the impact that their implementation would have upon the service lives. In this section some basic aspects of structural reliability are introduced with reference to Melchers (1999). Detailed description about the structural reliability theory can be found in textbooks such as Thoft-Christensen and Baker (1982), Ang and Tang (1984), Nowak and Collins (2012).

In the most general sense, the reliability of a structure is its ability to perform its intended function for a specified interval of time under specified conditions. The structural reliability is often characterized by safety, serviceability, and durability. The lack of reliability represents the probability of failure. In a mathematical sense it is the probability that a structure will not attain each specified limit state (ultimate or serviceability) during a specified reference period. Mathematically reliability of a structure or a component is defined as its probability of survival, defined here as

$$P_s = 1 - P_f \quad (2.10)$$

where  $P_s$  is the probability of survival and  $P_f$  is the Probability of failure. “Failure” in the reliability analysis not only means structural failure, e.g. collapse, but in most cases it refers to a situation when the performance of the structure exceeds a predefined limits. For example: initiation of rebar corrosion is called a failure in that limit state when the chloride content at the concrete cover depth exceeds a critical value. In general, the probability of failure of the structure or a component is defined as

$$P_f = P_r [R \leq S] \quad (2.11)$$

where  $R$  and  $S$  represents the resistance and the load respectively. Depending upon how  $R$  and  $S$  are related to the time, the failure probability can also be defined with respect to time. In every structure both  $R$  and  $S$  changes with time, thus the reliability of such a structure also varies with time. Nevertheless, often both resistance and loading are characterized as time-independent variables for a certain time span, e.g. one year, 10 years. These problems are solved by means of time-independent reliability analysis, in which the safety of a structure is estimated for a certain instant of time but it is valid for the period of time assumed in the characterization of the variables. On the other hand, some reliability problems may require considering that either the resistance or loading effects or both to be modelled as time-dependent variables. Such cases are regarded as time-variant reliability problems.

One approach to predict the structure’s reliability or its service life under future performance conditions is through probability-based techniques involving time

dependent reliability analyses. By using these techniques, a quantitative measure of structural reliability is provided to integrate information on design requirements, material and structural degradation, damage accumulation, environmental factors, and non-destructive evaluation technology. The technique can also investigate the role of in-service inspection and maintenance strategies in enhancing reliability and extending service life. The resistance  $R(t)$  of a structure and the applied loads  $S(t)$ , both are stochastic functions of time. At any time  $t$ , the limit state  $G(t)$  can be defined as

$$G(t) = R(t) - S(t) \quad (2.12)$$

And the probability of failure is given by

$$P_f(t) = P_r [R(t) \leq S(t)] = P_r [G(t) \leq 0] \quad (2.13)$$

According to equation (2.13), the probability of failure increases continuously with time (Melchers 1999). Considering continuous distributions, the failure probability  $P_f$  at a certain moment of time can be determined by using the convolution integral (Melchers, 1999)

$$P_f(t) = P_r [G(t) \leq 0] = \int_0^{\infty} F_R(s, t) f_s(s, t) ds \quad (2.14)$$

in which  $F_R(s, t)$  is the cumulative distribution function of  $G(t)$ ,  $f_s(s, t)$  is the probability density function of  $S(t)$  and  $s$  is the common quantity or measure of  $R$  and  $S$ . Generally, it is represented by the amount of overlap of the probability density

functions  $f_R$  and  $f_S$  as shown in Figure 2.13. Since this overlap may vary with time,  $P_f$  may also be a function of time.

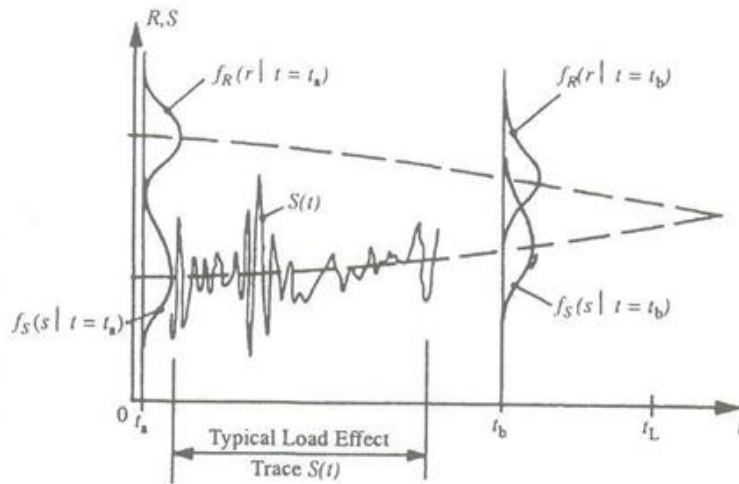


**Figure 2.13** Schematic representation of time-dependent reliability problem (*from Melchers 1999*)

In time-dependent reliability analysis, the quantity of interest is not the instantaneous probability of failure, but rather the probability of failure over an interval of time  $[0, t_L]$ , where  $t_L$  may represent the lifetime or service life of the structure. The determination of this probability of failure is not a straightforward task. This probability of failure can be obtained by integrating the above instantaneous probability of failure over the interval  $[0, t_L]$ . In practice, the probability of failure with respect to the occurrence of each possible failure mode can be analysed using various reliability analysis procedures, including FORM, SORM and Monte Carlo Simulations. A detailed discussion on these methods of reliability analysis is beyond the scope of this thesis. Detailed discussion of these methods can be found in Melchers (1999). Recently stochastic gamma process has also been employed for time-dependent reliability

analysis of deterioration structures subject to monotonic degradation process (Van Noortwijk 2003, Van Noortwijk 2009, Chen and Alani 2012, Chen and Alani 2013, Edirisinghe et al. 2013).

#### *2.6.4 Background on maintenance interventions*

Maintenance can be defined as a set of activities that are carried out to retain the structure in or restore it to a state in which it can perform its required function (Van Noortwijk 2003). It also refers to the operations performed to keep the structure in an acceptable performance level from both serviceability and a safety point of view. Inspections, repairs and replacements are the possible maintenance actions. In lifecycle maintenance of structure, there are basically two types of maintenance strategies:

- \* Corrective maintenance
- \* Preventive maintenance

In corrective maintenance repair is done after failure (or required serviceability level or safety level is exceeded) has occurred so as to restore the structure into the required level. It aims to return the element to functional state, either by repairing or replacing action. Preventive maintenance is carried out at predetermined intervals or corresponding to prescribed criteria, and intended to reduce the probability of failure or the performance degradation (Frangopol et al. 2000a, Mullard and Stewart 2012, Van Noortwijk 2003). For highway bridges, some preventive maintenance currently in practice include cathodic protection, saline treatment, painting of steelwork, and

concrete patch repairs. A schematic representation of corrective and preventive maintenance and its effect in lifecycle cost analysis is shown in Figure 2.14.

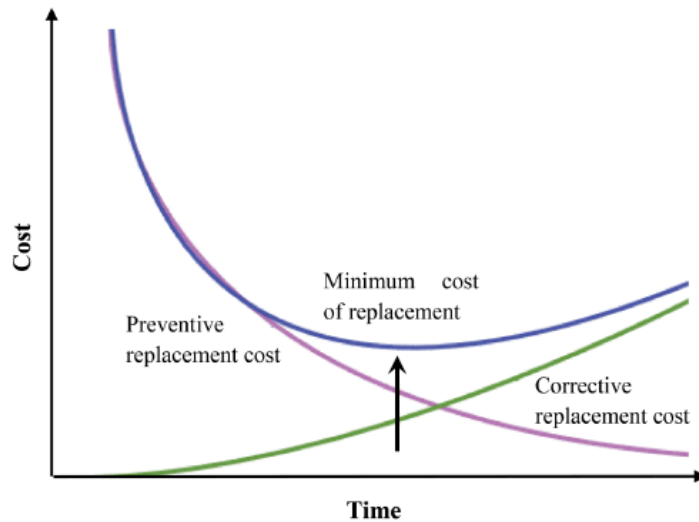


**Figure 2.14** Schematic representation of lifecycle cost and its components

The main objective of the lifecycle cost management is to find the optimum time of repair by balancing risk and cost associated with a failure. In order to make optimal maintenance decision of deteriorating civil infrastructures there are two maintenance models available (Van Noortwijk and Frangopol 2004):

- \* Condition-based maintenance model
- \* Reliability-based maintenance model

Condition-based maintenance model (Rijkswaterstaat's model) has been applied for justification and optimisation of maintenance measures by the Netherlands Ministry of Transport, Public Works and Water Management (Van Noortwijk 1998). Reliability-based maintenance model (Frangopol's model) contributed to the further development

of the bridge management methodology that has been set up by the UK Highways Agency (Frangopol 2003). In general, although both models can be applied to determine the best maintenance strategy to ensure an adequate level of reliability at minimal lifecycle cost, they have slight differences in terms of their application. Basically in reliability-based model, maintenance decision is made with respect to predefined target reliability index while in condition based model, maintenance decision is made with respect to predefined condition states. Another difference is that Frangopol's model uses Monte Carlo simulations, whereas Rijkswaterstaat's model uses analytical method for the evaluation of probability of failure. Hence, Rijkswaterstaat's model avoids the complexities in evaluation of structural reliability. More information on these maintenance models can be found in Van Noortwijk and Frangopol (2004).

#### *2.6.5 Existing investigations on lifecycle management*

In the past decades, many studies have been carried out in the time-dependent reliability of corrosion damaged RC structure. The methodology developed by Ellingwood and Mori (1993) was one of the first attempts to assess time dependent reliability of aging structures considering both the randomness of resistance and the stochastic nature of load defined by Poissons' model. They proposed an adoptive Monte Carlo simulation procedure to evaluate time-dependent system reliability. Their methodology was further used by Ellingwood and Mori (1997) to evaluate the optimized maintenance measures for aging structures and also have been used in many studies for assessing either remaining service life of deteriorating concrete bridges or time-dependent reliability of ageing concrete structures (Enright and Frangopol 1998a,

Enright and Frangopol 1998b, Hong 2000, Mori and Ellingwood 2006). The aforementioned reliability studies mainly concentrated on the evaluation of time-dependent flexural strength of the corrosion degraded RC structural members. Very few efforts have been made in the past for the evaluation of time- dependent bond strength and shear strength analysis of corrosion degraded RC structural members (Thoft-Christensen 1998, Val et al. 1998, Vu and Stewart 2000).

Val (2005) examined the effect of corrosion of reinforcing steel on flexural and shear strength, and subsequently on reliability, of reinforced concrete beams. Suo and Stewart (2009) used a time-dependent reliability analysis combined with visual inspection data to predict the likelihood and extent of corrosion-induced cracking in RC structures. Bhargava et al. (2011a, b) presented a time-dependent reliability of corrosion affected RC beam in terms of two limit states: (a) flexural failure, and (b) shear failure. However, in most of these earlier reliability studies probabilities of failure were evaluated by using Monte Carlo Simulations. The major disadvantage of Monte Carlo Simulation is its computational intensiveness. Furthermore, the strength degradation due to reinforcement corrosion was only considered as function of sectional loss of the rebar.

Frangopol (1997, 1999) developed the basis for lifetime reliability analysis and a whole lifecycle cost analysis of corrosion damaged concrete structure. Frangopol and Das (1999) defined bridge reliability states and proposed a reliability-based maintenance approach for bridges. Later, Frangopol et al. (2000a, b) further presented realistic examples of optimum bridge maintenance planning based on minimum expected costs. Kong and Frangopol (2003) studied lifecycle cost optimization of highway bridges with

or without preventive maintenance using Monte Carlo simulations. Similar approach of lifecycle cost analysis of corroded RC structures considering different limit states can also be found in literatures (Val and Stewart 2003, Val 2005, Yang et al. 2006, Ehlen et al. 2009, Mullard and Stewart, 2012).

Recently, Edirisinghe et al. (2013) used condition-based maintenance model to evaluate the optimal repair time of the deteriorating building. Chen and Alani (2013) studied the optimal repair strategy for corrosion damaged RC structure by using condition-based maintenance model based on concrete cover cracking. However, up to author's knowledge till now no effort has been made to study the lifecycle management of corrosion damaged RC structures with consideration of realistic behaviour of damages caused by reinforcement corrosion in both ultimate and serviceability limit states.

## **2.7 Summary and conclusions**

In this chapter, an overview of the effect of reinforcement corrosion on the structural behaviour of RC structure is presented. From the review of existing studies following conclusions are drawn:

- \* Performance deterioration of corrosion damaged RC structures mainly depends on the loss of rebar area, cracking in concrete cover and bond strength degradation between rebar and surrounding concrete. Bond strength loss at steel-concrete interface can lead to significant reduction in the residual load carrying capacity.

- \* Only few investigations have been carried out in corrosion propagation and even less in the residual strength of the corroded RC structure. Additionally, theoretical studies on the prediction of crack development in concrete due to reinforcement corrosion are limited, with specific reference to realistic concrete properties.
  
- \* Although few attempts have been made using analytical approach but there is still a need of reliable model which considers the critical mechanical factors affecting the residual strength of corroded RC structures. Research on life cycle performance of corroded RC structures associated with serviceability (i.e. concrete cover cracking) and ultimate (i.e. bond strength and flexural strength) limit states considering the realistic behaviour of corrosion induced damages is very limited.
  
- \* In lifecycle performance assessment, implication of the gamma process on time-dependent reliability analysis is less studied. Furthermore, condition-based maintenance model to investigate the optimal repair strategy of corrosion damaged RC structure with consideration of realistic behaviour of damages caused by reinforcement corrosion is not yet studied.

## **Chapter 3 Development of Corrosion Induced Cracking Model**

### **3.1 Introduction**

Corrosion induced cracking of the concrete cover is the most serious effect caused by corrosion of reinforcement in RC structures. Usually, corrosion- induced concrete cover cracking, which affects the normal performance of a RC structure, appears before corrosion has any significant influence on the strength of the structure (Chernin et al. 2010, Vidal et al. 2004, Alonso et al. 1998). At the same time, appearance of corrosion induced cracks on the surface of a RC structure is the main visual indicator of the corrosion presence in the structure (Chernin et al. 2012, Saether 2011). Thus for effective performance assessment of the existing RC structures, it is important to investigate under which conditions such cracks are formed and how they propagate with the progress of corrosion. Furthermore, it is necessary and beneficial to predict the internal damages such as residual strength deterioration from the observable surface condition (i.e. cover surface cracking).

A comprehensive review of the most recent research literature in Chapter 2 has shown that, although considerable investigations have been carried out during the last decades regarding crack initiation relatively less studies have been carried out in the crack propagation and residual life phase. Few studies have also been undertaken regarding the influence of reinforcement corrosion and concrete cracking on the reliability of RC structures. However, limited works has been carried out on the theoretical investigations of corrosion induced cover cracking process by considering realistic concrete material properties such as tensile softening behaviour of cracked concrete.

This chapter presents a simple and realistic analytical model of evolution of cover cracking due to reinforcement corrosion by using fracture mechanics considering the critical mechanical factors such as residual tensile strength, reduced tensile stiffness and radial pressure at bond interface. Concrete cover is assumed as a thick walled cylinder with axis-symmetrical displacement caused by uniform internal pressure exerted by the expansive corrosion products. Furthermore, the effect of volume increase of corrosion product on confinement of concrete cover is assumed to be negligible. During the analysis of stress distribution in concrete, both elastic and fracture mechanics are employed as appropriate. The cracked concrete is considered as anisotropic material and its residual strength is determined by adopting realistic bilinear tension softening law of cracked concrete. Crack width at the different location of concrete cover are evaluated for different phases of cracking by considering expansive corrosion pressure, radial and hoop stress corresponding to corrosion level. A programme in MatLab is developed to execute all the computations. The method proposed in this study is then demonstrated by numerical examples. Corrosion induced crack formation and its propagation in corrosion damage RC structures with respect to weight loss of the rebar is predicted.

The analytical results of cover surface cracking are examined by the experimental data available. Then the effect of concrete geometry on the formation of longitudinal crack width is discussed. The merit of the proposed approach is that this methodology provides a fundamental framework for the effective condition assessment of corrosion damaged RC structures.

### 3.2 Structural deterioration

The effect of corrosion on the performance deterioration of corroded RC structures during their whole lifetime is illustrated in Figure 3.1 (Chen and Nepal 2015b). Three phases are considered in the process i.e. crack initiation phase, crack propagation phase and residual life phase. The crack initiation phase starts from the time of construction and ends at the time when the corrosion induced cracking initiates at the interface between the steel rebar and the concrete cover. After cracking occurs at the cover surface, the bond strength between the steel reinforcement and the surrounding concrete starts decreasing and the performance of the concrete structures deteriorates gradually. Due to further corrosion of steel rebar, cracking propagates and widens in the concrete cover and then reaches an unacceptable level. At this stage, the structures reach their serviceability limit state. The residual phase starts from the serviceability limit until reaching the ultimate limit state, after which structures finally reach the stage of collapse.

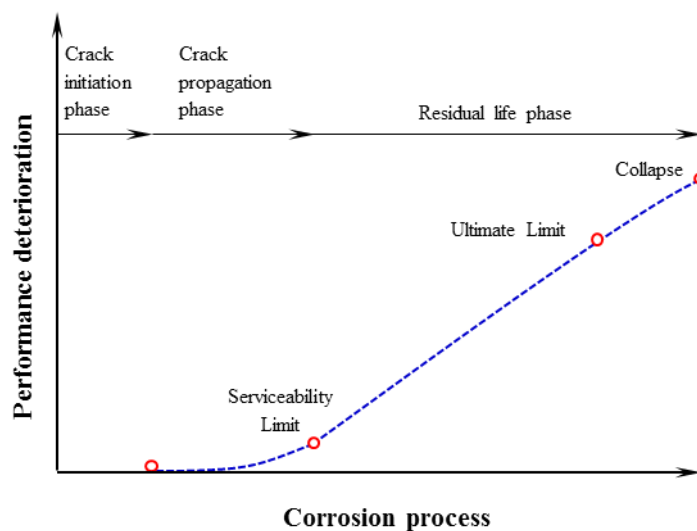


**Figure 3.1** Schematic representation of performance deterioration due to reinforcement corrosion in lifecycle of RC structures

As mentioned in Figure 3.1, crack propagation and residual life phases plays the significant role in lifecycle performance of any RC structures exposed to aggressive environment. For the time-dependent reliability analysis of these structures, quantification of the damages associated with the propagation of the reinforcement corrosion is required. The main types of damages associated with reinforcement corrosion are: i) loss of cross-sectional area of the rebar, ii) cracking in the concrete cover and iii) loss of residual strength of the structure.

To measure the damages in servicing structures, only crack width may be measured without disturbing the functionality of the structure but for other types of damages destructive examination is required and this is practically impossible. Therefore, for the structures in service, non-destructive examination is required. Most of the non-destructive techniques used for the monitoring and evaluation of damages caused by corrosion are basically based on the electrochemical measurements where the annual mean corrosion rate is estimated in terms of the corrosion current density  $i_{corr}$  (Val et al. 1998). The estimated  $i_{corr}$  can then be transformed into the loss of metal by using the diffusion law related to the growth of expansive corrosion products as discussed in Chapter 2. Reduction in cross-sectional area of steel rebar at any time can help in quantifying the existing residual strength and predicting the future performance of the corrosion-damaged RC structures. In this chapter analytical formulations for the evaluation of sectional loss of the rebar and associated crack growth in the concrete cover surface are presented.

### 3.3 Determination of sectional loss of rebar and corrosion induced expansion

In general, loss in rebar cross section is represented by the mass loss or the cross sectional area loss of the rebar. Therefore, the reduced diameter of the rebar  $D_{bx}$  from its original dimension  $D_b$  can be estimated in terms of attack penetration  $x$  (pitting or homogeneous corrosion), as utilised by Vidal et al. (2004), expressed here as

$$D_{bx} = D_b - \alpha_p x \quad (3.1)$$

where  $\alpha_p$  is an attack penetration factor as defined in Chapter 2.  $\alpha_p$  indicates the localised corrosion at the earlier stage when  $4 < \alpha_p < 8$  and homogeneous corrosion at later stage when  $\alpha_p = 2$ . Hence, the corresponding corrosion level  $X_p$  is defined as the ratio of the mass loss of the corroded rebar  $\Delta M_s$  to the original mass of the rebar  $M_o$ , namely

$$X_p = \frac{\Delta M_s}{M_o} = \frac{\Delta A_b}{A_b} = 1 - \frac{D_{bx}^2}{D_b^2} \quad (3.2)$$

where  $\Delta A_b$  is the cross-sectional area loss of the corroded rebar and  $A_b$  is the cross-sectional area of the original rebar. The mass of the rust products formed during corrosion process  $M_r$  can be defined as  $M_r = \Delta M_s / \gamma_{mol}$  and can be obtained from equation (2.7). The corresponding density of the rust products can be determined from  $\rho_r = \rho_s / \gamma_{mol} \gamma_{vol}$ , in which  $\rho_s$  is the density of the steel taken as  $\rho_s = 7850 \text{ kg/m}^3$  (Pantazopoulou and Papoulia 2001, Bhargava et al. 2006).  $\gamma_{mol}$  is the corresponding

molecular weight and  $\gamma_{vol}$  is the volume ratio of the corrosion products to its parent metal as given in Table 2.1 of Chapter 2. In many theoretical model,  $\gamma_{vol}$  is usually taken between 2 and 4 (Wang and Liu 2004, Bhargava et al. 2006, Pantazopoulou and Papoulia 2001, Papakonstantinou and Shinozuka, 2013). From equation (3.2), the volume of the rust products  $V_r$  is calculated from  $V_r = \gamma_{vol} A_b X_p$ . The corresponding volume increase per unit length of the rebar is given by  $\Delta V = V_r - \Delta V_s$ , in which  $\Delta V_s$  is the volume loss of the corroded rebar. This increase in volume creates a radial displacement at the bond interface  $u_{bx}$ , and can be obtained from

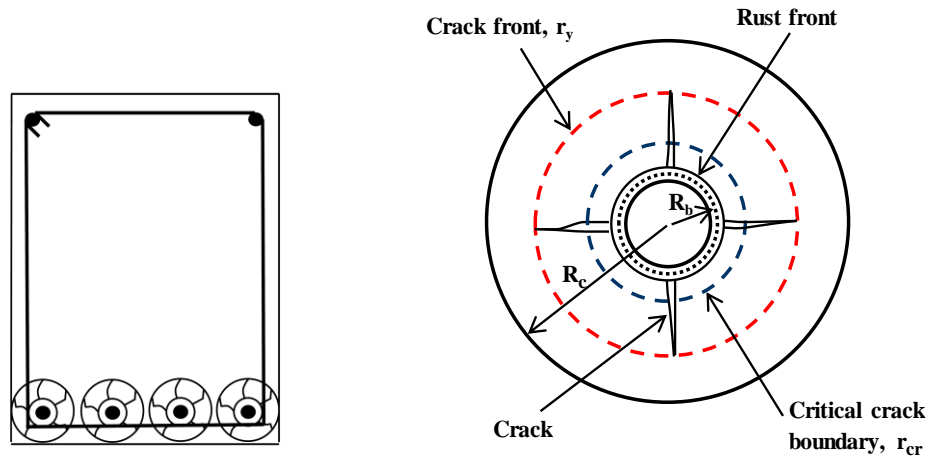
$$u_{bx} = \frac{\Delta V}{\pi D_b} = \frac{1}{4} (\gamma_{vol} - 1) D_b X_p \quad (3.3)$$

The prescribed displacement  $u_{bx}$  related to corrosion level  $X_p$  will be considered as the boundary condition of the boundary-value problem for analysing concrete cracking development in this chapter and predicting bond strength evolution in Chapter 4. It is assumed here that uniform displacements are exerted around the bond interface to simplify the calculations, although reinforcement corrosion may start from the places close to the free surfaces of the concrete cover and thus the steel rebar may not corrode uniformly around the rebar surface at the beginning of natural corrosion (Xia et al. 2012). However, as pitting corrosion progresses, it appears as uniform corrosion in the later stage, as demonstrated in the long-term natural corrosion experimental studies by Zhang et al. (2010). The assumption for uniform expansive pressure at the bond interface is reasonable, as shown in many studies such as Balafas and Burgoyne (2011),

Bhargava et al. (2006, 2007), Chen and Xiao (2012), Chernin et al. (2010) and Zhong et al. (2010).

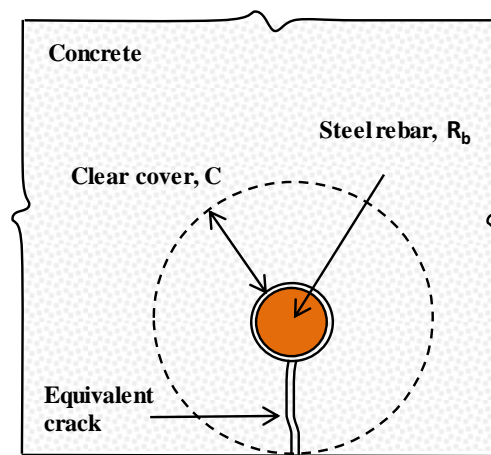
### 3.4 Modelling cover concrete as thick-walled cylinder model

In order to analyse concrete cover cracking process due to reinforcement corrosion, the thick-walled cylinder model as discussed in the Chapter 2 which has been widely utilised in many studies (Bhargava et al. 2007, Chen and Alani 2013, Wang and Liu 2004, Pantazopoulou and Papoulia 2001, Liu and Weyers 1998) is considered in this study. The schematic representation of thick walled cylinder model is shown in Figure 3.2. In the thick walled cylinder model for cover concrete cracking induced by reinforcement corrosion, the steel rebar has an initial radius  $R_b$ , embedded in the concrete with clear cover thickness  $C$ , as shown in Figure 3.2. This model can be considered as an axis-symmetrical problem subject to the assumed uniform expansion of corrosion at bond interface. Due to the expansive displacement applied around the bond surface, the hoop stress in the thick-walled cylinder is typically a principle tensile stress whereas the radial stress is a principle compressive stress. When the hoop stress reaches the tensile strength of concrete, the radial splitting cracks propagate from the bond interface ( $R_b = D_b / 2$ ) towards the free surface of concrete cover ( $R_c = C + D_b / 2$ ), as indicated in Figure 3.2(b). Existing experimental studies shows that although at early stage of crack propagation several cracks appear in the concrete cover, by the end of the test there is single crack that finally breaks the cover on the weakest side of the concrete cover (Balafas and Burgoyne 2010). Hence in experimental studies the concept of equivalent crack width is frequently used to define cover surface crack width. In this study, the concept of equivalent crack width as



(a) Reinforced bar and the surrounding concrete

(b) Crack propagation from bond interface to concrete cover surface



(c) Thick-walled cylinder with equivalent crack

**Figure 3.2** Idealisation of cover concrete as thick-walled cylinder model for predicting concrete crack development and residual bond strength evolution (Note: figures not drawn to scale)

defined by Vidal et al (2004) and previously utilised in many literatures (Molina et al. 1993, Coronelli 2002, Chen and Alani 2013, Wang and Liu 2004), as shown in Figure 3.2 (c) is also considered. During the analysis of cover cracking process, it is essential to analyse the stress (and strain) distribution in the concrete cylinder. It is therefore

analysed by using both elastic mechanics (Timoshenko and Goodier 1970) and fracture mechanics (Bazant and Planas 1998), wherever appropriate.

### 3.5 Modelling cracked concrete as cohesive crack model

As discussed earlier in the literatures review, a common limitation of the most existing analytical models for cover concrete cracking is in consideration of anisotropic properties of cracked concrete with representation of realistic tensile softening behavior of cracked concrete. Hence in order to consider the anisotropic properties of cracked concrete, fracture mechanics based on cohesive crack model is utilized.

Concrete cracking could be modelled as a process of tension softening if the cracking is considered as cohesive and the crack width does not exceed a limited value (Bazant and Planas 1998, Jirasek and Bazant 2001). In the cohesive crack model, the stress transferred through the cohesive cracks is assumed to be a function of crack opening (softening curve). In this study, the bilinear softening curve, described in CEB-FIP (1990) and shown in Figure 3.3, is adopted, since this curve gives reasonable approximations for cracked concrete in tension, expressed here as

$$\sigma_{\theta} = \sigma_w = f_t(a - bW) \quad (3.4)$$

where  $\sigma_w$  is the residual tensile stress acting across cohesive cracks,  $f_t$  is the maximum tensile strength of concrete at onset of cracking,  $W$  is the normalized crack width defined as  $W = f_t w(r) / G_F$  in which  $G_F$  is the fracture energy of the concrete which depends on maximum aggregate size and strength of concrete.

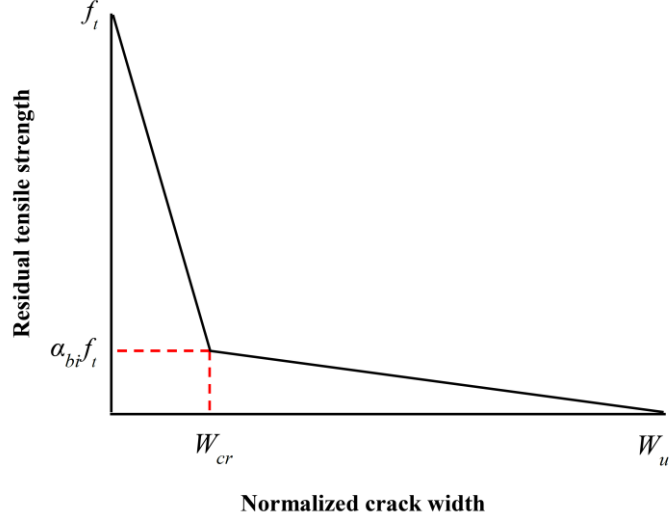


**Figure 3.3** Bilinear tension softening curve for cohesive cracking in the concrete around the rebar

The value of  $G_F$  is adopted between 180 to 200 N/m in this thesis.  $w(r)$  is the actual crack width at any point  $r$  between  $R_b$  and  $R_c$ . Coefficients  $a$  and  $b$  are the bilinear coefficients, depending on the pre-critical stage ( $0 \leq W \leq W_{cr}$ ) and post-critical stage ( $W_{cr} \leq W \leq W_u$ ) of crack width, defined as

$$a = a^{cr} = 1 \quad ; \quad b = b^{cr} = \frac{1 - \alpha_{bi}}{W_{cr}} \quad \text{for pre-critical cracking stage} \quad (3.5a)$$

$$a = a^u = \frac{\alpha_{bi} W_u}{W_u - W_{cr}} \quad ; \quad b = b^u = \frac{\alpha_{bi}}{W_u - W_{cr}} \quad \text{for post-critical cracking stage} \quad (3.5b)$$

in which  $\alpha_{bi}$  is coefficient of bilinear softening curve,  $W_{cr}$  (associated with actual critical crack width  $w_{cr}$ ) and  $W_u$  (associated with actual ultimate cohesive crack width  $w_u$ ) are normalized critical and ultimate crack widths respectively, which can be

determined from experiments for concrete. In the CEB-FIP (1990), the coefficient  $\alpha_{bi}$  is given as  $\alpha_{bi} = 0.15$ ,  $W_{cr}$  and  $W_u$  can be evaluated from concrete strength, fracture energy and maximum aggregate size  $D_a$ .

### 3.6 Mathematical formulations for isotropic thick-walled cylinder

Intact concrete in the thick walled cylinder, can be treated as isotropic elastic material subject to axis-symmetrical actions (Bhargava et al. 2006, Pantazopoulou and Papoulia 2001, Chen and Alani 2013). Hence, the governing equations suggested by Timoshenko and Goodier (1970) can be used for the axis symmetric displacement  $u$ , radial stress  $\sigma_r$  and hoop stress  $\sigma_\theta$  at any point  $r$  between rebar surface  $R_b$  and concrete cover surface  $R_c$ .

$$u = K_1 r + K_2 \frac{1}{r} \quad (3.6)$$

$$\sigma_r = \frac{E}{1-\nu} K_1 - \frac{E}{1+\nu} K_2 \frac{1}{r^2} \quad (3.7a)$$

$$\sigma_\theta = \frac{E}{1-\nu} K_1 + \frac{E}{1+\nu} K_2 \frac{1}{r^2} \quad (3.7b)$$

Where  $E$  is the effective modulus of elasticity of concrete, defined as  $E = E_c / (1 + \theta_c)$ , in which  $E_c$  is modulus of elasticity and  $\theta_c$  is creep coefficient of concrete,  $\nu$  is the Poisson's ratio of intact concrete. In this study  $\theta_c = 2.0$  and  $\nu = 0.18$

as previously used in many studies (Wang and Liu 2004, Bhargava et al. 2006, Pantazopoulou and Papoulia 2001, Papakonstantinou and Shinozuka 2013, Chernin et al. 2010) are adopted. As defined earlier,  $u$  is the radial displacement related to hoop strain  $\varepsilon_\theta$  and radial strain  $\varepsilon_r$ ,  $\varepsilon_\theta$  is defined as  $\varepsilon_\theta = \frac{u}{r}$  and  $\varepsilon_r$  is the first derivative of hoop strain defined as  $\varepsilon_r = \frac{du}{dr}$ .  $K_1$  and  $K_2$  are the coefficients determined by using two boundary conditions i.e. displacement at the internal boundary  $u_r|_{r=R_b} = u_b$  and free surface condition at the concrete cover surface i.e. radial pressure  $\sigma_r|_{r=R_c} = 0$ .

### 3.7 Mathematical formulations for anisotropic thick-walled cylinder

When cracking exists in the cover concrete, the total hoop strain  $\varepsilon_\theta$  of the cracked concrete consists of fracture strain  $\varepsilon_\theta^f$  and linear elastic strain between cracks  $\varepsilon_\theta^e$  (Chen and Alani 2013). The fracture strain is generated by a total number of  $n_c$  cracks, defined as  $n_c = 2\pi R_c / L_c$  in which  $L_c$  is minimum admissible crack band width estimated from  $L_c \approx 3D_a$  where  $D_a$  is maximum aggregate size of concrete (Bazant and Planas 1998). According to the experimental data available in Nielsen and Bicanic (2002), the typical value of total crack number in thick-walled cylinder model for cover cracking is approximately three or four. Therefore in this study total four numbers of cracks are considered for the analysis as previously utilized by Chen and Alani (2013). The linear elastic strain between cracks is associated with the residual tensile hoop stress  $\sigma_\theta = \sigma_w$ , defined, respectively, as

$$\varepsilon_{\theta}^f = \frac{n_c w(r)}{2\pi r} = bl_o \frac{f_t}{E} \frac{W}{r} \quad (3.8a)$$

$$\varepsilon_{\theta}^e = \frac{\sigma_{\theta}}{E} = \frac{f_t}{E} (a - bW) \quad (3.8b)$$

Where  $l_o$  is material coefficient defined as  $l_o = n_c l_{ch} / (2\pi b)$  in which  $l_{ch}$  is characteristic length  $l_{ch} = EG_F / f_t^2$  defined in Bazant and Planas (1998). The total hoop strain  $\varepsilon_{\theta}$  of the cracked concrete is then given by

$$\varepsilon_{\theta} = \varepsilon_{\theta}^f + \varepsilon_{\theta}^e = \frac{f_t}{E} \left[ (a - bW) + bl_o \frac{W}{r} \right] \quad (3.9)$$

The radial displacement  $u$  of the cracked cover concrete for the axis-symmetrical problem is therefore calculated from

$$u = \varepsilon_{\theta} r = \frac{f_t}{E} [(a - bW)r + bl_o W] \quad (3.10)$$

For the cracked cover concrete modelled as axis-symmetrical elastic continuum, the governing equation for the thick-walled cylinder is given in Pantazopoulou and Papoulia (2001) as

$$\frac{d^2 u}{dr^2} + \frac{1}{r} \frac{du}{dr} - \beta \frac{u}{r^2} = 0 \quad (3.11)$$

$$\sigma_r = \frac{E}{1 - \nu^2} (\varepsilon_r + \nu \sqrt{\beta} \varepsilon_{\theta}) \quad (3.12a)$$

$$\sigma_{\theta} = \frac{1}{1-\nu^2} [\nu\sqrt{\beta} \varepsilon_r + \beta\varepsilon_{\theta}] \quad (3.12b)$$

where  $\beta$  is the reduction factor of residual tensile stiffness defined as

$$\beta = \frac{E_{\theta}}{E} = \frac{\varepsilon_{\theta}^e}{\varepsilon_{\theta}^e + \varepsilon_{\theta}^f} = \frac{(a-bW)r}{(a-bW)r + bl_oW} \quad (3.13)$$

By utilising radial displacement  $u$  given in equation (3.10) and  $\beta$  given in equation (3.13), a new governing equation from equation (3.11) for directly solving the normalized crack width  $W$  is constructed as

$$(l_o - r) \frac{d^2W}{dr^2} + (l_o - 3r) \frac{1}{r} \frac{dW}{dr} = 0 \quad (3.14)$$

The general solution to the aforementioned second-order linear homogeneous differential equation is

$$W = C_1 \delta(l_o, r) + C_2 \quad (3.15)$$

where  $\delta(l_o, r) = \left[ \frac{1}{l_o(l_o - r)} - \frac{1}{l_o^2} \ln \left| \frac{l_o - r}{r} \right| \right]$ , constant coefficients  $C_1$  and  $C_2$  in the

general solution can be determined from two boundary conditions of the boundary-value problem, depending on the phase of crack development in the concrete cover.

After the normalized crack width  $W$  is obtained, the radial displacement  $u$  over the

thick-walled cylinder is calculated from equation (3.10). The radial strain over the cracked concrete is then given by

$$\varepsilon_r = \frac{du}{dr} = \frac{f_t}{E} \left[ (a - bW) + b(l_o - r) \frac{dW}{dr} \right] \quad (3.16)$$

The first derivative of normalized crack width  $W$  with respect to radial distance  $r$  is given as

$$\frac{dW}{dr} = C_1 \frac{1}{r(l_o - r^2)} \quad (3.17)$$

From the relationship between stress and strain with consideration of tensile stiffness reduction, the radial stress of the cracked concrete can be obtained from equation (3.12a), expressed here as

$$\sigma_r = \frac{E}{1-\nu^2} (\varepsilon_r + \nu\sqrt{\beta}\varepsilon_\theta) = \frac{f_t}{1-\nu^2} \left[ (1 + \nu\sqrt{\beta})(a - bW) + b(l_o - r) \frac{dW}{dr} + \nu\sqrt{\beta}bl_o \frac{W}{r} \right] \quad (3.18)$$

### 3.7.1 Crack initiation at bond interface

Before cracking, intact concrete can be treated as isotropic elastic materials, hence the governing equation and stress distributions for the thick-walled cylinder as mentioned section 3.3 are used for the axis-symmetrical elastic continuum problem. The displacement boundary condition at the bond interface ( $R_b$ ) and the free surface condition at concrete cover surface ( $R_c$ ) are described here as

$$u_r \Big|_{r=R_b} = u_{bx} \quad (3.19a)$$

$$\sigma_r \Big|_{r=R_c} = 0 \quad (3.19b)$$

where the prescribed displacement  $u_{bx}$  is related to corrosion level  $X_p$ , as given in equation (3.3). From the given boundary conditions, the radial and hoop stresses in the cover concrete are obtained from equations (3.7a) and (3.7b) as

$$\sigma_r = \frac{ER_b^2}{(1-\nu)R_b^2 + (1+\nu)R_c^2} \left( 1 - \frac{R_c^2}{r^2} \right) \frac{(\gamma_{vol} - 1)}{2} X_p \quad (3.20a)$$

$$\sigma_\theta = \frac{ER_b^2}{(1-\nu)R_b^2 + (1+\nu)R_c^2} \left( 1 + \frac{R_c^2}{r^2} \right) \frac{(\gamma_{vol} - 1)}{2} X_p \quad (3.20b)$$

It is found that the hoop stress is in tension whereas the radial stress is in compression over the concrete cover. The cover concrete initiates cracking when the hoop stress  $\sigma_\theta$  at the bond interface reaches the tensile strength  $f_t$ . From equation (3.20b), the corrosion level at the time when cracking initiates ( $X_p^I$ ) is estimated from

$$X_p^I = \frac{2}{(\gamma_{vol} - 1)} \frac{f_t}{E} \frac{(1-\nu) + (1+\nu)(1+2C/D_b)^2}{1+(1+2C/D_b)^2} \quad (3.21)$$

The equation (3.21) shows that the corrosion level for crack initiation at the bond interface largely depends on the rust volume expansion factor  $\gamma_{vol}$  and the ratio of

cover thickness to rebar diameter  $C/D_b$ . Normalised crack width at rebar surface corresponding to corrosion level  $X_p$  and the corresponding stiffness reduction factor can now be obtained from equation (3.10) and equation (3.13) respectively, given by

$$W_b = \frac{1}{b(l_o - R_b)} \left( \frac{E}{f_t} u_{bx} - aR_b \right) \quad (3.22a)$$

$$\beta_b = \frac{1}{1 + \left[ \frac{bl_o W_{bx}}{(a - bW_{bx}) R_b} \right]} \quad (3.22b)$$

### 3.7.2 Crack propagation through concrete cover

Once crack initiates at the rebar surface, it propagates towards the cover surface. Due to the bilinear tension softening of the cover concrete two cases are now considered, i.e. crack propagation before crack width at the bond interface reaches the critical value ( $W_b \leq W_{cr}$ ) and crack propagation when crack width at the bond surface exceeds the critical value ( $W_b > W_{cr}$ ).

#### **Case with $W_b \leq W_{cr}$**

Here, the thick-walled cylinder is divided into two zones, i.e. a cracked inner ring ( $R_b \leq r \leq r_y$ ) and an intact outer ring ( $r_y \leq r \leq R_c$ ) where  $r_y$  is the radius of crack front. At the crack front ( $r = r_y$ ) the crack width is zero and the tensile hoop stress reaches the concrete tensile strength  $f_t$ . The boundary conditions for this case are expressed as

$$u_r |_{r=R_b} = u_{bx}, \quad W |_{r=r_y} = 0 \quad \text{for } R_b \leq r \leq r_y \quad (3.23a)$$

$$\sigma_\theta |_{r=r_y} = f_t, \quad \sigma_r |_{r=R_c} = 0 \quad \text{for } r_y \leq r \leq R_c \quad (3.23b)$$

Defining a general crack width function associated with material coefficient  $l_o$  and radius  $r$  within the thick-walled cylinder

$$\delta(r_1, r_2) = \frac{r_1 - r_2}{l_o(l_o - r_1)(l_o - r_2)} + \frac{1}{l_o^2} \ln \frac{r_1 |l_o - r_2|}{r_2 |l_o - r_1|} \quad (3.24)$$

By utilising the boundary conditions and the general solution for the normalized crack width in equation (3.15), the normalized crack width over the cracked inner ring is given by

$$W = \frac{1}{(1 - \alpha_{bi})(l_o^{cr} - R_b)} \left( \frac{E}{f_t} u_{bx} - R_b \right) \frac{\delta^{cr}(r_y, r)}{\delta^{cr}(r_y, R_b)} W_{cr} \quad (3.25)$$

where superscript  $cr$  in material coefficient  $l_o$  and crack width function  $\delta$  indicates that the material coefficient  $l_o^{cr}$  is calculated by using the coefficients of bilinear tension softening curve for the pre-critical stage in equation (3.5a). The crack front ( $r_y$ ) can be determined by utilising the continuity condition of radial stress crossing the intact and cracked zones, where the obtained normalized crack width in equation (3.25) is considered.

When the crack front reaches the concrete cover surface ( $r_y = R_c$ ), the corresponding corrosion level at the time to crack on the concrete cover surface  $X_p^C$  is determined, from equation (3.25) and by using the normalized crack width at the bond interface, given by

$$X_p^C = \frac{2}{(\gamma_{vol} - 1)} \frac{f_t}{E} \left( 1 + (1 + \nu) \left( 1 + 2 \frac{C}{D_b} \right) \eta_x^{cr}(R_c, R_b) \right) \quad (3.26)$$

where coefficient  $\eta_x^{cr}(R_c, R_b)$  is determined by the general coefficient  $\eta_x(R_c, R_b) = (l_o - R_b)(l_o - R_c)\delta(R_c, R_b)$  by using  $l_o = l_o^{cr}$ . From equation (3.26), the corrosion level at the time when cracks reach the cover surface depends on the concrete properties, rust volume expansion factor  $\gamma_{vol}$  and the ratio of cover thickness to rebar diameter  $C/D_b$ .

**Case with  $W_b > W_{cr}$**

The thick-walled cylinder is now divided into three zones shown in Figure 3.2(b), a cracked inner ring where crack width exceeds critical value ( $R_b \leq r \leq r_{cr}$ ) where  $r_{cr}$  is radius of critical crack boundary, a cracked middle ring where crack width does not exceed critical value ( $r_{cr} \leq r \leq r_y$ ) and an intact outer ring ( $r_y \leq r \leq R_c$ ). In this case, the boundary conditions are expressed as

$$u|_{r=R_b} = u_{bx} \quad , \quad W|_{r=r_{cr}} = W_{cr} \quad , \quad \text{for } R_b \leq r \leq r_{cr} \quad (3.27a)$$

$$W|_{r=r_{cr}}=W_{cr} \ , \ W|_{r=r_y}=0, \quad \text{for } r_{cr} \leq r \leq r_y \quad (3.27b)$$

$$\sigma_{\theta}|_{r=r_y}=f_t \ , \ \sigma_r|_{r=R_c}=0, \quad \text{for } r_y \leq r \leq R_c \quad (3.27c)$$

By implementing these boundary conditions and utilising the general solution in equation (3.15), the normalized crack widths over the cracked inner ring and within the cracked middle ring are given, respectively, by

$$W = \frac{1}{\alpha_{bi}(l_o^u - R_b)} \left( \frac{E}{f_t} u_{bx} - \frac{\alpha_{bi} W_u}{(W_u - W_{cr})} R_b \right) \frac{\delta^u(r_{cr}, r)}{\delta^u(r_{cr}, R_b)} (W_u - W_{cr}) + \frac{\delta^u(r, R_b)}{\delta^u(r_{cr}, R_b)} W_{cr}$$

for  $R_b \leq r \leq r_{cr}$  (3.28a)

$$W = \frac{\delta^{cr}(r_y, r)}{\delta^{cr}(r_y, r_{cr})} W_{cr} \quad \text{for } r_{cr} \leq r \leq r_y \quad (3.28b)$$

where superscript  $u$  in material coefficient  $l_o$  and crack width function  $\delta$  represents that the material coefficient  $l_o^u$  is calculated by the post-critical coefficients in equation (3.5b). The crack front ( $r_y$ ) and the critical crack boundary ( $r_{cr}$ ) are obtained from additional two boundary conditions of the continuity of radial stresses at both the crack front and at the critical crack boundary, where the relevant normalized crack width in equation (3.28) is considered.

By using the obtained crack width at the bond interface, the corrosion level at the time to crack on the cover surface for this case  $X_p^C$  is estimated by

$$X_p^c = \frac{2}{(\gamma_{vol}-1)} \frac{f_t}{E} \frac{\alpha_{bi} W_u}{(W_u - W_{cr})} \left( 1 + \frac{(l_o^u - R_b) W_{cr}}{R_b W_u} + \frac{1 - \alpha_{bi}}{\alpha_{bi}} \frac{(l_o^{cr} - R_c)}{R_b} \frac{\eta_x^u(r_{cr}^c, R_b)}{\eta_x^{cr}(R_c, r_{cr}^c)} \frac{(W_u - W_{cr})}{W_u} \right) \quad (3.29)$$

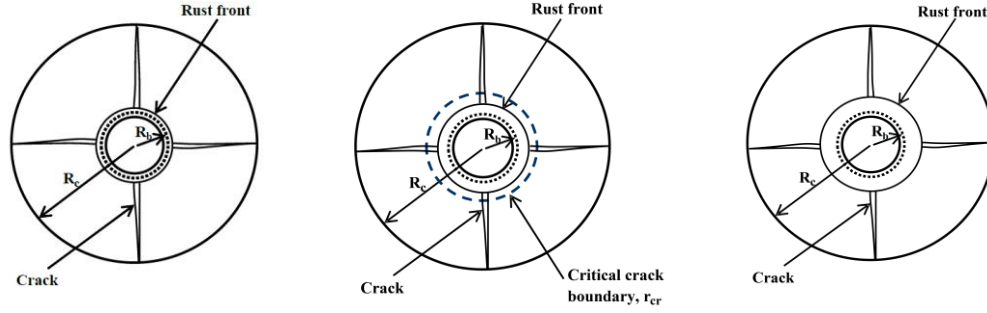
where  $\eta_x^u$  is determined by the general coefficient  $\eta_x$  in which  $l_o = l_o^u$ , as discussed in equation (3.26). At the time to crack on the concrete cover surface, the crack front is taken as  $r_y = R_c$  and the critical crack boundary  $r_{cr}^c$  is given by

$$(1 + \nu) R_c (l_o^{cr} - R_c) \delta^{cr}(R_c, r_{cr}^c) = 1 - \alpha_{bi} \quad (3.30)$$

Here again, the corrosion level at the time to crack is a function of concrete properties, rust volume expansion factor and the ratio of cover thickness to rebar diameter.

### 3.7.3 Completely cracked concrete cover

After crack front reaches the cover surface, the concrete cover becomes completely cracked. Depending on the crack widths at the bond interface  $W_b$  and at the cover surface  $W_c$ , three cases are considered, i.e. crack width over the concrete cover does not exceed the critical value ( $W_b \leq W_{cr}$  and  $W_c \leq W_{cr}$ ), critical crack width propagates through the concrete cover ( $W_b > W_{cr}$  and  $W_c < W_{cr}$ ), and crack width over the concrete cover exceeds the critical value ( $W_b > W_{cr}$  and  $W_c > W_{cr}$ ), as shown in Figure 3.4.



- a)  $W_b \leq W_{cr}$  and  $W_c \leq W_{cr}$     b)  $W_b > W_{cr}$  and  $W_c < W_{cr}$     c)  $W_b > W_{cr}$  and  $W_c > W_{cr}$

**Figure 3.4** Idealisation of completely cracked concrete cover (Note: figures not drawn to scale)

**Case with  $W_b \leq W_{cr}$  and  $W_c \leq W_{cr}$**

Here, a single cracked zone within the concrete cover exists, and the crack width at the bond interface does not exceed the critical value at the time to crack. The boundary conditions described in equations 3.19(a,b) are used for this case. By introducing the boundary conditions and ignoring the Poisson's effect associated with the hoop strain due to completely cracked concrete, the normalized crack width on the concrete cover surface  $W_c$  is obtained from

$$W_c = \frac{1}{(1 - \alpha_{bi})\eta_w^{cr}(R_c, R_b)} \left( \frac{1}{2}(\gamma_{vol} - 1) \frac{E}{f_t} R_b X_p - R_b - R_c \eta_x^{cr}(R_c, R_b) \right) W_{cr} \quad (3.31)$$

where coefficient  $\eta_w^{cr}(R_c, R_b)$  is determined by the general coefficient  $\eta_w(R_c, R_b) = (l_o - R_b)[1 - R_c(l_o - R_c)\delta(R_c, R_b)]$  by using  $l_o = l_o^{cr}$ . Once  $W_c$  is known the actual crack width at the concrete cover surface is evaluated from  $w_{cx} = G_F W_c / f_t$ . The normalized crack width over the concrete cover is then expressed as

$$W = \frac{1}{(1 - \alpha_{bi})(l_o^{cr} - R_b)} \left( \frac{E}{f_t} u_{bx} - R_b \right) \frac{\delta^{cr}(R_c, r)}{\delta^{cr}(R_c, R_b)} W_{cr} + \frac{\delta^{cr}(r, R_b)}{\delta^{cr}(R_c, R_b)} W_c \quad (3.32)$$

**Case with  $W_b > W_{cr}$  and  $W_c < W_{cr}$**

The critical crack front divides the thick-walled cylinder into two zones, a cracked inner ring where crack width exceeds the critical value ( $R_b \leq r \leq r_{cr}$ ) and a cracked outer ring where crack width does not exceed the critical value ( $r_{cr} \leq r \leq R_c$ ), giving the boundary conditions as

$$u|_{r=R_b} = u_{bx} \quad , \quad W|_{r=r_{cr}} = W_{cr} \quad , \quad \text{for } R_b \leq r \leq r_{cr} \quad (3.33a)$$

$$W|_{r=r_{cr}} = W_{cr} \quad , \quad \sigma_r|_{r=R_c} = 0 \quad , \quad \text{for } r_{cr} \leq r \leq R_c \quad \dots \quad (3.33b)$$

From these boundary conditions, the normalized crack width at the concrete cover surface  $W_c$  is given as

$$W_c = \frac{1}{(1 - \alpha_{bi})\eta_w^{cr}(R_c, r_{cr})} \left[ (1 - \alpha)(l_o^{cr} - r_{cr}) - R_c \eta_x^{cr}(R_c, r_{cr}) \right] W_{cr} \quad (3.34)$$

where the critical crack boundary ( $r_{cr}$ ) between the outer ring and the inner ring is obtained from the continuity condition of radial stresses crossing two rings. The normalized crack width within the cracked inner ring is then calculated from

$$W = \left[ \frac{1}{(1 - \alpha_{bi})(l_o^u - R_b)} \left( \frac{E}{f_t} \bar{u}_b(x_p) - R_b \right) \delta^u(r_{cr}, r) + \delta^u(r, R_b) \right] \frac{W_{cr}}{\delta^u(r_{cr}, R_b)} \quad (3.35)$$

**Case with  $W_b > W_{cr}$  and  $W_c > W_{cr}$**

The crack width over the concrete cover now exceeds the critical value, and the boundary conditions for this case are given in equations 3.19(a,b). From the boundary conditions, the normalized crack width at cover surface  $W_c$  is obtained from

$$W_c = \frac{1}{\eta_w''(R_c, R_b)} \left( \frac{1}{2} (\gamma_{vol} - 1) \frac{E}{f_t} \frac{(W_u - W_{cr})}{\alpha_{bi} W_u} R_b X_p - R_b - R_c \eta_x''(R_c, R_b) \right) W_u \quad (3.36)$$

where coefficient  $\eta_w''(R_c, R_b)$  is determined by general coefficient  $\eta_w(R_c, R_b)$  in which  $l_o = l_o^u$ . The Normalized crack width within the cracked concrete cover is expressed as

$$W = \frac{1}{\alpha_{bi}(l_o^u - R_b)} \left( \frac{E}{f_t} u_{bx} - \frac{\alpha_{bi} W_u}{(W_u - W_{cr})} R_b \right) \frac{\delta''(R_c, r)}{\delta''(R_c, R_b)} (W_u - W_{cr}) + \frac{\delta''(r, R_b)}{\delta''(R_c, R_b)} W_c \quad (3.37)$$

The corrosion level at the time when cracks in the cover concrete reach the ultimate cohesive width ( $X_p^U$ ) is determined from equations (3.36) and (3.3), given by

$$X_p^U = \frac{2}{\pi(\gamma_{vol} - 1)} \frac{f_t}{E} \frac{n_c l_{ch}}{D_b} W_u \quad (3.38)$$

Similarly, from the above equation it is clear that the corrosion level at the time for cracks to reach ultimate cohesive width is related to material properties and rust volume expansion factor.

### **3.8 Numerical example 1**

#### *3.8.1 Evolution of visible crack at the concrete cover surface*

In order to demonstrate the effectiveness of the proposed approach, the published experimental data of Vu et al. (2005) and Andrade et al. (1993) on corrosion cracking test is adopted. These investigations made use of bars with diameter in the range of 10-16 mm, with cover to rebar diameter ratios between 1.5 and 7.0 and concrete compressive strength ranged from 30 to 52 MPa. Accelerated corrosion tests were conducted by using current densities of  $100 \mu\text{A}/\text{cm}^2$ . The other material properties of concrete i.e. tensile strength and modulus of elasticity utilized in the model is evaluated from EC2 (2004) corresponding to characteristic compressive strength of concrete. The concrete fracture energy  $G_F = 200 \text{ N/m}$  is adopted. The critical and ultimate cohesive crack widths required for this study have been obtained from CEB-FIP (1990) for adopted maximum aggregate size of 16 mm.

The theoretical predictions of the amount of corrosion level required to develop visible crack at the concrete cover surface from the developed approach are then compared with experimental data observed by Vu et al. (2005) and Andrade et al. (1993). In this study visible crack is defined as the crack of width of 0.05mm as defined in reference literatures Vu et al. (2005) and Andrade et al. (1993). It can be seen from Table 3.1 that the predicted results in general agree with the experimental results. Some discrepancies in the results may be due to complexity of the cracking process.

**Table 3.1** Comparison of experimental and predicted corrosion level associated with visible cracking

References	Cover thickness $C$ (mm)	Rebar diameter $D_b$ (mm)	Compressive strength, $f_{ck}$ (MPa)	Tensile strength $f_t$ (MPa)	Observed (%)	Predicted (%)
Vu et al. (2005)	25	16	52.7	4.55	0.74	0.66
	50	16	—	—	1.62	1.45
	25	16	20	3.06	0.44	0.43
	50	16	—	—	1.33	1.32
Andrade et al. (1993)	20	16		3.55	0.36	0.38
	30	16		3.55	0.53	0.61

### 3.9 Numerical example 2

#### 3.9.1 Evolution of cracking at the concrete cover surface

In order to demonstrate the applicability of proposed approach for predicting crack evolution due to accumulation of corrosion product, analyses are now carried out by considering a simply supported RC beam with minimum service life of 50 years designed to resist very aggressive environment as defined by Eurocode 2. The cross-sectional width and effective depth of beam are  $b=300$  mm and  $d=560$  mm, respectively. Four steel rebars with diameter  $D_b=16$  mm are provided as the tensile reinforcement and two rebars of diameter  $D_{sc}=12$  mm are provided as the compressive steel with clear cover thickness  $C=40$  mm along with the stirrup of diameter  $D_{st}=6$  mm at spacing of 50 mm and is subjected to mean annual corrosion

current per unit length  $i_{corr} = 6 \mu\text{A}/\text{cm}^2$ . The characteristic compressive strength of concrete is assumed as  $f_{ck} = 40 \text{ Mpa}$  and corresponding concrete properties such as tensile strength and modulus of elasticity are obtained from Eurocode 2. Four numbers of cracks are assumed to be formed in the concrete cover and crack width in the cover concrete is represented by the equivalent crack width, as defined in Vidal et al (2014). The concrete fracture energy  $G_F = 200 \text{ N/m}$  is adopted, and the ultimate cohesive crack width  $w_u = 1.52 \text{ mm}$  and the critical crack width  $w_{cr} = 0.21 \text{ mm}$  are estimated from CEB-FIP (1990) for the given compressive strength and adopted maximum aggregate size of 16 mm.

The results in Figure 3.5 show the analytically predicted equivalent cover surface crack width as a function of corrosion level in percentage. The predicted results are then compared with published experimental data (accelerated or natural corrosion) obtained from various references (Vidal et al. 2004, Coronelli et al. 2013, Khan et al. 2014, Mangat and Elgarf 1999a, Torres-Acosta et al. 2007, Almusallam et al. 1996, Rodriguez et al. 1994, Xia et al. 2012). These investigations made use of bars with diameter in the range of 12-20 mm, with cover to rebar diameter ratios between 1.5 and 5.0. Concrete compressive strength ranged from 30 to 52 MPa and in case of accelerated corrosion test impressed current densities varied between 0.1 and 30 mA/cm<sup>2</sup>. It can be seen from Figure 3.5 that the predicted crack width increases as reinforcement corrosion level increases, agreeing well with the referred experimental results in particular with the measured crack width in the condition of natural corrosion. At corrosion level of about 1.6%, concrete cover is thoroughly cracked and the crack width at the cover surface continuously increase with further progress of corrosion reaching its ultimate cohesive value at the corrosion level of approximately 18%.

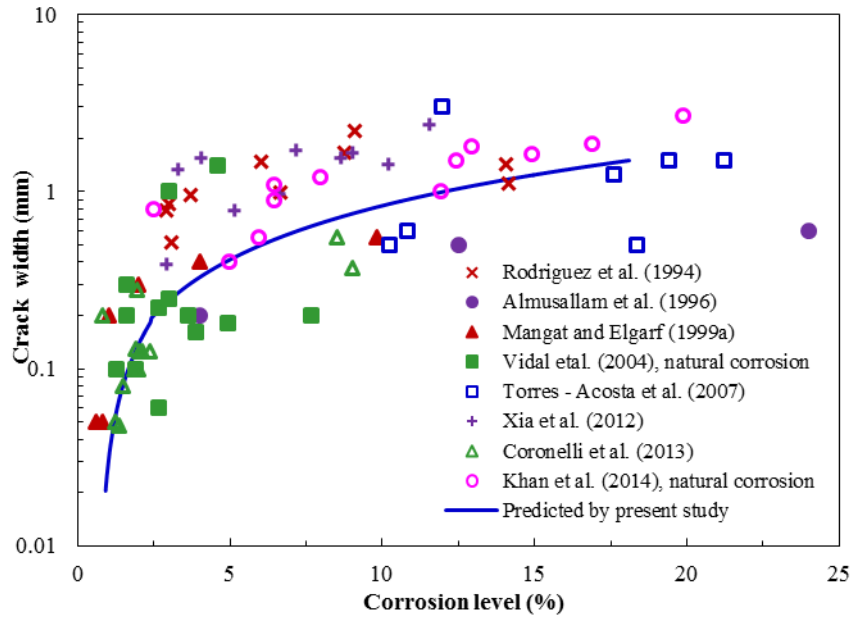


**Figure 3.5** Analytical prediction of equivalent cover surface crack width versus corrosion level, compared with experimental test results available from various sources

Although the relationship between corrosion level and the crack growth in the concrete cover surface depends on number of parameters, but it is clear from the Figure 3.5 that cracking at the cover surface develops well before the reduction in rebar becomes significant.

### 3.9.2 Comparison of cracking at the bond interface and cover surface

During the routine inspections of concrete bridges, cracking in concrete cover is the most important information recorded for condition rating. Based on the condition ratings collected during inspections, Bridge Management Systems (BMSs) are developed for optimum allocation of limited resources available (Liu and Frangopol 2005). Depending on the size of the cracks, these defects in concrete cover due to corrosion can be classified in different categories such as spalling, minor and major

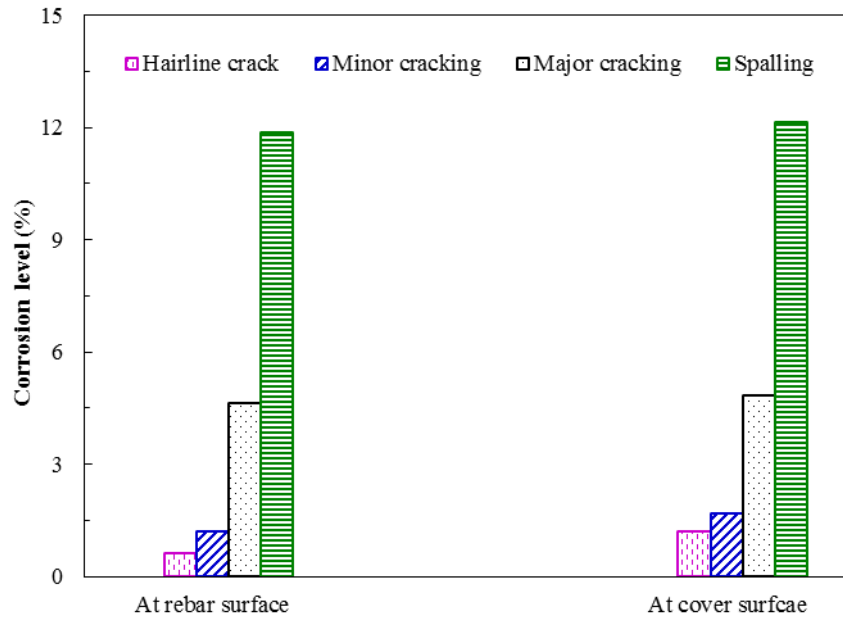


**Figure 3.6** Defects in concrete cover versus corrosion level

cracking etc. These defects predicted by the present analytical study occurring during the corrosion process is shown in Figure 3.6. In Figure 3.6, the vertical axis represents the corrosion level in percentage and the horizontal axis represents the different types of defects developed. Depending on the crack width developed, the defects in concrete cover due to reinforcement corrosion are classified here as hairline crack (0.05 mm), minor cracking (0.1 mm), major cracking (0.4 mm) and spalling (1.0 mm). The results here are presented for the defects occurring both at the rebar surface and concrete cover surface. In case of rebar surface, minor cracking occurs comparatively at low level of corrosion. However there is no significant difference in the higher stage of defects. For instance in both cases (i.e. at rebar surface and cover surface) at corrosion level of about 5%, major cracking appear while at about 11% of corrosion spalling of the concrete cover takes place in. This is due to fact that in later stage of corrosion, crack width at the cover surface is close to rebar surface and becomes ultimate cohesive with at the same stage of corrosion.

### 3.9.3 Effect of concrete geometry on corrosion induced cover cracking

The results in Figure 3.7 show the corrosion level required to produce visible crack at the concrete cover surface for various cover to rebar diameter ratio ( $C/D_b$ ). As expected, the formation of visible crack in the concrete cover surface is delayed in higher  $C/D_b$  ratio. Influence of corrosion level on cover defects at the cover surface for different cover depth is studied in Figure 3.8. In the analysis various values of cover depth ranging from 32 mm, 40 mm and 48 mm are considered.

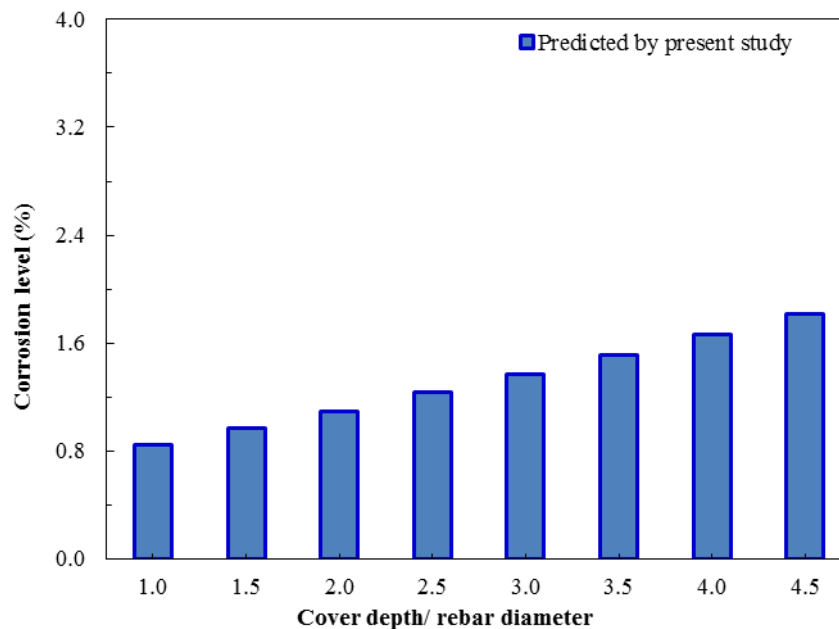


**Figure 3.7** Corrosion level associated with formation of visible crack for various cover/rebar diameter ratios

From the results it is clear that although the formation of defect until the stage of minor cracking is delayed for larger cover depth, after the stage of minor cracking there is no significant influence of cover depths on the propagation of defects till spalling.

This agrees with the experimental findings of Rodriguez et al. (1994), Alonso et al (1998) and Vidal et al. (2004).

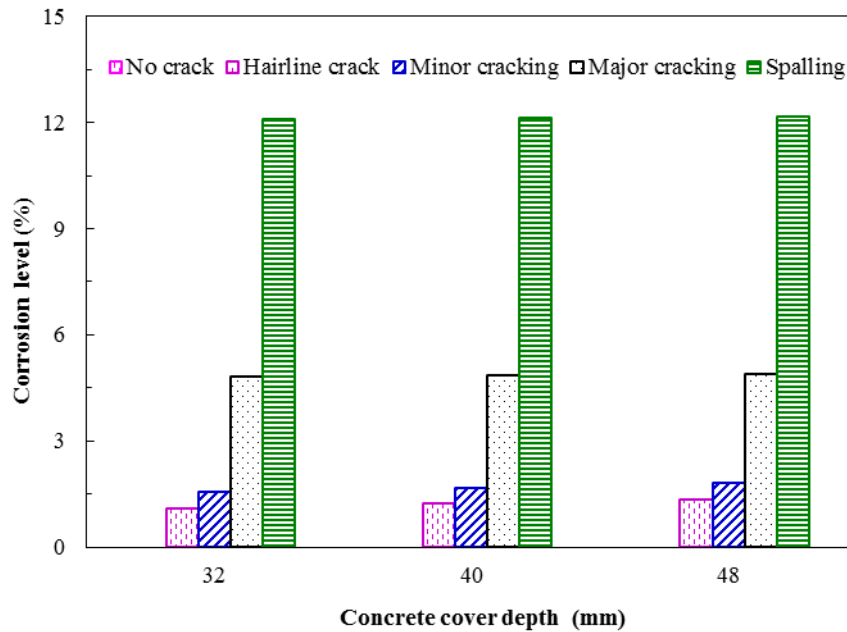


**Figure 3.8** Corrosion level at different stages of cracking at the cover surface for various concrete cover depths

### 3.10 Summary and conclusions

In this chapter a new analytical method for analysing the evolution of corrosion induced concrete cover cracking is proposed based on the thick-walled cylinder model and the use of realistic concrete properties. Cracked concrete is considered as anisotropic in nature and its residual strength is determined by using realistic tensile softening behaviour of cracked concrete. A governing equation for directly solving crack width within the cover concrete is established and general closed form solution is obtained for the proposed boundary value problem. Finally the development of concrete cracking caused by reinforcement corrosion at various stages is investigated as a function of

corrosion level. The applicability of the proposed methodology is demonstrated by using numerical examples. The predicted result for crack growth with respect to reinforcement corrosion is then validated by experimental data available.

The results obtained from the numerical analysis following conclusions are drawn: a) Crack width in the concrete cover increases with progress of reinforcement corrosion and the cracking at the concrete cover surface becomes visible well before the reduction in rebar cross section area becomes significant; b) In early stage of corrosion defects in rebar surface becomes prominent but in later stage of corrosion, defects at both the concrete cover surface and bond interface develop in the same rate; c) The formation of minor cracking is delayed for larger cover depths.

## **Chapter 4 Development of Bond Strength Degradation Model**

### **4.1 Introduction**

Bond strength acting at the rebar surface has the interaction mechanism that enables the force transfer between rebar and the surrounding concrete. Hence bond strength maintains the composite action in RC structures. When composite action is disrupted, load carrying capacity is also affected (Rodriguez et al. 1994, Coronelli 2002, Nepal et al. 2013). This in turn changes the overall behaviour of the RC structures. Hence, for the satisfactory performance of RC structure adequate bond between rebar and surrounding concrete is essential.

Bond strength deterioration of corrosion damaged RC structure is the hidden effect that does not have direct observation or measurement in the field. Moreover, design codes and standards are primarily focused on new construction and do not provide information about characteristics values for the bond strength of corroded rebar. Hence, evaluation of bond strength degradation is essential parameter for the condition assessment of the corroded RC structures which ultimately helps in correctly predicting the residual strength and remaining service life of the corroded RC structures. Meanwhile, further understanding of the effect of reinforcement corrosion on the structural behaviour of deteriorating RC structures can be useful for asset managers to make cost effective decisions related to the inspection, repair, strengthening, replacement and demolition of such structures. This can ultimately help in achieving the goal of sustainable infrastructure management.

From the review of the existing research in the field of bond strength behaviour of corrosion damaged RC structures, it can be concluded that corrosion in reinforcement can cause considerable reduction of bond strength. Losses of up to 90% of the initial bond strength have been observed for only about 5-7% of the corrosion level in specimens without transverse reinforcement. On the basis of these experimental results, empirical models for the relationship of the bond strength of corroded reinforcement with corrosion level have been proposed, such as in the studies by Auyeung et al. (2000), Bhargava et al. (2007), Lee et al. (2002) and Stanish et al. (1999). Furthermore some empirical formulae have also been proposed to describe the influence of crack width on the bond strength of the corroded plain rebar based on the experimental results (Cairns et al. 2006). The applicability of these empirical models to real RC structures serving in aggressive environments may be limited, since they are mainly evaluated from specific concrete specimens and test procedures in the experiments. On the other hand, numerical investigations on the influence of reinforcement corrosion on bond strength have been conducted by using powerful finite element methods, giving conclusions similar to those from experimental investigations (Lundgren 2002, Amleh and Ghosh 2006).

In addition, attempts have also been made to develop analytical models for predicting bond strength degradation due to reinforcement corrosion. Coronelli (2002) proposed an analytical model for estimating the bond strength of corroded reinforcement in concrete. Later, Wang and Liu (2004) improved the analytical model by using the corrosion pressure estimated from the thick-walled cylinder model with consideration of the nonlinear stress-strain relation of the cracked concrete. Recently, Bhargava et al. (2007) utilised similar approach and proposed an analytical model. However, most of

the existing analytical models ignore the anisotropic behaviour of the cracked concrete affected by reinforcement corrosion. These models may be unable to correctly predict the crack width growth of the cover concrete and the pressure evolution at the bond interface as corrosion progresses. Therefore, there is a need to develop a new analytical model that can predict the residual bond strength of the corroded RC structures.

This chapter presents a new analytical model for predicting bond strength evolution for RC structures affected by reinforcement corrosion. The thick-walled cylinder model subject to increasing displacement generated by the expansive corrosion products at the bond interface as defined in Chapter 3, is adopted for constructing new governing equations for the ultimate bond strength. From the proposed analytical model of the crack width in the concrete cover presented in Chapter 3, the radial corrosion pressure, confinement stress and the adhesion stress acting at the bond interface are determined. The ultimate bond strength is then estimated by considering the contributions from adhesion, confinement and corrosion pressure related to corrosion level. The merit of the proposed method is that the bond strength degradation is directly related to crack growth over corrosion process. Finally, the proposed analytical model is verified by comparing the predicted results with experimental and field data available from various sources. Influence of geometrical properties and confinement conditions of the concrete on the bond strength deterioration have also been discussed.

#### **4.2 Mechanism of bond strength of corroded rebar**

The bond strength of plain rebars relies on adhesion and friction between rebar and the surrounding concrete. However, the bond strength of deformed rebars, which are most

commonly used in RC structures and are mainly concerned in this study, depends on chemical adhesion between the rebar and surrounding concrete, frictional forces at the interface and mechanical interlocking of the ribs against the concrete surface (ACI 2003). The schematic representation of bond mechanism of the typical deformed rebar is shown in Figure 4.1.

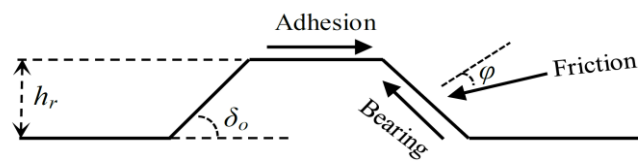


**Figure 4.1** Bond mechanisms for deformed rebar

The chemical adhesion between the steel reinforcement and the surrounding concrete is the weak bond. Therefore, during the early stage of corrosion the weak bond is broken at a very low stress. Bond strength is then mainly contributed by mechanical interlocking, friction and confinement stress acting at steel-concrete interface. At low level of corrosion when there is no longitudinal cracking, the corrosion products have beneficial effect on the bond strength because it increases the surface roughness and hence the frictional force (Coronelli 2002). At higher corrosion level, corrosion affects the bond properties between the rebar and the surrounding concrete by changing the shape and angle of the ribs of the deformed rebar. Corrosion also influences the mechanical interlocking at the bond interface by further reducing the adhesion and frictional force caused by the accumulation of corrosion products. Furthermore, corrosion also reduces the confinement action between concrete and steel by creating cracks in the concrete. With further progress of corrosion, cracking in the concrete cover continues on widening which simultaneously decreases the confinement stress

and finally the residual confinement stress provided by the cracked concrete is released and is contributed only by the transverse reinforcement. (Tastani and Pantazopoulou 2010, Coronelli 2002, Li and Yuan 2013). Therefore corrosion in reinforcement threatens all these factors required for good bonding condition of the RC structure.

### 4.3 Evaluation of ultimate bond strength

To consider the effects of reinforcement corrosion, Coronelli (2002) has proposed an analytical model to evaluate the ultimate bond strength of deformed corroded rebar by modifying the original model provided by Cairns and Abdullah (1996). The ultimate bond strength was defined by considering three types of forces acting at the steel-concrete interface namely friction, bearing and radial forces as shown in Figure 4.2. The friction, bearing and radial forces were associated with roughness of the rebar surface, mechanical interlocking between ribs and concrete, and corrosion pressure acting at the steel concrete interface respectively.

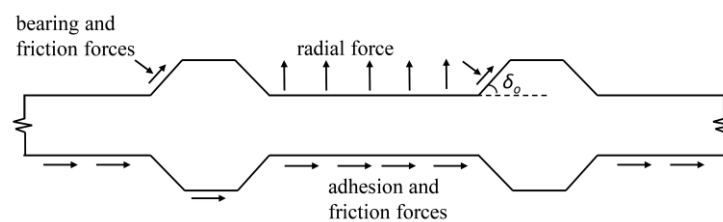


**Figure 4.2** Bond mechanisms for corroded deformed rebar

Hence, from the modified model of Coronelli (2002), the ultimate bond strength ( $T_{ubx}$ ) is obtained from the total contribution of three types of stresses acting at the bond interface i.e. adhesion stress ( $T_{adx}$ ), confinement stress ( $T_{cnfx}$ ) and corrosion stress

$(T_{corr_x})$ , as given in equation (4.1), expressed as

$$T_{ubx} = T_{adx} + T_{cnfx} + T_{corr_x} \quad (4.1)$$

The above equation (4.1) gives the ultimate bond strength of corroded rebar at any corrosion level  $X_p$ . Unlike in most of the existing design codes (CEB-FIP 1990, EC2 2004, FIB 2010), the definition of the bond strength in equation (4.1) not only defined as the function of concrete compressive strength but also as the three different stresses acting at the steel concrete interface. The bond strength in equation (4.1) depends on various mechanical and geometrical properties of the steel and concrete. The analytical formulation of each component of bond stress is now discussed in upcoming sections 4.4, 4.5 and 4.6.

#### 4.4 Evaluation of adhesion stress

The adhesion stress acting at the bond interface ( $T_{adx}$ ) is related to the interface cohesion, defined as non-splitting component associated with the friction and adhesion stress acting on inclined rib faces, given by Coronelli (2002) as a function of corrosion level

$$T_{adx} = \frac{n_r A_{rx} f_{coh_x} [\cot \delta_o + \tan(\delta_o + \varphi)]}{\pi D_{bx} S_r} \quad (4.2)$$

where  $A_{rx} = \pi D_{bx} h_{rx}$  is the reduced rib area in plane at right angle to rebar axis in which  $h_{rx} = 0.07 D_{bx}$  is the reduced rib height of the rebar due to corrosion;  $S_r = 0.6 D_b$

is the rib spacing (Wang and Liu, 2004),  $n_r$  is the number of transverse ribs at section,  $f_{cohx} = 2 - 10(x - x_c)$  is the adhesion strength coefficient in which  $x_c$  is the corrosion depth corresponding to the thorough cracking of the concrete cover and can be obtained once  $X_p^C$  is known,  $\tan(\delta_o + \varphi)$  can be estimated from  $1.57 - 0.785x$  (Coronelli and Gambarova 2000) in which  $\delta_o$  is the orientation of the rib is usually taken as  $45^\circ$  and  $\varphi$  is the angle of friction between steel and concrete as shown in Figure 4.1.

#### 4.5 Evaluation of confinement stress

The bond strength contribution due to confinement stress is given by  $T_{cnfx} = k_{cnfx} P_{cnfx}$  where  $k_{cnfx} = 0.8n_r \tan(\delta_o + \varphi) / \pi$  is the coefficient of confinement stress and  $P_{cnfx}$  is the confinement pressure (Coronelli 2002, Coronelli and Gambarova 2000). According to the study carried out by Cairns and Abdullah (1996) in deformed rebar, bond failure may be caused by the splitting of cover or by shearing-off the concrete keys between the bar ribs (splitting and pullout failure respectively). The splitting failure may be activated by the formation of splitting cracks in the concrete cover caused by the expansion of corrosion product (Coronelli 2002). To incorporate the confinement stress associated with the splitting cracks and the stirrups, the maximum confining pressure at splitting bond failure proposed by Giuriani et al. (1991) is now considered. In confined concrete the confinement pressure is the total contribution of cracked concrete  $P_{cnfx,c}$  and the stirrups  $P_{cnfx,st}$  given by

$$P_{cnfx} = P_{cnfx,c} + P_{cnfx,st} \quad (4.3)$$

In case of unconfined concrete, confinement stress is only provided by the cracked concrete. The confinement stress provided by the cracked concrete is due to the confining action provided by the residual stress transmitted between the faces of cracked concrete (Giuriani et al. 1991), defined as

$$P_{cnf,c} = \frac{b - n_p D_b}{D_b} \times \sigma_{rc} \quad (4.4)$$

where  $b$  is the width of the section considered,  $n_p$  is the number of longitudinal rebar,  $D_b$  is diameter of rebar and  $\sigma_{rc}$  is the residual tensile stress in cracked concrete. Introducing the characteristics of thick walled cylinder model, and assuming the splitting cracks formed are cohesive in nature with bilinear softening property as defined in Chapter 3, the confinement stress of the cracked concrete due to reinforcement corrosion can be obtained from equation (4.4) (Chen and Nepal 2015a, b), expressed here as

$$P_{cnf,c} = \frac{2C}{D_{bx}} \times f_t \frac{D_a (w_u - w_{bx})}{w_u (D_a + k_c w_{bx})} \quad (4.5)$$

where  $w_{bx} = G_F W_{bx} / f_t$  is actual crack width at the rebar surface associated with corrosion level obtained from equation (3.22),  $k_c$  is the constant taken as 167, and  $D_a$  is the maximum aggregate size. From equation (4.5) it is clear that the confinement stress provided by the cracked concrete depends on crack width at the rebar surface  $w_{bx}$ . Therefore, with increase in  $w_{bx}$  the confinement stress provided by the cracked

concrete decreases and ultimately becomes negligible when crack reaches its ultimate cohesive value  $w_u$ .

The relationship for the confinement pressure contributed by the stirrups is also proposed by Giuriani et al. (1991) as the stress in the stirrup legs that increases with the crack opening, defined here as

$$P_{cnf, st} = \frac{n_{st} A_{st}}{n_p D_b S_{st}} \times \sigma_{st} \quad (4.6)$$

where  $A_{st}$  is the cross-section area of stirrup leg with diameter of  $D_{st}$ ,  $S_{st}$  is the spacing of stirrup,  $n_{st}$  is the number of stirrup leg in the section  $n_p$  is the number of longitudinal rebar and  $\sigma_{st}$  is the maximum stress of transverse reinforcement close to splitting crack. In order to consider the influence of reinforcement corrosion on the confinement contribution of steel stirrups in the thick walled cylinder model, the original relations proposed by Giuriani et al. (1991) is modified by Chen and Nepal (2015a), as

$$P_{cnfx, st} = \frac{n_{st} A_{st}}{D_{bx} S_{st}} \times E_{st} \sqrt{\frac{a_2 w_{bx}^2}{\alpha_{st}^2 D_{st}^2} + \frac{a_1 w_{bx}}{\alpha_{st} D_{st}} + a_o} \quad (4.7)$$

$E_{st}$  is the modulus of elasticity of steel,  $\alpha_{st}$  is the shape factor of stirrup taken as 2,  $a_2$ ,  $a_1$  and  $a_o$  are the coefficients related to the local bond-slip law of the stirrups, and given in Giuriani et al. (1991). In this study  $E_{st}$  is taken as 200 GPa (EC2 2004). As

shown in equation (4.7), the confinement stress due to stirrup increases with the increase in crack width at rebar surface. However, bond strength contribution due to stirrup has limited value and has been estimate as suggested by ACI (2003). Therefore, in this study, the confinement stress is analytically expressed as a function of corrosion level  $X_p$  and limited confinement contribution from stirrups is considered.

#### 4.6 Evaluation of corrosion stress

Due to the accumulation of corrosion product pressure is built-up at steel-concrete interface. This corrosion pressure gives some contribution to bond strength through friction mechanism between rebar surface and the surrounding concrete. The bond strength contributed from corrosion pressure due to reinforcement corrosion ( $T_{corr}$ ) is expressed in Coronelli (2002) as

$$T_{corr} = \mu_x P_{corr} \quad (4.8)$$

where  $\mu_x$  is the coefficient of the friction between the corroded rebar and cracked concrete defined as  $\mu_x = 0.37 - 0.26(x - x_c)$  in which  $x$  and  $x_c$  are the corrosion depth corresponding to  $X_p$  and  $X_p^C$  respectively.  $P_{corr}$  is the corrosion pressure or the radial stress  $\sigma_r$  acting at the bond interface  $R_b$  due to the accumulation of the corrosion product. For the evaluation of corrosion pressure, a thick walled cylinder model used in Chapter 3 for the analytical modelling of concrete cover cracking has been adopted. Therefore,  $P_{corr}$  is the radial pressure exerted by the expansive corrosion products at the bond interface and defined in general equation (3.18), which can be

determined from the discussion for various phases in the preceded section. In the phase before cracking initiates at the bond interface, the radial pressure is estimated from equation (3.20a). During the period of crack propagation from the bond interface to the concrete cover, in the case when crack width at the bond interface does not exceed the critical value ( $0 < W_b \leq W_{cr}$ ), the radial corrosion pressure  $P_{corr}$  is expressed here as

$$P_{corr} = \frac{f_t}{1-\nu^2} \left[ (1+\nu\sqrt{\beta_{bx}^{cr}}) \left( 1 - (1-\alpha_{bi}) \frac{W_{bx}^{cr}}{W_{cr}} \right) + (1-\alpha_{bi})(l_o^{cr} - R_b)W_{,r}^{cr} + \nu(1-\alpha_{bi})\sqrt{\beta_{bx}^{cr}} \frac{l_o^{cr}}{R_b} \frac{W_{bx}^{cr}}{W_{cr}} \right] \quad (4.9)$$

where  $W_{bx}^{cr}$  and  $\beta_{bx}^{cr}$  are the normalized crack width and stiffness reduction factor as defined in equations (3.22a) and (3.22b) of Chapter 3 respectively, expressed here as

$$W_{bx}^{cr} = \frac{W_{cr}}{(1-\alpha_{bi})(l_o^{cr} - R_b)} \left( \frac{E}{f_t} u_{bx} - R_b \right) \quad (4.10)$$

$$\beta_{bx}^{cr} = \frac{W_{cr} - (1-\alpha_{bi})W_{bx}^{cr}}{W_{cr} - (1-\alpha_{bi})W_{bx}^{cr} \left( 1 - \frac{l_o^{cr}}{R_b} \right)} \quad (4.11)$$

Similarly, in the case when crack width at the bond interface exceeds the critical value ( $W_{cr} < W_b \leq W_u$ ), the radial stress is rewritten here as

$$P_{corr} = \frac{f_t}{1-\nu^2} \frac{\alpha_{bi}}{(W_u - W_{cr})} \left[ (1+\nu\sqrt{\beta_{bx}^u})(W_u - W_{bx}^u) + (l_o^u - R_b)W_{,r}^u + \nu\sqrt{\beta_{bx}^u} \frac{l_o^u}{R_b} W_{bx}^u \right] \quad (4.12)$$

where  $W_{bx}^u$  and  $\beta_{bx}^u$  are related to post-critical material coefficient, obtained from

$$W_{bx}^u = \frac{1}{\alpha_{bi}(l_o^u - R_b)} \left( \frac{E}{f_t} u_{bx} (W_u - W_{cr}) - \alpha_{bi} W_u R_b \right) \quad (4.13)$$

$$\beta_{bx}^u = \frac{\alpha_{bi} (W_u - W_{bx}^u)}{\alpha_{bi} \left[ W_u - W_{bx}^u \left( 1 - \frac{l_o^u}{R_b} \right) \right]} \quad (4.14)$$

$W_{,r}^{cr}$  and  $W_{,r}^u$  are the first derivative of the normalized crack width with respect to radius  $r$  at the bond interface as defined in equation (3.17) of Chapter 3 in which  $l_o = l_o^{cr}$  and  $l_o = l_o^u$  respectively, as

$$W_{,r}^{cr} = C_1 \frac{1}{R_b (l_o^{cr} - R_b)^2} \quad (4.15a)$$

$$W_{,r}^u = C_1 \frac{1}{R_b (l_o^u - R_b)^2} \quad (4.15b)$$

The constant  $C_1$  in the equation (4.15) for both partially and fully cracked stage of concrete cover depends on different stages of cracking at the bond interface and cover surface and can be obtained from equation (3.15) of Chapter 3.

#### 4.7 Numerical example 1

To investigate the performance of the proposed analytical model for predicting bond strength deterioration with corrosion propagation in corroded RC structures, numerical analyses are now carried out by taking published experimental data of Lee et al. (2002)

and analytical results of Bhargava et al. (2007) and Pantazopoulou and Papoulia (2001).

#### 4.7.1 Comparison of corrosion pressure with existing models

The results in Figure 4.3 show the comparison of predicted corrosion pressure at the bond interface with analytical results by Pantazopoulou and Papoulia (2001) and Bhargava et al. (2007). The results are obtained for the experimental sample S2 in Liu and Weyers (1998) with cover thickness  $C = 70$  mm, compressive strength  $f_{ck} = 31.5$  MPa, corrosion rate  $i_{corr} = 1.79 \mu\text{A}/\text{cm}^2$ , rebar diameter  $D_b = 16$  mm and  $\gamma_{mol} = 0.57$ . Here, other parameters required in the proposed model are estimated by using methods given in Stewart and Rosowsky (1998) and CEB-FIP (1990). From the results in Figure 4.3, the predicted bursting pressure exerted by the accumulation of the corrosion

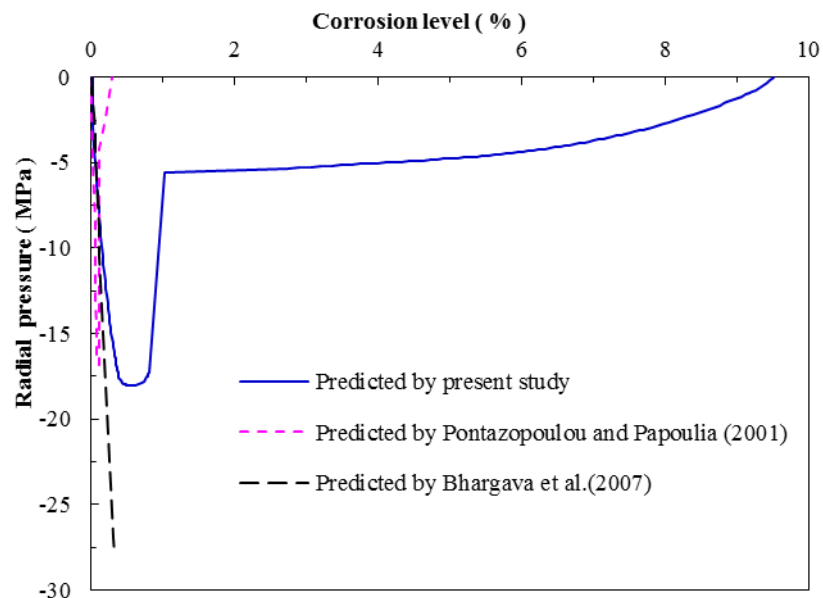


**Figure 4.3** Predicted radial corrosion pressure at bond interface as a function of corrosion level, compared with other analytical results

products at the bond interface has a maximum value of 17.9 MPa at the corrosion level of 0.66% at the time when crack front propagates to about 2/3 of the cover. When cracking approaches the cover surface, a sudden release of the corrosion pressure takes place and the residual pressure maintains only less than a third of the maximum value. As corrosion further progresses the corrosion pressure gradually decays to zero until crack width reaches the ultimate cohesive value. The bursting pressure predicted by Pantazopoulou and Papoulia (2001) gives a close maximum value but vanishes completely once crack front reaches the cover surface, since the residual strength of the cracked cover concrete is not considered in their study. The prediction of radial pressure by Bhargava et al. (2007) increases steadily as corrosion level increases, without considering the effects of cracking in the surrounding concrete and the tension softening of the cracked concrete. As demonstrated in the experimental investigations by Law et al. (2011), substantial residual bond strength exists for both with and without steel stirrups after cracks appear on the cover surface, and then the bond strength gradually decreases to a smaller value even at concrete crack width of 1.4 mm. Therefore, the proposed analytical model gives more appropriate predictions for corrosion pressure at the bond interface since the realistic properties of the cracked concrete, such as anisotropic behaviour, cohesive cracking, residual tensile strength and reduced tensile stiffness, are considered in the proposed model.

#### *4.7.2 Comparison of bond strength degradation with existing models*

The results for the ultimate bond strength predicted by the proposed analytical model are now further compared with the experimental data by Lee et al. (2002) and analytical results by Bhargava et al. (2007), as shown in Figure 4.4.

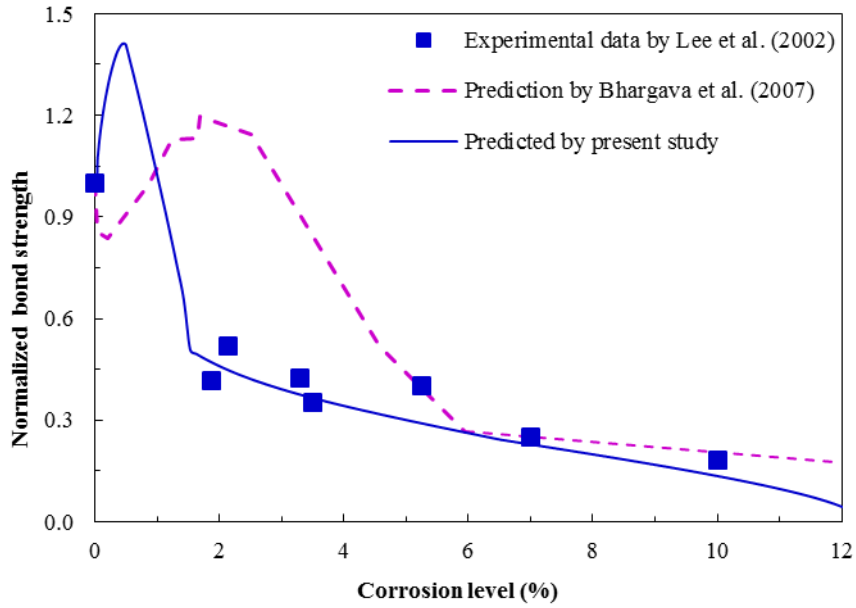


**Figure 4.4** Predicted ultimate bond strength as a function of corrosion level, compared with other analytical results and experimental data

As mentioned earlier in Chapter 2, Lee et al. (2002) undertook the pull-out tests to study rebar corrosion induced bond strength deterioration. A single rebar of a diameter of 13 mm was centrally embedded in the concrete cube of 65 mm in dimensions with a clear cover of 39 mm. The compressive strength of concrete was measured 42.1 MPa, which is utilized for evaluating necessary concrete parameters for calculations. Concrete fracture energy  $G_F = 190$  N/m and the volume ratio of the corrosion products is taken as  $\gamma_{vol} = 2.5$  are adopted. Then a curve for the ultimate bond strength evolution is obtained from the proposed model as reinforcement corrosion progresses. In Figure 4.4, the vertical axis represents the normalized residual bond strength, which has been calculated by dividing the ultimate bond strength of corroded element ( $T_{ubx}$ ) by the ultimate bond strength of non-corroded element ( $T_{ubo}$ ). The ultimate bond strength of non-corroded element has been evaluated from equation (4.1) considering corrosion level ( $X_p$ ) and its corresponding corrosion depth ( $x$ ), radial displacement ( $u_{bx}$ ) and

crack width at rebar surface ( $w_{bx}$ ) equal to zero. Similarly, the normalized bond strength of Lee et al. (2002) and Bhargava et al. (2007) is also evaluated by dividing the bond strength of corroded specimen by non-corroded specimen. The results show that the proposed analytical model can provide predictions in better agreement with the experimental data, comparing with the analytical results by Bhargava et al. (2007). Again, this is because the proposed model adopts more realistic estimates of concrete properties, by considering the anisotropic nature of the cracked concrete and the influence of concrete crack growth.

#### *4.7.3 Role of each stresses in contribution of residual bond strength*

Figure 4.5 shows the predicted results for the ultimate bond strength and its components, contributed by adhesion, confinement and corrosion pressure, as a function of corrosion level. As mentioned in Chapter 2, Auyeunga et al. (2000) conducted experiments to measure the bond strength of concrete specimens without transverse reinforcement stirrups due to rebar corrosion. In their experiments, the dimensions of the concrete specimens were measured as 175 mm×175 mm×350 mm, and a bar of a diameter of 19 mm was placed at the centre of the specimen. The compressive strength of concrete was taken as 28 MPa, which is here again used for estimating other concrete parameters required in the calculations by using maximum aggregate size of 16 mm. Concrete fracture energy  $G_F = 190$  N/m and the volume ratio of the corrosion products  $\gamma_{vol} = 2.5$  are adopted. The predicted ultimate bond strength matches well with the experimental results of Auyenga et al. (2000) at various corrosion levels.

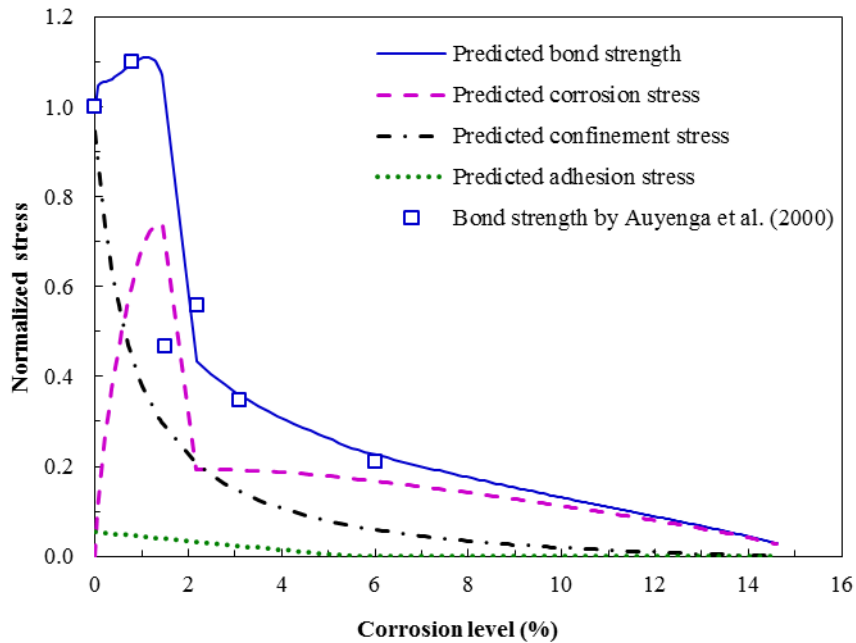


**Figure 4.5** Analytically predicted various contributions of ultimate bond strength as a function of corrosion level, compared with the experimental results of Auyunga et al.

(2000)

From the results, the confinement and the corrosion pressure have major contributions to the ultimate bond strength. As reinforcement corrosion progresses, the relatively small contribution of adhesion stress gradually decreases to zero, while the contribution of confinement from the surrounding concrete drops fast at low corrosion level and then gently vanishes at high corrosion level. This may be due to many factors caused by the reinforcement corrosion and concrete cracking, such as reduction in geometrical properties of the ribs of deformed rebar, deterioration of mechanical interlocking caused by accumulating corrosion products, growth of concrete crack width at the rebar surface, and decrease in the residual strength of the cracked concrete. However, the contribution of corrosion pressure at the bond interface increases in the early stage of the crack propagation phase, but has a sharp drop when concrete cracking approaches the cover surface and then gradually decays with increase of corrosion level. The

reason for the initial increase of corrosion pressure contribution is that the bursting stress at the rebar surface caused by the expansive corrosion products increases in the early stage of crack propagation phase, as shown in Figure 4.5, and the roughness of rebar may also increase in this stage. As corrosion level further increases, the corrosion pressure contribution decreases gradually to zero at the corrosion level of approximately 15%.

#### **4.8 Case-study of Ullasund Bridge**

In order to obtain the better understanding of the bond strength behaviour of corroding rebar in reality, a case study is undertaken here to demonstrate the applicability of the proposed model for evaluating bond strength deterioration of corroded RC structures. The field data of the Ullasund Bridge, Norway, published by Horringmoe et al. (2007), are considered in analysis. The Ullasund Bridge was demolished in 1998, only after 29 years of service in harsh environments. From the pieces of concrete collected from the demolished Ullasund Bridge, a total number of 22 cubic specimens with dimensions of 150 mm × 150 mm × 150 mm and single ribbed rebar of diameter 25 mm were prepared for investigations. The yield strength of the rebar was measured as 400 MPa and the compressive strength of the concrete was 40.3 MPa. Bond strength of each specimen was evaluated by pull-out test and the corresponding corrosion level was determined by sandblasting method. Due to lack of details in situ measured material properties, some material properties required for this analytical model are assumed such as  $G_F = 200$  N/m and the volume ratio of the corrosion products is taken as  $\gamma_{vol} = 2.0$ . Corrosion current density of  $1 \mu\text{A}/\text{cm}^2$  is considered, representing nominal amount of mean annual current density measured in field structures (Broomfield , 1997). Here

again, the equivalent critical crack width  $w_{cr} = 0.2$  mm and ultimate crack width  $w_u = 1.6$  mm are obtained from CEB-FIP (1990) for the corresponding concrete compressive strength and the adopted maximum aggregate size  $D_a = 16$  mm. Other parameters such as concrete tensile strength  $f_t = 4.6$  MPa and modulus of elasticity of the concrete  $E_c = 37.1$  GPa are obtained from EC2 (2004).

#### *4.8.1 Effect of reinforcement corrosion on residual bond strength*

The predicted results of residual bond strength as a function of corrosion level ( $X_p$ ) in percentage are shown in Figure 4.6, and are compared with the field data of the Ullasund Bridge. The predicted results are in good agreement with the available field data. The analytical prediction by this study shows that at the low corrosion level (<1%) there is about 40% increase in bond strength, but further increase in corrosion leads to significant reduction in bond strength as observed in the field data. As discussed earlier, this rapid reduction in bond strength is associated with many factors, including loss of mechanical interlocking, reduction in friction and confinement stress acting at the bond interface, and widening of cracks in the concrete cover. The predicted bond strength after the corrosion level of 2.5% is slightly lower than field data. This may be due to the difference between the material properties of the concrete assumed in the present model and the actual material properties of the Ullasund Bridge. The difference may be also due to the complexity of the reinforcement corrosion and cover cracking mechanism in reality. However, it clearly shows that the bond strength of RC structures exposed in aggressive environment is seriously affected by reinforcement corrosion.

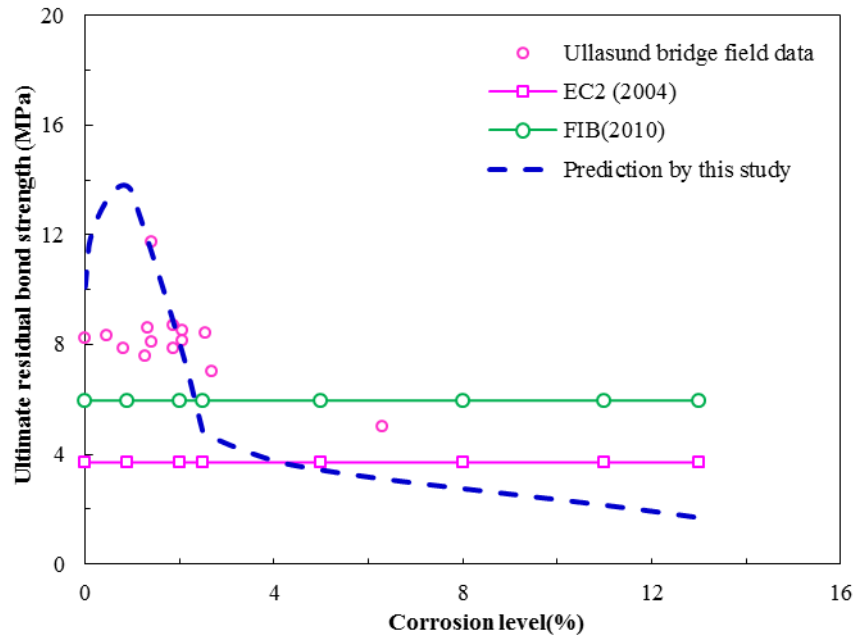


**Figure 4.6** Residual bond strength versus corrosion level, compared with available filed test data of the Ullasund Bridge and with the ultimate bond strength values given by EC2 (2004) and FIB (2010)

In order to compare the results of bond strength deterioration predicted by present study with the bond strength given by design codes, the predicted results are compared with the maximum ultimate bond strength ( $T_{ub,max}$ ) and design ultimate bond strength ( $T_{ub,des}$ ) of intact rebar given by FIB (2010) and EC2 (2004). The design values are evaluated by using empirical equations  $T_{ub,max} = 5(f_{ck}/20)^{1/4}$  and  $T_{ub,des} = 0.315(f_{ck})^{2/3}$ , as given in design codes, respectively. It is interesting to see that at about 2.5% corrosion level the specimen reaches the value of  $T_{ub,max}$  whereas at about 4% corrosion level it reaches the value given by  $T_{ub,des}$ .

#### 4.8.2 Effect of cover surface defects on residual bond strength

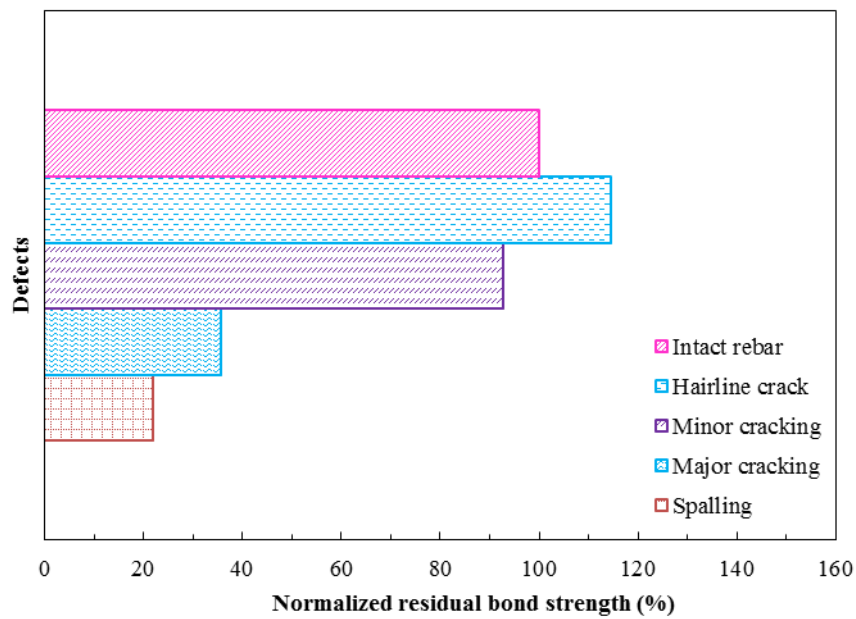


**Figure 4.7** Normalized residual bond strength versus cover surface defects of the Ullasund Bridge

Influence of cover concrete cracking on the residual bond strength is presented in Figure 4.7. Here the cover surface cracking is represented by defects in the concrete cover surface and is defined as in Chapter 3. From the results it is clear that the defects at the concrete cover surface have considerable effect on residual bond strength maintaining only 20% of the initial strength when the cover defect reaches at the stage of spalling.

#### 4.8.3 Effect of concrete geometry on residual bond strength

In absence of transverse reinforcement, the confinement stress is only contributed by concrete cover. Hence it is beneficial to understand the role of cover depth on bond strength deterioration of corroded RC elements. However systematic studies on the

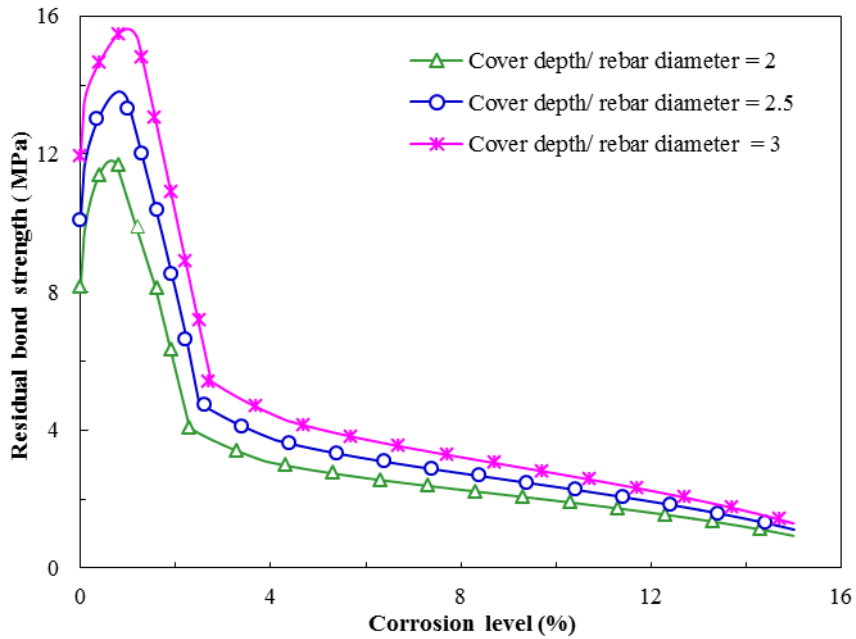


**Figure 4.8** Predicted residual bond strength versus corrosion level for various cover depth to rebar diameter ratios of the Ullasund Bridge

effect of cover depth to rebar diameter ratios ( $C/D_b$ ) are relatively limited. Therefore the effect of cover depth on the bond strength deterioration process is now studied in Figure 4.8 and Figure 4.9. In the analysis, cover depth to rebar diameter ratios ( $C/D_b$ ) of 2, 2.5 and 3.0 are considered.

The results in Figure 4.8 and Figure 4.9 indicate that the predicted bond strength increases as the cover depth to rebar diameter ratio increases. As shown in Figure 4.8, up to a corrosion level of 1.5%, bond strength increases and then decreases for a given corrosion level. For instance, the bond strength of intact rebar increased from 8 MPa to 12 MPa, when  $C/D_b$  ratio is increased from 2 to 3. When corrosion level reaches at 4%, in case of lower  $C/D_b$  ratio (i.e.  $C/D_b = 2.0$ ) only 3 MPa of bond strength is maintained whereas bond strength of approximately 3.7 MPa is maintained in higher

$C/D_b$  (i.e.  $C/D_b = 3.0$ ). This indicates that at higher level of corrosion the influence of the  $C/D_b$  ratio on bond strength of corroded rebar is not significant as that in the intact rebar. This pattern is similar to the finding of experimental studies conducted by Al-Sulaimani et al. (1990) and Rodriguez et al. (1994). In all three cases of cover depths, as the corrosion progresses, cracking in concrete cover increase which ultimately decreases the bond strength. Furthermore, the bond strength in all three cases decreases dramatically when crack width is approximately 0.2 mm. It is interesting to see that in all three cases of cover depth the bond strength becomes negligible when crack width reaches its ultimate cohesive value. This may be due to the significant reduction in confinement stress caused by the formation of wider crack opening.

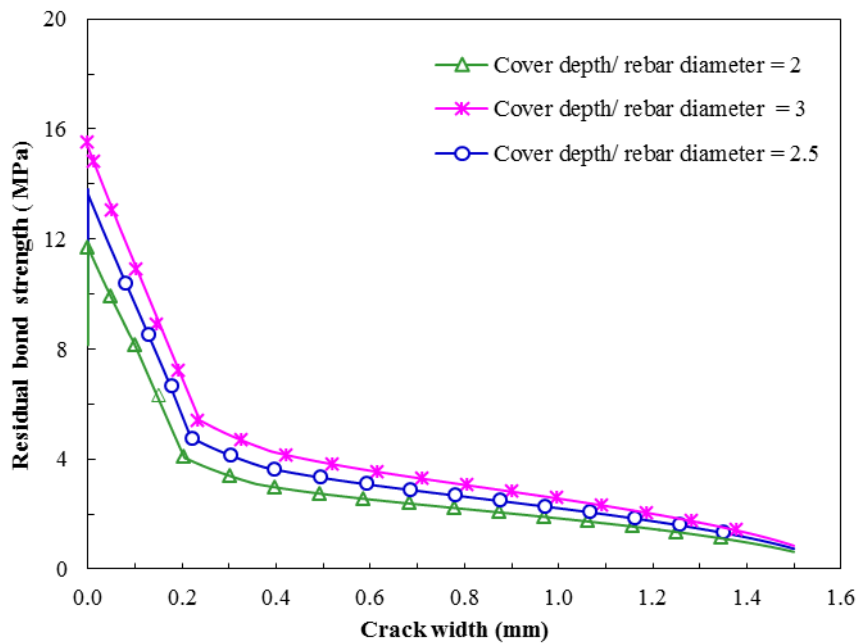


**Figure 4.9** Predicted residual bond strength versus cover surface crack width for various cover depth to rebar diameter ratios of the Ullasund Bridge

## 4.9 Numerical example 2

In this section the methodology mentioned in the preceding sections is applied to analyse the role of transverse reinforcement on residual bond strength capacity of corrosion affected RC beam. A numerical example of simply supported RC beam of 5.0 m span of a bridge exposed to an aggressive environment is now utilised. The cross-sectional width and effective depth of beam are  $b = 300$  mm and  $d = 560$  mm, respectively. Four steel rebars with diameter  $D_b = 16$  mm are provided as the tensile reinforcement and two rebars of diameter  $D_b = 12$  mm are provided as the compressive steel with clear cover thickness  $C = 40$  mm along with the stirrup of diameter  $D_{st} = 8$  at spacing of 50 mm and is subjected to mean annual corrosion current per unit length  $i_{corr} = 6 \mu\text{A}/\text{cm}^2$ . Volume ratio of corrosion product is considered as 2.5. The characteristic compressive strength of concrete is assumed as  $f_{ck} = 40$  MPa and corresponding concrete properties such as tensile strength and modulus of elasticity are obtained from EC2 (2004). The critical and ultimate cohesive crack width required for this study have been obtained from CEB-FIP (1990) for adopted fracture energy of 190 N/m and maximum aggregate size of 16 mm.

### 4.9.1 Effect of reinforcement corrosion on residual bond strength

The effect of reinforcement corrosion on unconfined and confined specimens is presented in Figure 4.10 and 4.11 respectively. In Figure 4.10, here again normalized residual bond strength as a function of corrosion level predicted by present study is plotted in Figure 4.10 and then compared with the published experimental and field test data available from various references (Al-Sulaimani et al. 1990, Almusallam et

al.1996, Auyeung et al. 2000, Chung et al. 2008a, Lee et al. 2002, Law et al. 2011, Rodriguez et al. 1994, Fang et al. 2004, Mangat and Elgarf 1999a, Zhao et al. 2013).

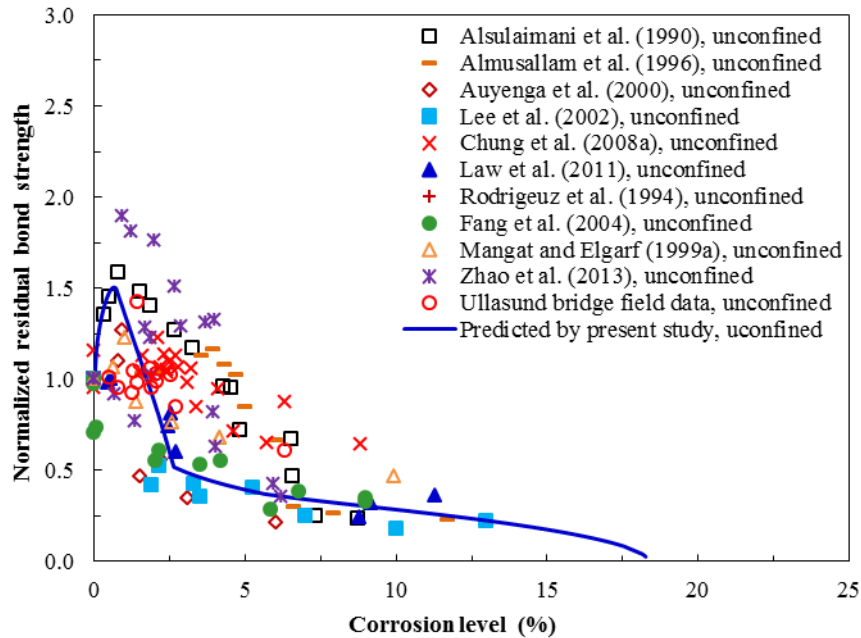


**Figure 4.10** Analytical prediction of normalized residual bond strength versus corrosion level for unconfined beam, compared with experimental test results available from various sources

In these experimental studies, different test specimens with rebar diameters ranging from 8 up to 25 mm and with cover to rebar diameter ratio of 1.0 to 7.5 were utilised. Furthermore, significant variations are also found on the concrete compressive strengths ranging from 30 to 70 MPa. The impressed current densities also varied over a wide range with the values between 0.1 and 30 mA/cm<sup>2</sup>. Therefore, as expected, although the results of published experimental data presented in Figure 4.10 demonstrate a significant scatter, they concluded that the corrosion of reinforcement has considerable influence on bond strength of unconfined specimen. Here again, the trend of bond strength evolution predicted by the present study is in good agreement with the

experimental data. At low corrosion level (<1%), bond strength increases by about a half but further increase in corrosion leads to considerable reduction of bond strength and becomes negligible when corrosion level is about 18%. This rapid reduction in bond strength is associated with many factors including reduction of corrosion and confinement stresses. It is interesting to see that the trend of bond strength deterioration reported in the field study of Ullasund Bridge (Horringmoe et al. 2007), is close to that of the laboratory experimental data published in other references.

Transverse reinforcement provides additional confinement to the longitudinal reinforcement. Therefore the study on role of transverse reinforcement (stirrup) in bond strength deterioration is of great importance. However, comparatively fewer experimental studies are available for specimens with transverse reinforcement than for specimens without transverse reinforcement. In order to study the behaviour of bond strength deterioration of confined specimen (with stirrup), the residual bond strength of confined specimen predicted by the present analytical study is plotted in Figure 4.11 as function of corrosion level and compared with the published experiment data obtained from various reference literatures (Rodriguez et al. 1994, Fang et al. 2004, Shima 2001). These investigations made use of rebar with diameters in the range 12 to 20 mm, with cover depth to rebar diameter ratios  $C/D_b$  between 1.2 to 5.0 and varying with. The use of transverse reinforcement also varied from 6 mm to 10 mm diameter at distance of 40 mm to 100 mm. Concrete compressive strength ranged from 30 to 52 MPa and the impressed current densities varied between 0.1 and 30 mA/cm<sup>2</sup>. In general the predicted trend for residual bond strength deterioration of unconfined specimen with respect to corrosion level agrees well with the available experimental data. As expected, the bond strength is better maintained in specimen with transverse

reinforcement than in specimens without such reinforcement, due to the confinement provided by the transverse reinforcement. Hence, the beneficial effect of stirrups is that it limits and delays the bond strength deterioration but it is still unavoidable at high corrosion level.

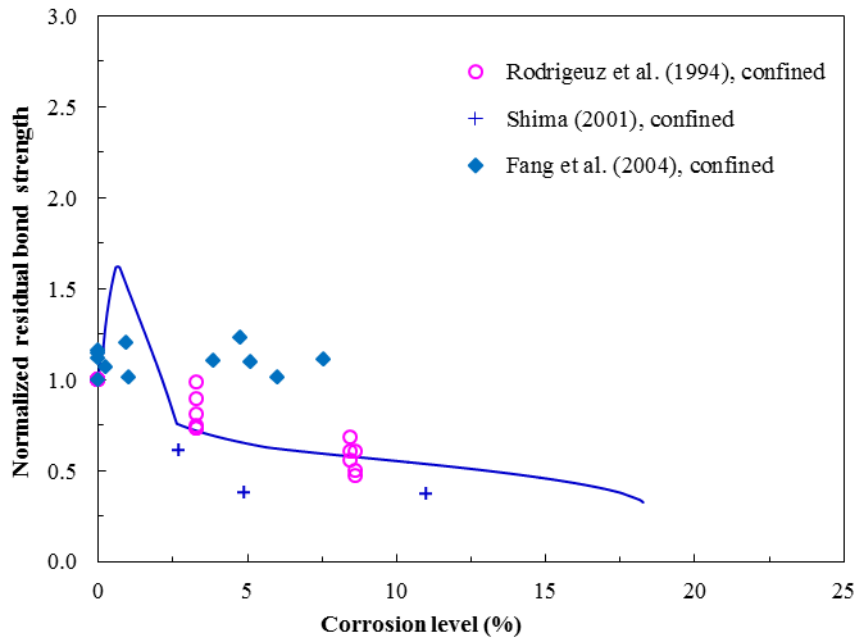


**Figure 4.11** Analytical prediction of normalized residual bond strength versus corrosion level for confined beam, compared with experimental test results available from various sources

#### 4.9.2 Effect of cover surface cracking on residual bond strength

Cracking in the concrete cover is only the visible sign of defects caused by reinforcement corrosion. Moreover, cracking in concrete cover is an important parameter which helps in condition monitoring of the RC structures. . It is necessary to predict the internal damages such as residual strength deterioration from the observable surface condition during the routine inspection or maintenance process. Therefore, it is

always beneficial to establish a prediction method to quantitatively assess the structural performance by assessing cracking in the concrete cover. Hence in this section, effect of cracking in the concrete cover surface on bond strength behavior of unconfined and confined specimen is presented in Figures 4.12 and 4.13 respectively.

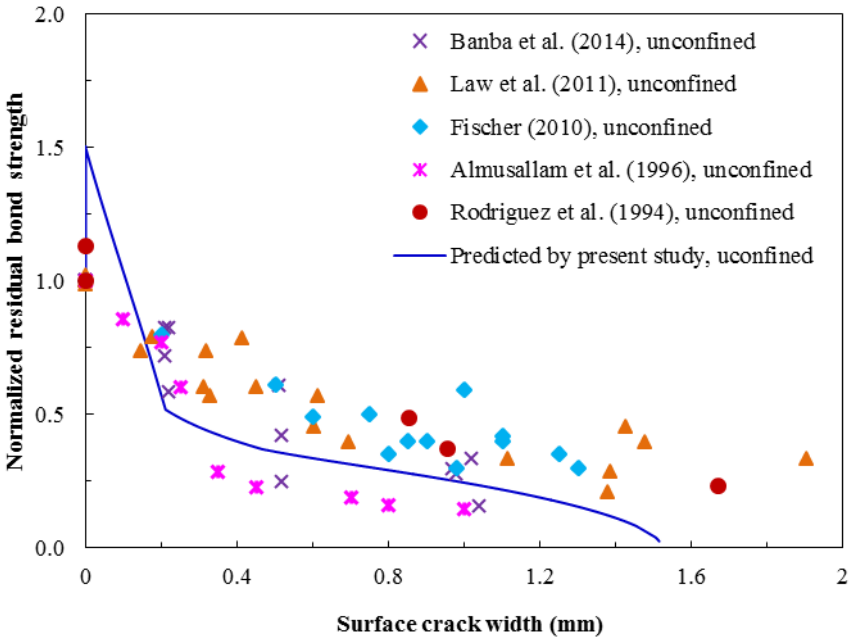


**Figure 4.12** Analytical prediction of normalized residual bond strength versus surface crack width for unconfined beam, compared with experimental test results available from various sources

The results of normalized residual bond strength versus surface crack width for unconfined specimen predicted by the present analytical study are plotted in Figure 4.12 and compared with the published experiment data obtained from various reference literatures (Banba et al. 2014, Law et al. 2011, Fischer 2010, Almusallam et al. 1996, Rodriguez et al. 1994). Here again, the trend of bond strength deterioration with increase in surface crack width predicted by the present study is in good agreement with the experimental investigations of the reference literatures. At the initial stage of

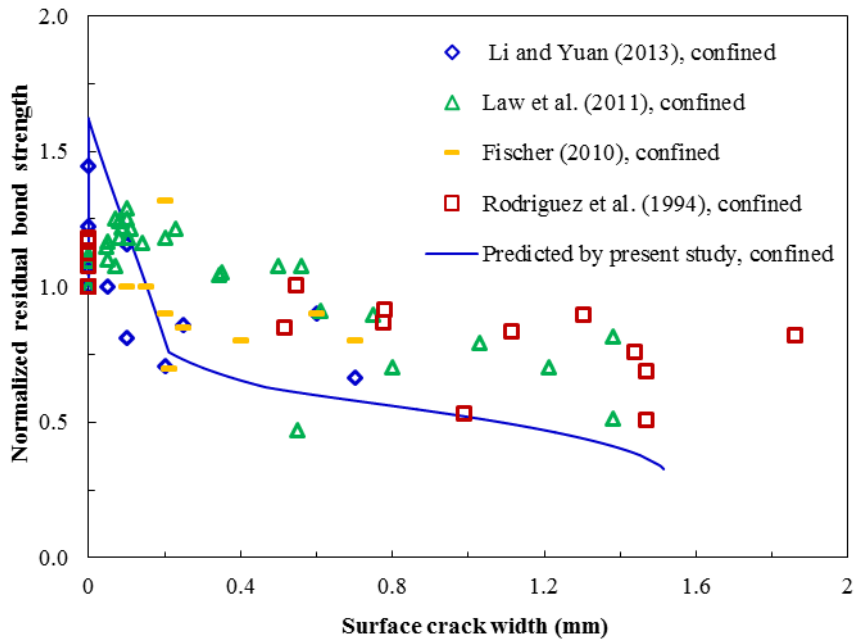


**Figure 4.13** Analytical prediction of normalized residual bond strength versus equivalent cover surface crack width for confined beam, compared with experimental test results available from various sources

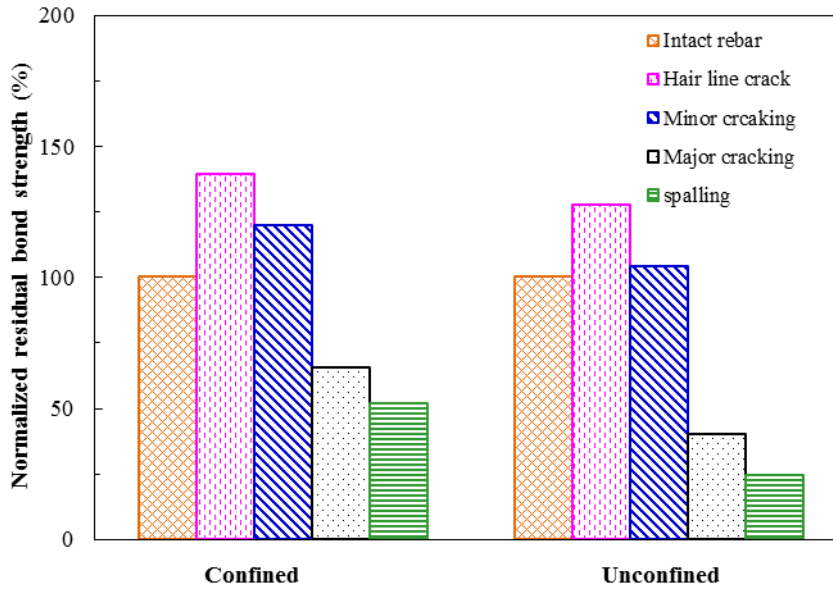
surface cracking the bond strength is about 50% higher than that in the non-corroded stage. It decreases considerably with further increase in surface crack width and lost 50% of initial strength (non-corroded) stage when the surface crack width is about 0.2 mm. Further progress of cracking causes significant reduction in bond strength and when the crack width is approximately 1.5 mm, the bond strength of unconfined specimen becomes negligible

Figure 4.13 shows the residual bond strength of confined specimen predicted by the present analytical study as function of surface crack width and compared with the published experiment data obtained from various references (Li and Yuan 2013, Law et al. 2011, Fischer 2010, Rodriguez et al. 1994). Despite the lower value of normalized residual bond strength in predicted results, in general the predicted trend for residual

bond strength deterioration of unconfined specimen with respect to surface crack width agree well with the available experimental data. The lower value of normalized residual bond strength might be due to the difference in material properties, concrete geometry and the rate of corrosion density adopted in this study and that used in the experimental investigations. At the initial stage of surface cracking the bond strength is about 60% higher than that in the non-corroded stage. It decreases considerably with further increase in surface crack width and lost 70% of initial strength (non-corroded) stage when the surface crack width is about 1.5 mm.

Similarly to the case for unconfined specimen, in Figure 4.13, the residual bond strength of confined specimen decreases with increase in surface crack width. But in case of confined specimen residual bond strength still exist when crack width is about 1.5 mm (ultimate cohesive value). This is due to the fact that in confined specimen stirrup provides some residual confining action together with the cracked concrete cover. Hence, the results from Figure 4.12 and Figure 4.13 show that at same value of surface crack width, unconfined specimen is more vulnerable than confined specimen.

Influence of different types of cover surface defects on the bond strength of corroded RC beam is presented in Figure 4.14. Here again the cover defects have the same definition as in Chapter 3. From the results, till minor cracking in the concrete cover, there is increase in residual bond strength of both confined and unconfined specimens. As the defects reach to major cracking stage, bond strength decreases significantly. At this stage of defect (major cracking), 51% of the initial bond strength is maintained in confined specimen whereas only 24% of its initial strength is maintained in unconfined specimen. This clearly shows that, defects in concrete cover have significant effect on



**Figure 4.14** Normalized residual bond strength versus cover surface defects for confined and unconfined beam

residual bond strength of corroded RC beam. Additionally, the results from Figure 4.14 show that at the same stage of defects in the concrete cover, unconfined concrete is more susceptible than confined concrete, as expected.

#### 4.10 Summary and conclusions

In this section a new analytical method for predicting the ultimate bond strength evolution in corrosion damaged RC structures is proposed on the basis of the thick walled cylinder model and the use of realistic concrete properties. The governing analytical formulations for adhesion, confinement and corrosion stresses have been proposed, which directly depend on crack developed in concrete cover. The proposed model can provide reliable results for residual bond strength as reinforcement corrosion progresses, which agree well with the experimental and field data available from various sources. Furthermore, role of cover surface crack width on bond strength

deterioration has also been analysed. The behaviour of confined and unconfined specimen with increase in surface crack width has also been investigated.

From the results obtained by the proposed analytical model, following conclusions can be drawn: a) The process of bond strength evolution caused by reinforcement corrosion can be described as three phases associated with crack development in the cover concrete, i.e. crack initiation phase, crack propagation phase and residual life phase; b) The ultimate bond strength increases at low level of reinforcement corrosion (typically less than 1-2%) during the crack propagation phase, but decreases significantly when concrete cracking propagates to the cover surface and then gradually decays to zero at the time when crack reaches the ultimate cohesive width for unconfined specimen; c) When surface crack width reaches its ultimate cohesive value, confined specimen still possess 30% of its initial strength whereas no residual bond strength is observed in unconfined specimen and it has also been found that increasing cover depth residual bond strength increases at uncorroded stage and in residual life phase the bond strength deteriorates with the same gradient; d) The confinement from steel stirrups and defects in concrete cover makes significant changes to the ultimate bound strength, in particular to the residual bond strength during the residual life phase when the cover concrete is completely cracked.

## **Chapter 5 Development of Flexural Strength Degradation Model**

### **5.1 Introduction**

Corrosion of reinforcement affects the performance of corroded RC structures in different ways. They mainly depend on the loss of rebar area, cracking in concrete cover and bond strength degradation between rebar and concrete. Corrosion progress in concrete structures further affects the mechanical properties of both concrete and reinforcement. These changes in mechanical properties along with decreasing size of the rebar and increasing crack width in the concrete cover can lead to significant reduction in the residual load carrying capacity and stiffness of the RC structures (FIB 2010, Du et al. 2005, Pantazopoulou and Papoulia 2001). Moreover loss of bond at the bond interface between reinforcement and surrounding concrete indicates that the design guidance for ultimate moment resistance, which are dependent on strain compatibility at all sections, may become invalid and shift to a new compatibility condition. This in turn changes the overall behaviour of the RC structures.

From comprehensive literature review presented in Chapter 2, it can be concluded that many investigations have been carried out during the last decades regarding the prediction of corrosion initiation but comparatively fewer investigations have been carried out in corrosion propagation and even less with the residual structural capacity of the corroded RC structure. Limited studies have been carried out to investigate the effect of reinforcement corrosion on the mechanical characteristics and load carrying capacity of corroded RC structures where reinforcing bars were corroded by using accelerated corrosion techniques (Azad et al. 2010, Chung et al. 2008b, Zhang et al.

2012). Few attempts have also been made to develop theoretical methods for predicting the residual flexural strength of corroded RC structures (EI Maaddawy et al. 2005a, Wang and Liu 2010, Bhargava et al. 2007, Yang et al. 2013). However, the influence of bond strength loss on the residual flexural strength of corroded structures is not well understood. This chapter presents a simple analytical method for estimating the load carrying capacity of corrosion damaged concrete structures by considering different failure modes. The applicability of the proposed model is then demonstrated by comparing its predictions with the published experimental data available.

## **5.2 Mechanism of flexural strength of corroded RC beam**

In flexural analysis of any structural elements, defining the mechanical properties of concrete and steel is the first step. The mechanical properties of concrete and steel are generally analysed with the help of stress-strain curves. These curves are basically in an idealized form which can be used in the analysis of the RC elements. Here, the mechanical properties of concrete and steel are defined as mentioned in the EC2 (2004). To consider the effect of bond strength degradation on evaluating flexural strength of corroded RC beams, a typical cross section of doubly reinforced RC beam, as shown in Figure 5.1(a), is now considered. The strain and stress distribution across beam section under initial un-corroded condition of rebar are shown in Figures 5.1 (b) and Figure 5.1 (c) respectively, as given by Eurocode 2.

The symbols used in Figure 5.1 are defined as:  $b$  = width of beam;  $D$  = overall depth of the beam;  $d$  = effective depth of beam;  $d'$  = distance from centroid of the compression rebar to edge of the compression fibre;  $A_b$  = initial area of un-corroded

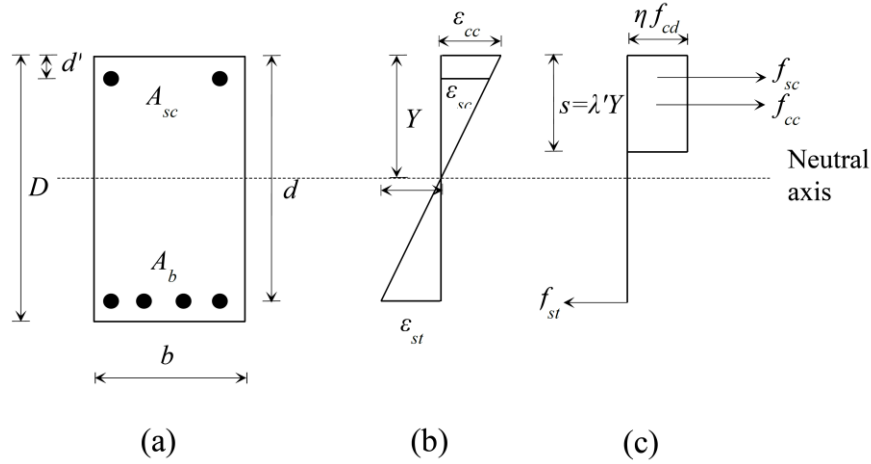


**Figure 5.1** Flexural analysis of a RC beam section: (a) typical cross section of RC beam, (b) strain distribution, (c) equivalent stress distribution

tensile steel rebar ;  $A_{sc}$  = initial area of un-corroded compression rebar with diameter of  $D_{sc}$ ;  $\epsilon_{cc} = 0.0035$  is ultimate tensile or compressive strain of concrete;  $\epsilon_{st}$  = strain of tensile rebar;  $\epsilon_{sc}$  = the strain of compression rebar respectively;  $Y$  = neutral axis depth from the edge of compression zone;  $f_{st}$  = tensile force acting at the centroid of tensile steel;  $f_{cd} = \alpha_{cc} f_{ck} / \gamma_c$  is the design strength of the concrete in which  $\alpha_{cc}$  is the constants taken as 0.85 for  $f_{ck} \leq 50$  MPa,  $f_{ck}$  is the characteristic compressive strength of the concrete and  $\gamma_c$  = partial factor of safety of the concrete taken as 1.5;  $s$  is the equivalent compression zone given by  $s = \lambda' Y$ ;  $\eta$  and  $\lambda'$  are the coefficients taken as 1 and 0.8 for  $f_{ck} \leq 50$  MPa. In this study concrete strength of  $f_{ck} \leq 50$  MPa is considered, as these are the concrete most commonly used in reinforced concrete construction. Analysis of concrete classes higher than 50 MPa can be easily done by defining parameters  $\epsilon_{cc}$ ;  $\eta$  and  $\lambda'$  for that particular strength. From Figure 5.1, in

uncorroded perfectly bonded beam the flexural strength of the RC beam can be evaluated by using condition of equilibrium, expressed here as

$$M_{uo} = f_{cc} \left( d - \frac{s}{2} \right) + f_{sc} (d - d') \quad (5.1)$$

where  $f_{cc} = \eta\lambda f_{cd} b Y$  is the compressive force of the concrete and  $f_{sc} = f_{yd} A_{sc}$  is the resultant compressive force in compression reinforcement. As there is the compatibility of strains between the reinforcement and adjacent concrete, steel strain in tension and in compression can be determined from the strain diagram of Figure 5.1(b), expressed here as

$$\frac{\varepsilon_{st}}{\varepsilon_{cc}} = \frac{d - Y}{Y}, \quad \frac{\varepsilon_{sc}}{\varepsilon_{cc}} = \frac{Y - d'}{Y} \quad (5.2a,b)$$

In intact condition, without rebar corrosion, the ultimate bond strength  $T_{ub,rqd}$  and the corresponding development length  $l_d$  required to prevent anchorage (bond) failure of the tensile steel rebar can be obtained from design codes such as EC2 (2004), expressed here as

$$T_{ub,rqd} = \frac{f_{yd} D_b}{4 l_d}, \quad l_d = \alpha_{bd} \frac{D_b f_{yd}}{4 f_{bd}} \quad (5.3a, b)$$

where  $f_{yd}$  is the design strength of tensile steel rebar given by  $f_{yk} / \gamma_s$  in which  $f_{yk}$  is the characteristic tensile strength and  $\gamma_s = 1.15$  is the partial factor of safety of the steel

rebar;  $f_{bd}$  is design bond strength obtained from  $f_{bd} = 0.315 f_{ck}^{0.67}$  for concrete strength  $f_{ck} \leq 60$  MPa and rebar diameter  $D_b \leq 32$  mm; and  $\alpha_{bd}$  is the coefficient depending on many factors including the shape of anchorage, types of confinement provided by the stirrups and concrete cover. During the process of reinforcement corrosion, when the existing ultimate bond strength of corroded rebar ( $T_{ubx}$ ) is sufficient to prevent the RC beam from the bond failure ( $T_{ub,rqd}$ ), the flexural capacity of the RC beam can be obtained by the conventional method based on compatibility condition. Therefore, in this stage any reduction of flexural strength is caused by the cross-sectional area loss of the rebar. Then the residual flexural strength can be evaluated by utilising the concept given by Cairns and Zhao (1993) that the corroded beam still follows the condition of equilibrium of resultant tensile and compressive forces acting at the beam section.

$$M_{ux} = f_{ccx} \left( d_x - \frac{s_x}{2} \right) + f_{scx} (d_x - d'_x) \quad (5.4)$$

where  $f_{ccx} = \eta \lambda f_{cd} b Y_x$  is the resultant compressive force of the concrete and  $f_{scx} = f_{yd} A_{scx}$  is the compressive force of the compression steel associated with corrosion. In equation (5.4) the parameters have the same definitions as that in equation (5.1) and quantities with subscript  $x$  are associated with corrosion level  $X_p$ . The evaluation of compression and tension force depends on failure modes and corresponding yielding of steel and concrete, this will be discussed in Sections 5.3 to 5.5.

### 5.3 Evaluation of flexural strength of corroded RC beam at bond failure

As the corrosion progresses, ultimate bond strength of the corroded reinforcement  $T_{ubx}$  decreases and will become less than the required bond strength  $T_{ub,rqd}$ . In this situation, due to insufficient bond strength at the bond interface, bond failure occurs. Hence the uniform tensile force  $f_{stx}$  generated in the corroded tensile rebar is governed by ultimate bond strength, given by

$$f_{stx} = n_b \pi D_{bx} l_d T_{ubx} \quad (5.5)$$

where  $n_b$  is the number of the bottom tensile rebar and  $T_{ubx}$  is the ultimate bond strength as defined in equation (4.1) of Chapter 4. Consequently strain acting at steel rebar is given by

$$\varepsilon_{stx} = \frac{f_{stx}}{A_{bx} E_{st}} \quad (5.6)$$

### 5.4 Evaluation of strain compatibility of corroded RC beam

In case of un-corroded perfectly bonded beam, strain compatibility at all sections exists as given by design codes. But due to the loss of bond strength over the region of corroded rebars, the compatibility condition of the perfectly bonded RC beam will shift to a new compatibility condition. In reality, corrosion of reinforcing bars may occur only within the partial length of the RC beam, such as in the area close to support and in the central part of beam (Castel et al. 2000, Tapan and Aboutaha 2008). Nevertheless, for simplicity whole length corrosion is considered in this study to define

the new compatibility condition of a corroded RC beam. Assuming the deformation of concrete at the rebar level is mainly due to plastic deformation occurring within the plastic equivalent region ( $L_{eq}$ ), a new strain compatibility condition of corroded RC beam can be expressed as (Wang and Liu 2010)

$$\frac{\varepsilon_{stx}}{\varepsilon_{ccx}} = g_x \frac{d_x - Y_x}{Y_x}, \quad \frac{\varepsilon_{scx}}{\varepsilon_{ccx}} = g_x \frac{Y_x - d'_x}{Y_x} \quad (5.7a,b)$$

The quantities with subscript  $x$  in equation (5.7) are associated with corrosion level  $X_p$  and the parameters have same meaning as that in equation (5.2).  $g_x$  is the interpolation factor between un-bonded and perfectly bonded beam given by

$$g_x = 1 - \left(1 - \frac{T_{ubx}}{T_{ubo}}\right) \left(1 - \frac{L_{eq}}{l_d}\right) \quad (5.8)$$

where plastic equivalent region  $L_{eq} = 9.3Y_x$  (Au and Du 2004),  $T_{ubo}$  is the ultimate bond strength of un-corroded rebar and can be obtained by considering corrosion level as zero in equation (4.1) of Chapter 4.

## 5.5 Evaluation of yielding of concrete and steel in corroded RC beam

Failure modes of flexural strain at compression fibre and tensile fibre can be determined by satisfying the limited values of  $\varepsilon_{stx}$ ,  $\varepsilon_{ccx}$  and  $\varepsilon_{scx}$  corresponding to  $\varepsilon_{cc} = 0.0035$  and  $\varepsilon_{st} = 0.002$  as given by EC2 (2004). Generally when tensile rebar

reaches its yielding stage, compressive rebar should reach its yielding stage (Mosley 2007). Therefore in this study yielding of tensile rebar is only considered.

*Failure mode 1:  $\varepsilon_{stx} \leq 0.002$  and  $\varepsilon_{ccx} \leq 0.0035$*

During the corrosion process, when anchorage failure occurs before yielding of the tensile rebar and the concrete (i.e.  $\varepsilon_{stx} \leq 0.002$  and  $\varepsilon_{ccx} \leq 0.0035$ ), the tensile stress acting along the corroded rebar  $f_{stx}$  is governed by the bond strength and hence can be evaluated from equation (5.5). From equilibrium of resultant tensile and compression forces acting at beam section, neutral axis depth  $Y_x$  is obtained from

$$Y_x = \frac{f_{stx} - f_{scx}}{\eta \lambda f_{cd} b} \quad (5.9)$$

where  $f_{scx} = f_{ydx} A_{scx}$  is the compressive force acting at the centroid of compression steel in which  $A_{scx}$  is the area of the compression steel,  $f_{ydx} = (1 - 0.5X_p) f_{yd}$  is the residual yield strength of corroded steel rebar corresponding to corrosion level  $X_p$  (Du et al. 2005). Hence, taking moment at the centroid of the tensile rebar, residual flexural strength of corroded RC beam can be evaluated by using equation (5.4)

*Failure mode 2:  $\varepsilon_{stx} > 0.002$  and  $\varepsilon_{ccx} \leq 0.0035$*

In case, when yielding of steel occurs before the bond failure (i.e.  $\varepsilon_{stx} > 0.002$  and  $\varepsilon_{ccx} \leq 0.0035$ ), tensile force is governed by the residual yield strength of the corroded rebar  $f_{ydx}$  and is obtained from  $f_{stx} = f_{ydx} A_{bx}$ . Then, from equilibrium of forces,  $Y_x$  in

equation (5.9) can be obtained by using the tensile force  $f_{stx}$ . Once  $Y_x$  is available the corresponding flexural strength is determined from equation (5.4).

*Failure mode 3:*  $\varepsilon_{stx} > 0.002$   $\varepsilon_{st} > 0.002$  and  $\varepsilon_{ccx} > 0.0035$

If both the tensile rebar and the concrete yield before anchorage failure (i.e.  $\varepsilon_{stx} > 0.002$  and  $\varepsilon_{ccx} > 0.0035$ ), strain of steel rebar will be governed by the yielding of the concrete. By using  $\varepsilon_{ccx} = \varepsilon_{cc} = 0.0035$ , strain of steel rebar  $\varepsilon_{stx}$  can be obtained from equation (5.7a), given by

$$\varepsilon_{stx} = \varepsilon_{cc} \frac{d_x - Y_x}{Y_x} g_x \quad (5.10)$$

The corresponding tensile stress  $f_{stx}$  and the neutral axis depth  $Y_x$  are then evaluated from equation (5.6) and equation (5.9), respectively and finally the corresponding flexural strength of corroded rebar is determined from equation (5.4).

## 5.6 Numerical example 1

### 5.6.1 Effect of reinforcement corrosion on residual strength

In order to demonstrate the effectiveness of the proposed approach, a typical corrosion affected RC beam used by Mangat and Elgarf (1999b) is employed in this study. In their experimental investigations a total of 111 under-reinforced RC beam specimens divided in nine groups (Group 1- Group 9), were subjected to accelerated corrosion damage and then tested under four point loading to evaluate the ultimate flexural

strength. In this study, Group 6 beam specimen is adopted for analysis, as shown in Figure 5.2. The RC beam was singly reinforced with two reinforcing bars as the tensile steel with clear cover depth of 20 mm and subjected to accelerated corrosion of 3 mA/cm<sup>2</sup>. The reinforcing bars were 10 mm in diameter and 1100 mm long, including the anchorage length in the form of U-shaped hooks at both ends. No stirrups were provided in the beam specimens, instead shear reinforcement was provided by means of external tubular collars so as to prevent shear failure and to ensure the development of full flexural resistance and typical flexural failure in the middle-third of beam span. The yield strength of the reinforcement was 520 MPa and the modulus of elasticity was 206 GPa. The average compressive strength of the concrete cubes after 28 days was 40 MPa and the maximum aggregate size was 10 mm. During the experiments, the failure of the corroded beams was initiated by bond failure at the longitudinal reinforcement interface. Therefore, the moment of resistance of the corroded beams was controlled by the bond of the rebars rather than the yielding of the tensile reinforcement at failure.

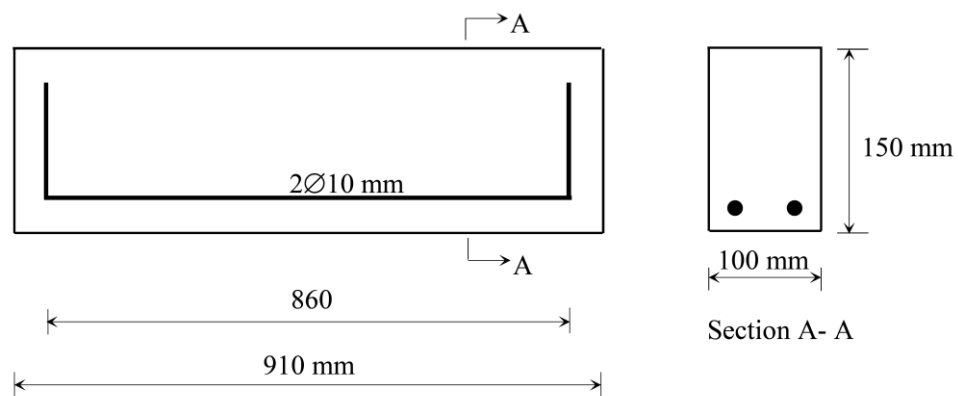


**Figure 5.2** A RC beam specimen and its cross section used in the experimental studies by Mangat and Elgarf (1999b)

For the purpose of analytical study, in this study, the unmeasured concrete properties are estimated or assumed for the experimental data available i.e. concrete fracture energy  $G_F = 160 \text{ N/m}$  and four numbers of cracks are assumed. The volume ratio of the corrosion products is also assumed as 3.0. The details of other material properties of the concrete considered for the validation of the proposed model are given in Table 5.1. Here again crack width in the cover concrete is represented by the equivalent crack width as defined in Chapter 3 as the cumulated crack width over the concrete cover.

**Table 5.1** Concrete material properties

Parameter	Symbol	Evaluation	Value	Reference
Compressive strength of cube	$f_{cu}$		40 MPa	
Compressive strength of cylinder	$f_{ck}$		37.5 MPa	[1]
Tensile strength	$f_t$	$0.39(f_{ck})^{2/3}$	4.4 MPa	[1]
Modulus of elasticity	$E_c$	$11.57(f_{ck} + 8)^{0.3}$	36.4 GPa	[1]
Ultimate crack width	$w_u$	$\alpha_f \frac{G_F}{0.3f_{ck}^{2/3}}$	0.37 mm	[2]
Critical crack width	$w_{cr}$	$2 \frac{G_F}{0.3f_{ck}^{2/3}} - 0.15w_u$	0.04 mm	[2]

Reference: (Eurocode 2, 2004) [1], (CEB-FIP, 1990) [2]

The residual flexural strength predicted by the present analytical method is plotted in Figure 5.3 as a function of the corrosion level and compared with the published experimental data of Mangat and Elgarf (1999b). In Figure 5.3, the horizontal axis represents the rebar mass loss in percentage as defined in equation (3.2) of Chapter 3

and the vertical axis represents the normalized residual flexural strength which is calculated by dividing the flexural capacity of corroded element by the capacity of the non-corroded element.

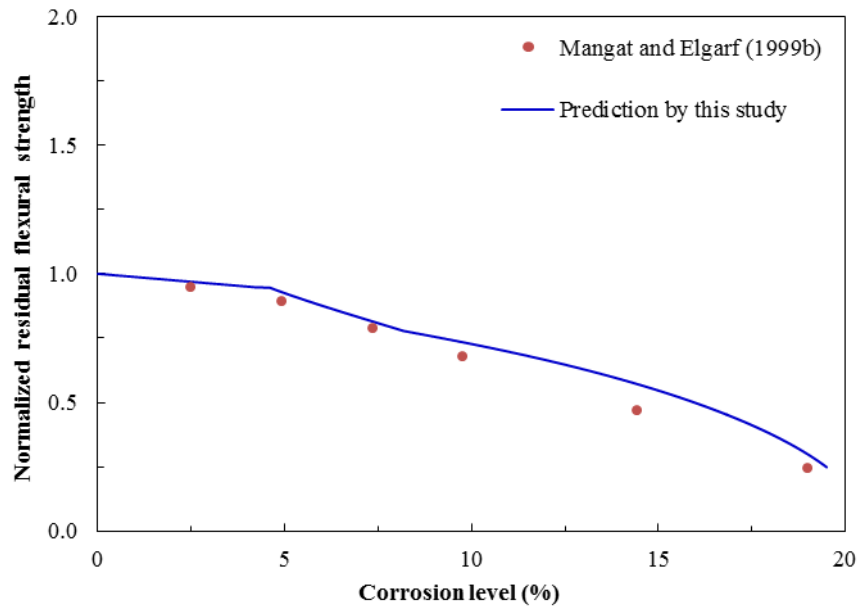


**Figure 5.3** Analytical prediction of normalized residual flexural strength versus corrosion level, compared with experimental test results of Mangat and Elgarf (1999b)

As shown in Figure 5.3, the flexural strength deterioration predicted by the present study is in good agreement with the published experimental data of Mangat and Elgarf (1999b). At initial corrosion stage, the flexural strength of the corroded beam remains almost the same as that for the un-corroded beam. When corrosion level reaches about 5% (critical point), considerable strength deterioration occurs maintaining only 25% of the strength at corrosion level of approximately 20%.

The results in Figure 5.4 show the deterioration process of bond strength and flexural strength caused by reinforcement corrosion. Here the normalized bond strength associated with corrosion level is obtained by dividing the ultimate bond strength of

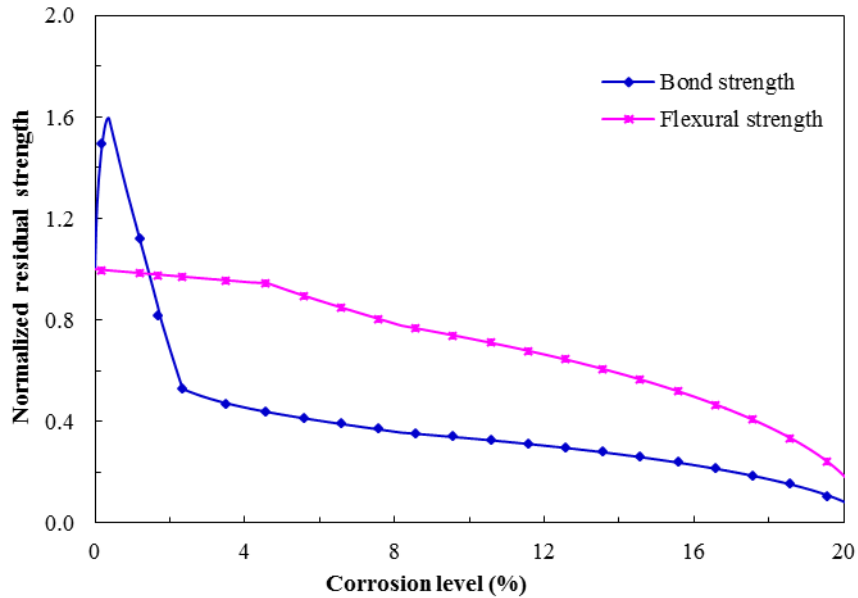


**Figure 5.4** Analytical prediction of normalized residual flexural strength and bond strength versus corrosion level

corroded rebar by the ultimate bond strength of non-corroded rebar as mentioned in Chapter 4. At low corrosion level (<1%), bond strength increases by about a half but further increase in corrosion leads to considerable reduction of bond strength. The bond strength is most severely reduced at the corrosion level between 1% and 2.5%. This rapid reduction in bond strength is associated with many factors including reduction of corrosion and confinement stresses. It can also be observed that at corrosion level of about 5%, bond strength decreases by about 60% whereas flexural strength decreases by only 10%. When corrosion level exceeds 5%, there is significant reduction in flexural strength, which is caused by decrease in bond strength indicating bond failure occurs before yielding of the steel rebar and the surrounding concrete. It is interesting to see that at about corrosion level of 20%, bond strength reduces only 10% of its residual strength while flexural capacity maintains 25% of its residual capacity. This clearly shows that, corrosion in reinforcement has more severe effect on bond strength than on the flexural strength of corroded RC beam.

In order to analyse the trend of flexural strength deterioration due to reinforcement corrosion, the predicted residual flexural strength by the present analytical method is plotted as a function of the corrosion level and compared with the published experimental data of various reference literatures in Figure 5.5. Here again the normalized residual flexural strength and corrosion level is evaluated as in the Figure 5.3. The experimental results of (Azad et al. 2007, Azad et al. 2010, Chung et al. 2008b) shows that before the critical point (i.e. approximately 6% in Chung et al. (2008b) and 4% in Azad et al. (2010) there is the negligible reduction in flexural strength, whereas after the critical point significant reduction of residual flexural strength has occurred agreeing well with the trend of flexural strength deterioration predicted by the present study. The reduction in flexural strength may be due to the significant reduction in bond strength, which is required to prevent beam from bond failure. Although, in the experimental investigations conducted by Azad et al. (2007), the author has mentioned that significant reduction in bond strength was responsible for flexural strength deterioration, the trend of flexural strength deterioration does not matched with the trend of present study.

This could be due to larger confinement stress poses by the cover concrete and the stirrups and also may be due to the development length provided is sufficient for yielding of the corroded tension reinforcement before bond failure. Furthermore, the residual flexural strength of the RC beam is calculated by ignoring the bond strength loss and by using the standard expression for the moment of resistance of under-reinforced beams given in Eurocode 2 ( 2004). The reduction in cross-sectional area of the reinforcing bar due to corrosion is considered in calculations and then the normalized residual flexural strength of the RC beam is plotted in Figure 5.5.

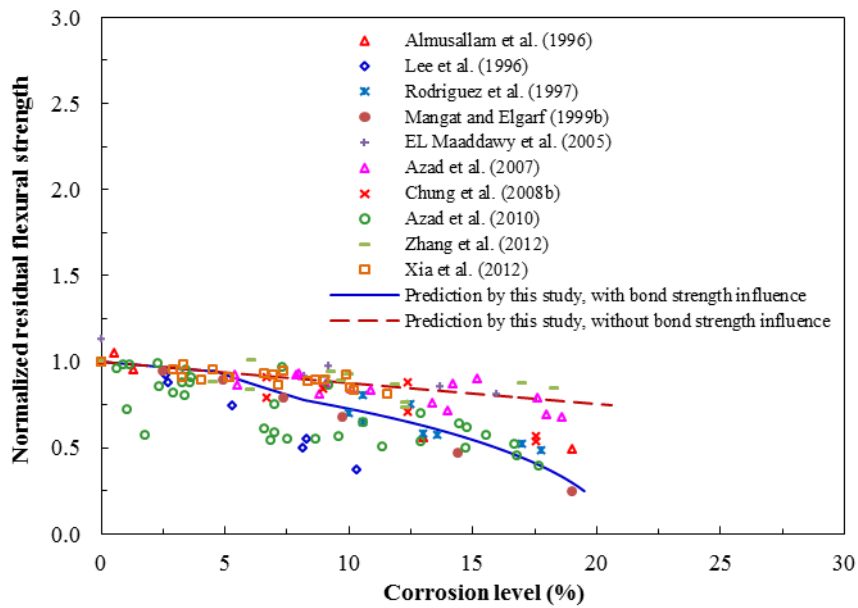


**Figure 5.5** Analytical prediction of normalized residual flexural strength versus corrosion level, compared with experimental test results available from various sources

It can be seen that in this case (i.e. without bond strength influence), the reduction in flexural strength follows approximately linear trend, which is similar to the trend of experimental investigations carried out by EI Maaddawy et al. (2005b), Zhang et al. (2012) and Xia et al. (2012). The experimental investigations carried out EI Maaddawy et al. (2005b), Xia et al. (2012) and Zhang et al. (2012) have not mentioned about the bond strength deterioration of those test specimens. Therefore it can be said that although bond strength decreases severely as the corrosion level increase, the gradual reduction of flexural strength in these tests results indicates that the severe reduction on their bond strength due to corrosion barely affected their ultimate flexural strength capacity at which reinforcement reached their ultimate yield strength. This may be due to the reasons that in these experimental investigations, the specimens were provided with sufficient development lengths and confinement for preventing bond failure hence allowing for yielding of the tensile reinforcement or the concrete.

It is clear from Figure 5.5 that the reduction in flexural strength for the case without bond strength influence is relatively low in comparison with the case with influence of bond strength loss. Thus, from Figure 5.5 it can be concluded that, at corrosion level less than the critical point of corrosion level, the reduction of the flexural strength is mainly caused by reduction in cross-sectional area of the rebar due to corrosion. On the other hand, the predicted results and the experimental results show that the flexural strength rapidly decreases with corrosion rate greater than the critical point which is due to rapid reduction of bond strength caused by corrosion and also because of the insufficient development length and confinement required for yielding of the corroded tension reinforcement. For instance, at a corrosion level of 20%, the residual flexure strength by using conventional method is about 80% percentage of the original strength whereas the corresponding flexural strength with considering influence of bond strength loss is only about 25%. This indicates that at relatively high corrosion level (>5%), bond strength reduction at the steel-concrete interface is the primary factor responsible for the deterioration of flexural strength of the corroded beam rather than the reduction in cross sectional area of the rebars.

#### *5.6.2 Effect of cover surface cracking on residual strength*

From the literatures review in Chapter 2, it is clear that no effort has been made to find the relationship between load carrying capacity and cover surface cracking of corrosion damaged RC structures suffering from bond strength deterioration. In this context, in order to investigate the effect of cover surface cracking on the structural behaviour of corroded RC structures, deterioration of bond strength and flexural strength of the RC beam considered in numerical example 1 is presented in Figure 5.6. Figure 5.6 shows

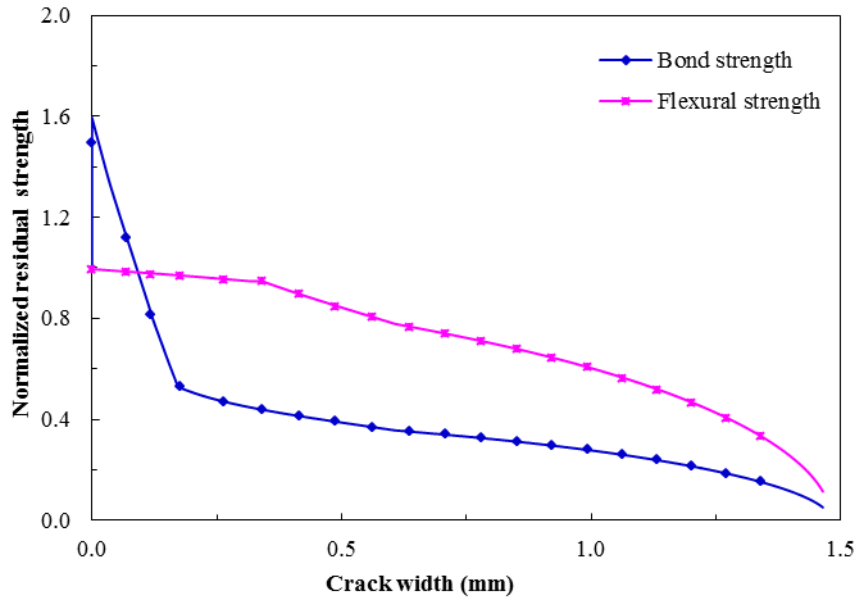


**Figure 5.6** Analytical prediction of normalized residual flexural strength and bond strength versus cover surface crack width

the results of normalized bond and flexural strength versus equivalent cover surface crack width. The cover surface crack width and bond strength of the corroded rebar are evaluated by using methodology mentioned in Chapter 3 and Chapter 4 respectively. Both flexural and bond strength of the RC beam continuously decreases with the increase of crack width at the concrete cover surface. Furthermore, Figure 5.6 demonstrates that the bond strength is most severely reduced at the crack width of 0.2 mm approximately while flexure strength is more severely reduced when crack width is 0.4 mm approximately. Moreover, the results indicate that bond strength is more affected by cover surface cracking than the flexural strength.

Depending on the size of cracks, the defects in concrete cover due to corrosion can be classified in different categories such as spalling; minor cracking and major cracking as mentioned in Chapter 3. Influence of different types of defect in concrete cover on the residual flexural strength of corroded RC beam is mentioned in Figure 5.7. From the

results, till minor cracking in the concrete cover there is no significance change in flexural strength, with major cracking flexural strength is reduced considerably maintaining only 60% of the initial strength.

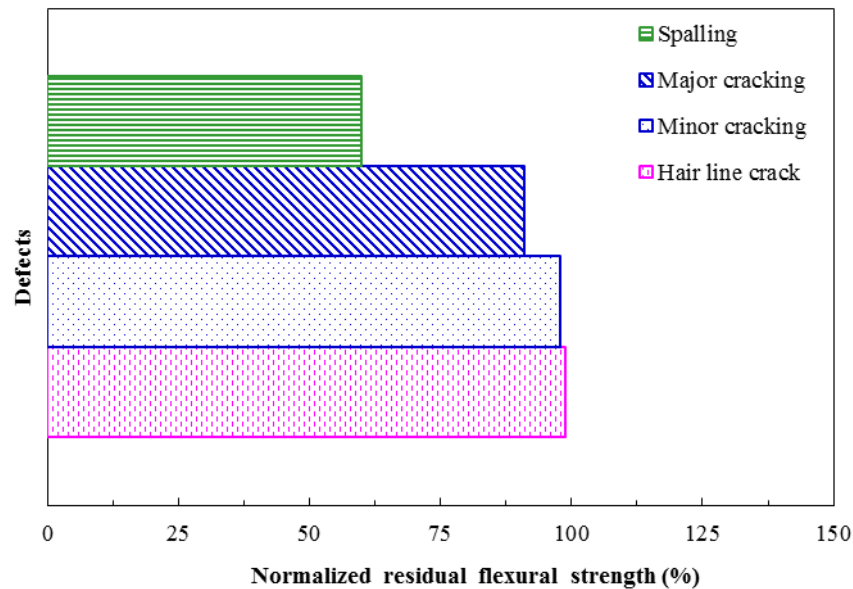


**Figure 5.7** Normalized residual flexural strength versus cover surface defects

### 5.6.3 Effect of concrete geometry on residual flexural strength

The influence of cover depth  $C$  on the flexural strength deterioration of corroded RC beam is presented in Figure 5.8, where cover depth to rebar diameter ratios ( $C/D_b$ ) of 1.5, 2 and 2.5 are considered. The results indicate that, residual flexural strength of corroded RC beam increases in larger cover depth. Furthermore, it also indicates that in case of larger cover depth, bond failure occurs at higher level of corrosion, which may be due to increase in confinement created by larger cover depth. Figure 5.9 shows the effect of cover surface defects on the residual flexural strength for different cover to rebar diameter ratios ( $C/D_b$ ). The cover surface defects are defined in the similar

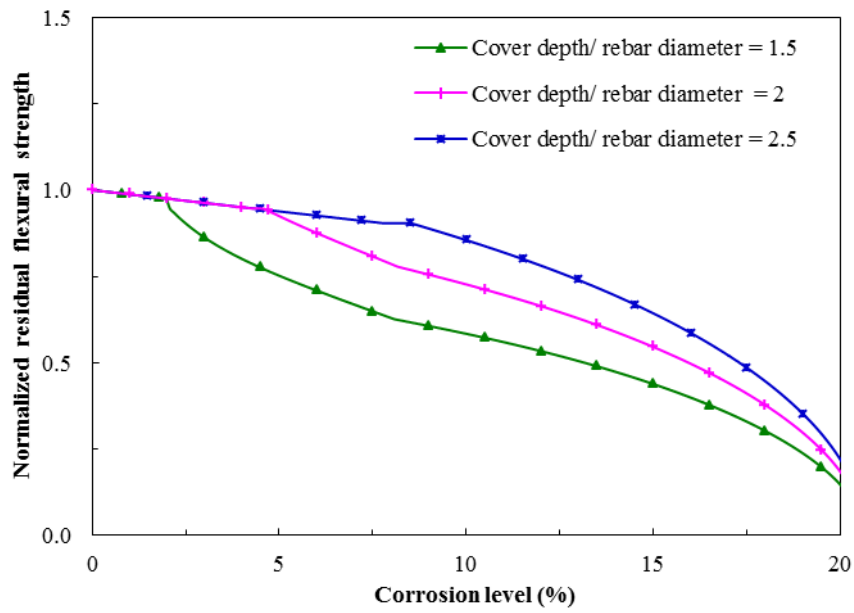


**Figure 5.8** Normalized residual flexural strength versus corrosion level evaluated for various cover depths

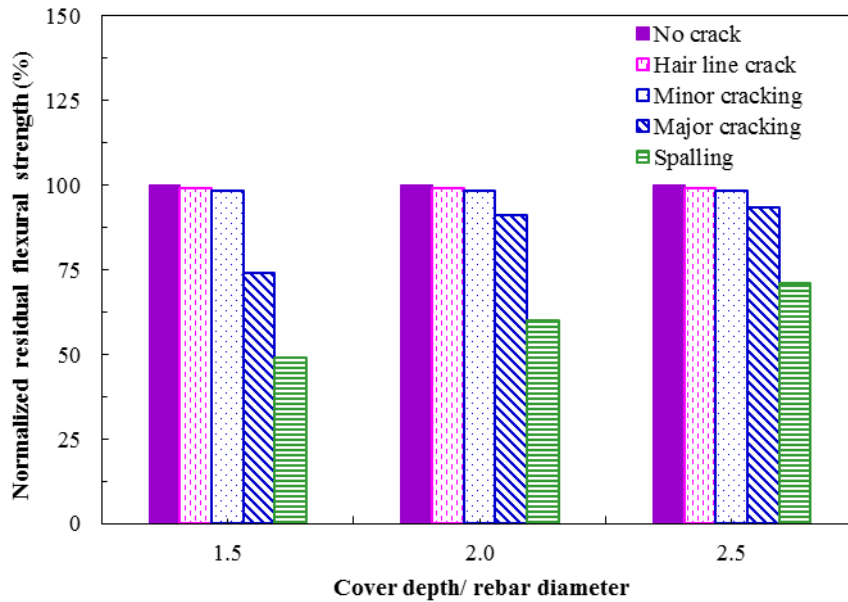


**Figure 5.9** Normalized residual flexural strength versus cover surface defects for different concrete cover depths

way as in Chapter 3. Here, at hairline crack (i.e. crack width of 0.05 mm), the residual flexural strength generally remains same as that in the intact stage for all three cases of concrete cover depths. However, with further growth of cracks width residual flexural strength decreases for all cases, but deterioration rate is slightly higher in the case with thinner concrete cover. At the stage of spalling (i.e. crack width of 1 mm) approximately 70% of its original strength is maintained in case of cover depth of  $C/D_b = 2.5$  whereas only about 50% is maintained in cover depth of  $C/D_b = 1.0$ .

## 5.7 Numerical example 2

In this section the role of stirrup on residual flexural strength capacity of corrosion affected RC beam is presented with the help of numerical example. A simply supported RC beam of 5.0 m span exposed to an aggressive environment is now utilised. The RC beam is operated in aggressive environments with mean annual corrosion current per unit length  $i_{corr} = 1 \mu\text{A}/\text{cm}^2$ . The beam is doubly reinforced with the cross-sectional width  $b = 300$  mm and effective depth  $d = 560$  mm. Four steel rebars with diameter  $D_b = 20$  mm are provided as the tensile reinforcement and two rebars of diameter  $D_{sc} = 16$  mm are provided as the compressive steel with clear cover thickness  $C = 40$  mm along with the stirrup of diameter  $D_{st} = 6$  mm at spacing of 100 mm. The concrete has a characteristic compressive strength  $f_{ck} = 40$  MPa, the yield strength of original reinforcing steel  $f_{yk} = 460$  MPa with modulus of elasticity  $E_{st} = 200$  GPa. The characteristic compressive strength of concrete is used for estimating other relevant properties of concrete i.e. tensile strength  $f_t = 4.6$  MPa; modulus of elasticity  $E_c = 37$  GPa ( Eurocode 2, 2004) as shown in Table 5.1. The concrete fracture energy

$G_F = 200\text{N/m}$  is adopted and ultimate cohesive crack width and critical crack width are estimated from CEB-FIP (1990) for given compressive strength and assumed maximum aggregate size of 20 mm as shown in Table 5.1. The volume ratio  $\gamma_{vol}$  of the corrosion products is taken as 2.0. During the analysis, deterioration of structural capacity of the aforementioned reinforced concrete beam is evaluated with respect to mass loss of reinforcing bar and cracking in concrete cover surface by using the method as mentioned in Section 5.6.

### 5.7.1 Effect of stirrups on residual flexural strength

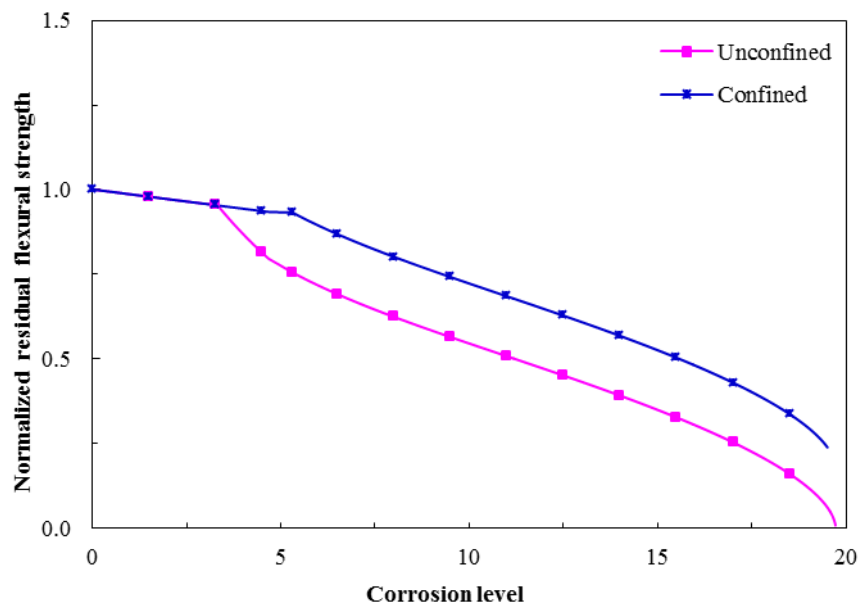


**Figure 5.10** Normalized residual flexural strength as a function of corrosion level evaluated for confined and unconfined beam

The results in Figure 5.10 show the residual strength behaviour of confined and unconfined concrete as function of corrosion level. The results show that the critical point of corrosion where the severe reduction of flexural strength takes place is

comparatively lower in unconfined concrete than in confined concrete. This is due to the increase in bond strength capacity provided by the stirrups in confined concrete. Furthermore, the flexural strength deterioration is comparatively less in confined concrete.

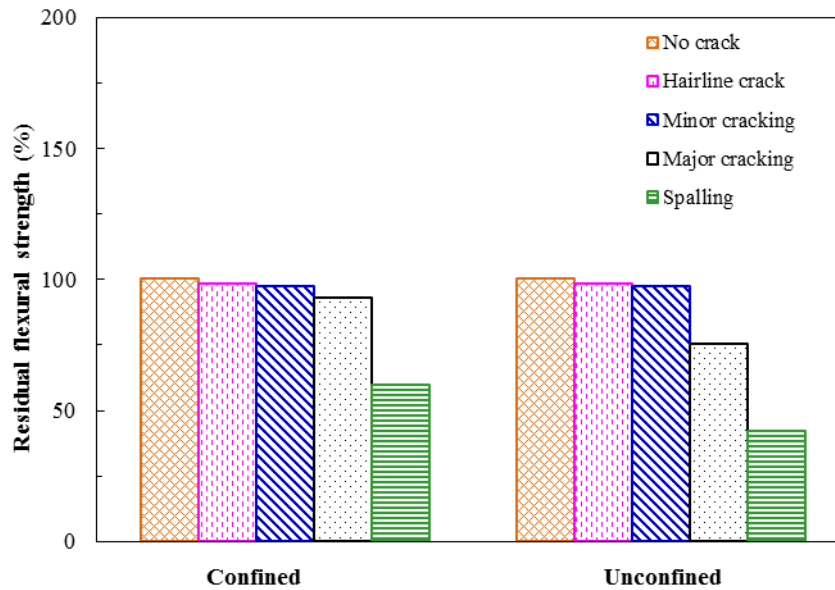


**Figure 5.11** Normalized residual flexural strength versus cover surface defects for confined and unconfined beam

Influence of different types of aforementioned defects in concrete cover on the structural behaviour of confined and unconfined RC beam is presented in Figure 5.11. From the results, till minor cracking appears in the concrete cover there is no significant change in residual flexural strength. As the defects reach to spalling stage, flexural strength decreases significantly. This clearly shows that, defects in concrete cover have significant effect on residual strength of corroded RC beam. Moreover, the reduction in residual strength in unconfined beam is relatively higher than in confined beam. For instance, when the defect in the concrete cover becomes spalling, the residual flexural strength of the confined beam maintains about 60% of its initial strength, whereas in

unconfined beam it only maintains 40% of its initial strength. This is due to the absence of transverse reinforcement (stirrups) in unconfined concrete. Hence, the results from Figure 5.11 show that, at the same stage of defects in the concrete cover, unconfined beam is more susceptible than confined beam.

## **5.8 Summary and conclusions**

In this section a new analytical method for evaluating the residual capacity of RC members with corroded reinforcing bars is proposed which is based on flexural analysis of RC beams that considers the realistic parameters associated with the flexural strength loss such as sectional area loss of rebar, bond strength degradation due to reinforcement corrosion as well as reduction in yield strength of the rebar. During the analysis, a new strain compatibility condition occurred due to insufficient bond strength is considered together with the different failure modes satisfying the equilibrium of compression and tensile forces acting in the corroded RC beam. At first, crack growth in concrete cover and bond strength deterioration caused by reinforcement corrosion are evaluated by analytical investigations as mentioned in Chapters 3 and 4. Then the flexural strength of corroded RC beam failing in bond is evaluated by using proposed methodology and then validated by the published experimental data. Growth of surface crack width with increase in reinforcement corrosion and its effect on bond strength deterioration and corresponding flexural strength deterioration are analyzed. Likewise, the behavior of flexural strength deterioration in corroded RC beam with different concrete geometry and confinement condition are also discussed.

On the basis of the results obtained from the numerical examples, following conclusions are drawn: a) The proposed approach is capable of evaluating structural performance and defects of corrosion damaged RC structures; b) Further progress of corrosion causes significant reduction in rebar size which in turn widens the crack in concrete cover, and consequently reduces residual strength of bond and flexural strength; c) Flexural strength decreases rapidly after 5% mass loss due to significant reduction in bond strength loss, hence indicating that bond strength degradation due to reinforcement corrosion is dominant factor causing deterioration of flexural strength; d) In case when sufficient confinement and/or development length is provided to ensure yielding of tensile reinforcement or concrete before bond failure, significant reduction in bond strength may barely affect the flexural strength. In that case reduction in flexural strength is caused by cross-sectional area loss of the reinforcing rebar due to corrosion and hence the gradual reduction of flexural strength takes place; e) Reinforcement corrosion has more impact on rebar bond strength, comparing with the flexural strength; f) Increase in cover depth and use of transverse reinforcement can reduce the rate of flexural strength deterioration of corroded beam failing in bond.

## **Chapter 6 Time-dependent Reliability Analysis and Optimized Maintenance Strategy**

### **6.1 Introduction**

From the previous chapters (Chapters 3 to 5), it can be concluded that the loss in area of reinforcement due to corrosion and the cracking or even spalling of the concrete cover directly influences the serviceability and ultimate resistance of the concrete structures by altering its bond strength and load carrying capacity. The reliability of the RC structures is mainly governed by their performance. Therefore the reliability of RC structures is threatened by deterioration caused by reinforcement corrosion. Time-dependent structural reliability analysis considering the uncertainties in performance degradation is a fundamental tool which can help in the efficient infrastructure asset management, allocating limited resources for periodic inspection and maintenance of such structures.

The review of existing research literature in Chapter 2 has shown that time-dependent structural reliability analysis is widely utilised to evaluate lifecycle performance and optimized maintenance strategy of corrosion damaged RC structures. However, existing studies on the evaluation of time-dependent reliability of the corrosion-degraded RC structures are mainly focused on the sectional loss of corroded rebar. Limited efforts have been made in lifecycle performance analysis of corrosion affected RC structures with consideration of the influence of mechanical factors such as realistic properties of cracked concrete, reduction in yield strength of rebar and bond strength loss on the whole life cycle performance. The integration of structural response measurements and

reliability-based performance assessment techniques has tremendous potential for structural safety and economic feasibility. Therefore, the need for reliability-based performance assessment together with the optimized maintenance strategy is evident for the sustainable infrastructure management.

This Chapter presents an approach for time-dependent reliability analysis of corrosion affected RC structures together with the optimized maintenance strategy. Initially, the analytical models developed in the previous Chapters (Chapter 3 to 5) are utilized to evaluate the performance degradation caused by reinforcement corrosion. In order to model the progression of structural resistance deterioration during the lifecycle of the RC structure, a gamma process model is adopted, to take uncertainties into account. The time-dependent reliability analysis is then applied to evaluate the probability of failure of the RC beam in predefined allowable deterioration limit. Then, optimal repair planning and maintenance strategies are determined by balancing the cost for maintenance and the risk of failure. Finally, the applications of the proposed approach are illustrated with numerical examples.

## **6.2 Lifecycle performance assessment**

In lifecycle modelling of corrosion damaged RC structures serving in aggressive environments, the effect of corrosion on the performance deterioration of corroded RC structures can be illustrated as in Figure 3.1 of Chapter 3. Hence, in this study a lifecycle of RC structure subjected to reinforcement corrosion is defined as the period from the completion of construction to collapse of the structure. Three phases are considered in the process i.e. crack initiation phase, crack propagation phase and

residual life phase. As observed from Figure 3.1, in the first phase structural resistance remains almost the same as the original capacity. In the second phase it deteriorates gradually until the third phase where the structural resistance deterioration rate is accelerated leading to the collapse of the structure. Therefore, as mentioned in Chapter 3, degradation of the structural resistance caused by reinforcement corrosion in whole life of RC structures can basically be discussed in terms of three factors: 1) sectional loss of rebar; 2) cover cracking and 3) strength (bond and flexural) deterioration. For time-dependent reliability analysis, quantification of these factors (damages) associated with reinforcement corrosion is required. Therefore, these damages are evaluated by using the formulations developed in Chapters 3-5.

### **6.3 Formulation of time-dependent reliability analysis**

As mentioned in Chapter 2, the structural reliability is characterized by an ability to perform without failure, by durability, repair ability, and maintainability. Hence, the structural reliability of the corrosion affected RC structures mainly depends on two parameters: structural resistance deterioration and actions on the structure. Both of these parameters are time-dependent in nature, hence the reliability of these structures is related to time. Reinforcement corrosion is a complex process, therefore there is possibility of high degree of uncertainties associated with both corrosion induced resistance deterioration and its effect on structural performance of these structures. The uncertainties associated with the resistance deterioration and the corresponding structural response can be dealt with the stochastic process (Papakonstantinou and Shinozuka 2013, Van Noortwijk 2009, Saydam and Frangopol 2014, Wellalage et al. 2015). Therefore, time-dependent structural reliability analysis based on the stochastic

approach could be helpful in evaluating the existing condition and predicting the future performance of these structures suffering from reinforcement corrosion.

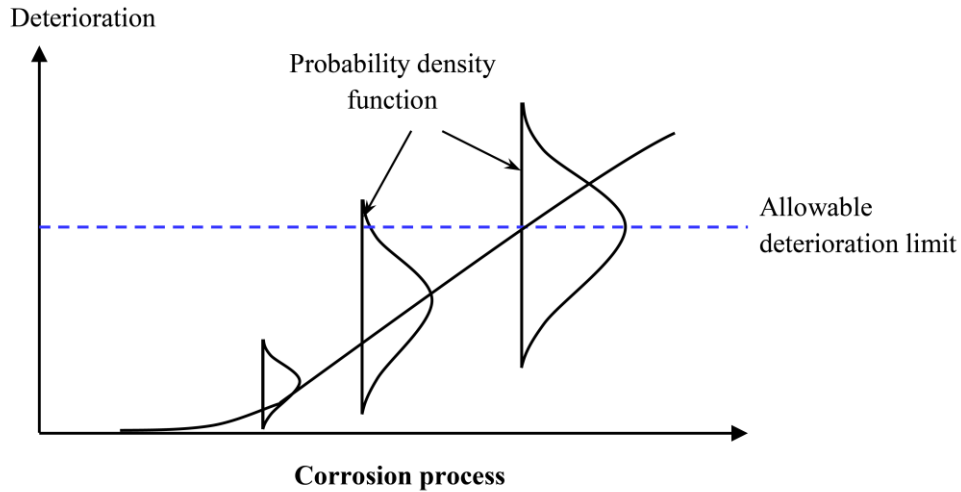


**Figure 6.1** Schematic presentation of time-dependent reliability problem in performance based assessment

In time-dependent reliability analysis of corrosion affected RC structures, the probability of structural failure ( $P_f$ ) varying with time can be evaluated by using performance based assessment. From the definition of performance based assessment, the probability of failure of the RC structure undergoing deterioration can be defined as the stage at which the structural performance or its corresponding deterioration reaches the intended threshold limit, as shown in Figure 6.1. The basic approach is based on the fact that the RC structure will not fail, if it does not reaches the threshold limit of deterioration, that will occur during the time interval  $[0, t]$ . Thus, the probability of the corrosion affected RC structure to fail during their lifetime ( $t$ ) is given by

$$P_f(t) = P_r(J(t) \geq L) \quad (6.1)$$

where  $L$  is the threshold limit or the maximum allowable limit of the structural deterioration and  $J(t)$  is the structural action (i.e. performance deterioration). Usually the performance criteria are defined as limit states, therefore the threshold limits can be chosen by using various maximum allowable limits of deterioration such as acceptable crack width limits for the serviceability limit state and strength loss of the structure for the ultimate limit state. This predefined limit state may vary in accordance with the requirement of the RC structures concerned.

#### **6.4 Stochastic deterioration modelling and probability of failure**

In order to deal with uncertainty associated with the deterioration caused by reinforcement corrosion, a stochastic process is now considered. In this section, gamma process is utilised for the stochastic modelling of the deterioration caused by reinforcement. The gamma process is often adopted for modelling a stochastic deterioration process to evaluate the resistance of deteriorating structures (Van Noortwijk and Frangopol 2004, Van Noortwijk 2009, Chen and Alani 2013). From Figure 6.2, it is clear that performance deterioration in corrosion affected RC structures is a continuous and increasing phenomenon. As defined earlier in Chapter 2, gamma process is suitable to model gradual damage monotonically accumulating over time. Hence, the gamma process is suitable for the stochastic modelling of structural resistance deterioration in corrosion affected RC structures during their lifecycle. The gamma process therefore can be employed for the stochastic modelling of performance degradation process in corrosion damaged RC structures occurring randomly in time, such as crack evolution inside concrete cover and residual strength deterioration. In this study, average rate of deterioration caused by reinforcement corrosion is denoted by

$J_x$ . In case of cover cracking, average rate of deterioration is given by  $J_x = w_{cx}$ . In condition (performance) assessment of the deteriorating RC structure, deterioration is evaluated by the ratio of structural strength deterioration over initial strength, therefore in case of the flexural strength deterioration, the average flexural strength deterioration ratio is represented by  $J_x$  and is given by

$$J_x = \frac{M_o - M_{ux}}{M_o} \quad (6.2)$$

where  $M_{ux}$  and  $M_o$  are the flexural strength of corroded and uncorroded RC beam respectively. From Figure 4.11 it is clear that after cracking of the concrete cover at the cover surface, the bond strength deterioration due to reinforcement corrosion is also a continuous and non-negative process. Therefore, gamma process is also utilized for the stochastic modelling of bond strength degradation. In the case of stochastic modelling of bond strength deterioration associated with the corrosion induced cracking at the concrete cover surface, average bond strength deterioration ratio is represented by  $J_x$  and is defined by

$$J_x = \frac{T_{ubo}(w_{cx}) - T_{ubx}(w_{cx})}{T_{ubo}(w_{cx})} \quad (6.3)$$

where  $w_{cx}$  is the cover surface crack width,  $T_{ubo}(w_{cx})$  and  $T_{ubx}(w_{cx})$  are the residual bond strength related with onset of cracking and further cracking at cover surface. In the gamma process deterioration model, cumulative resistance deterioration  $J$  is considered as a random quantity with the gamma distribution, and has shape parameter

$\eta_x > 0$  and scale parameter  $\lambda > 0$ . The probability density function of cumulative resistance deterioration  $J$  occurring over time  $t$  ( $t \geq 0$ ) corresponding to corrosion level  $X_p$  ( $X_p \geq 0$ ) can be expressed as

$$f_{J_x}(J) = Ga(J, \eta_x, \lambda) = \begin{cases} \frac{\lambda^{\eta_x}}{\Gamma(\eta_x)} J^{\eta_x - 1} e^{-\lambda J}, & \text{for } J \geq 0 \\ 0, & \text{elsewhere} \end{cases} \quad (6.4)$$

where  $\Gamma(\eta_x) = \int_0^{\infty} v^{\eta_x - 1} e^{-v} dv$  is the gamma function for shape parameter  $\eta_x$ ; the scale parameter  $\lambda$  could be estimated from statistical estimation methods such as a Maximum Likelihood Method by maximizing the logarithm of the likelihood function of the increment of the parameter. The shape function  $\eta_x$  is the time-dependent parameter and can be obtained from  $\eta_x = \lambda J_x$  (Chen and Alani 2013, Van Noortwijk and Frangopol, 2004). Assuming  $J_L$  as the maximum allowable limit of deterioration, from the definition of probability of failure and by integrating probability density function given in equation (6.4), the lifetime distribution of probability of failure is given by

$$P_f(t) = P_r[J_x \geq J_L] = \int_{J_L}^{\infty} f_{J_x}(J) dJ = \frac{\Gamma(\eta_x, J_L \lambda)}{\Gamma(\eta_x)} \quad (6.5)$$

where  $\Gamma(\eta, z) = \int_{v=z}^{\infty} v^{\eta - 1} e^{-v} dv$  is the incomplete gamma function for  $z \geq 0$  and  $\eta > 0$ .

Similarly, the lifetime distribution of structural reliability associated with structural resistance deterioration is given by

$$P_s(t) = 1 - \int_{J=J_L}^{\infty} f_{J_x}(J) dJ = \frac{\Gamma(\eta_x) - \Gamma(\eta_x, J_L \lambda)}{\Gamma(\eta_x)} \quad (6.6)$$

In performance based reliability analysis, the main question that needs to be answered is how the maximum allowable deterioration limit  $J_L$  is considered. There is a risk involved in making decision of  $J_L$ , as different allowable limits ( $J_L$ ) will result in different times for the structure to be unsafe or unserviceable. According to the DuraCrete (1998), a surface crack width of  $\approx 0.3$  mm is commonly considered to represent a serviceability limit state of the RC structures. Hence, for serviceability problem as characterized by cover surface cracking in this study the probability of failure in terms of structural serviceability is evaluated for three acceptable crack width limits: 0.3 mm, 0.4 mm and 0.5 mm. However, it is more difficult to decide an allowable limit of strength deterioration, since there is not such guidance available in the existing literatures. In this regard, while analyzing the RC structure in its ultimate limit state, the reduction in strength (bond and flexural) corresponding to predefined crack width limits are considered as the maximum allowable limit of strength deterioration.

## 6.5 Optimized maintenance strategy

After reviewing the existing literatures of reinforcement corrosion, it can be concluded that considerable amount of recourses have already been spent on maintenance of RC

structures such as roads, railways, bridges and buildings and is likely to increase in coming years. If no repair is undertaken, the resistance of these RC structures will deteriorate further until it reaches the ultimate limit or collapse. Structural repairs, therefore, are necessary and should be planned to improve the resistance of the deteriorating RC structure against increasing deterioration caused by reinforcement before reaching the predefined limit states during its service life. In order to reduce the economic impact of deteriorating RC structures, scientific techniques such as mathematical optimisation models are essential. This helps to determine the best maintenance strategy. Moreover, the best maintenance strategy is essential for effective maintenance planning required to keep the deteriorating RC structures safe and reliable to ensure an adequate level of structural reliability at minimal lifecycle cost. The effective maintenance strategy for the deteriorating RC structures could be determined on the basis of the balance of statistical estimations of failure probability and the costs for the repairs.

A characteristic feature of optimising maintenance is that the balanced decisions need to be made under uncertainties such as structural performance deterioration. In maintenance management, the most important uncertainty is generally the uncertainty in the time to failure (lifetime) and/or the rate of deterioration (Van Noortwijk 2009). In order to incorporate these uncertainties, a stochastic based time-dependent reliability analysis is necessary and is frequently used to determine the optimal maintenance strategy (Mullard and Stewart 2012, Liu and Frangopol 2005, Kim et al. 2013). In this section, evaluation of optimized maintenance strategy is presented by using condition-based maintenance model of Rijkswaterstaat, previously used by (Van Noortwijk 2003, Van Noortwijk and Frangopol 2004, Chen and Alani 2013). The main advantage of

Rijkswaterstaat's model is that it is computationally less demanding which can be easily used in practice. In order to optimized maintenance strategy represented here as repair time, the maintenance model based on the risk cost balanced criteria is also employed.

## 6.6 Evaluation of cost of maintenance and optimal maintenance decision

In evaluating the maintenance strategy of deteriorating structure, quantitative assessment of the costs associated with the maintenance is essential. The quantification of the maintenance costs can be obtained by modelling the maintenance of corrosion damaged RC structure as a discrete-time renewal process, whereby renewal process or the maintenance actions bring a deteriorating RC structure back into its original condition or as-good-as new state (Van Noortwijk 2009). Therefore, in general the cost of maintenance can be defined as the cost which is associated with combination of actions carried out to restore a component or structure to the initial condition. Mathematically a discrete renewal process  $\{N(n), n = 1, 2, 3, \dots\}$  is a non-negative integer-valued stochastic process that registers the successive renewals in the given time-interval. In which renewal times  $T_1, T_2, T_3, \dots$  are considered as the positive, independent, identically distributed, random quantities having the discrete probability function (Van Noortwijk and Frangopol 2004), expressed here as

$$P_r(T_k = i) = p_i \quad \text{for } i = 1, 2, \dots \quad (6.7)$$

where  $p_i$  represents the probability of a renewal in unit time  $i$  and  $T_k$  is the aforementioned renewal times . Assuming  $c_i$  as the cost associated with a renewal in

this unit time, the expected average costs over the bounded horizon  $[0, n]$   $C_e$  can be obtained by simply averaging the costs over an bounded horizon as a sum of the cost associated with the renewal ( $c_i$ ) and the additional expected cost during the interval  $(i, n]$ , given by

$$C_e(n) = \sum_{i=1}^n p_i [c_i + C_e(n-i)] \quad (6.8)$$

Because the planned lifetime maintenance of the most RC structures is very long compared with the possible renew cycle length, the strategy for risk cost balanced optimized maintenance during the lifetime can be approximately considered over an unbounded time horizon. From the renew reward theory and age replacement policy, the expected costs of repair over an unbounded horizon per unit time depend on the preventive maintenance cost  $C_p$ , the corrective maintenance cost  $C_F$  that includes the consequences caused by the failure and the expected renew cycle length, expressed as the ratio of the expected cycle cost and expected cycle length of renewal (Van Noortwijk 2003), expressed here as

$$\lim_{n \rightarrow \infty} \frac{C_e(n)}{n} = C_e(k) = \frac{\sum_{i=1}^k q_i C_F + \left(1 - \sum_{i=1}^k q_i\right) C_P}{\sum_{i=1}^k i q_i + k \left(1 - \sum_{i=1}^k q_i\right)} \quad (6.9)$$

where  $k=1,2,3,\dots$  represents the number of the age replacement intervals to be determined. The detail derivation of equation (6.9) is out of the scope of this thesis and can be found in Van Noortwijk (2003). From the aforementioned definition of failure of

the corrosion damaged RC structures and equation (6.5), the probability of failure per unit time at the  $i$ -th time interval can then be computed form

$$q_i = P_f(t_i) - P_f(t_i - 1), \text{ for } i = 1, 2, 3 \quad (6.10)$$

In equation (6.10), the preventive maintenance cost  $C_p$  and corrective maintenance cost  $C_F$  are the cost associated with preventive (mainly before failure) and corrective (mainly after failure) maintenance strategies respectively. In condition-based maintenance model, failure of the RC structure is the condition failure and the failure is defined as the event at which a structure fails to meet its predefined functional limit. An illustration corrective and preventive maintenance on the life cycle performance of the corroded RC structures is shown in Figure 6.2.

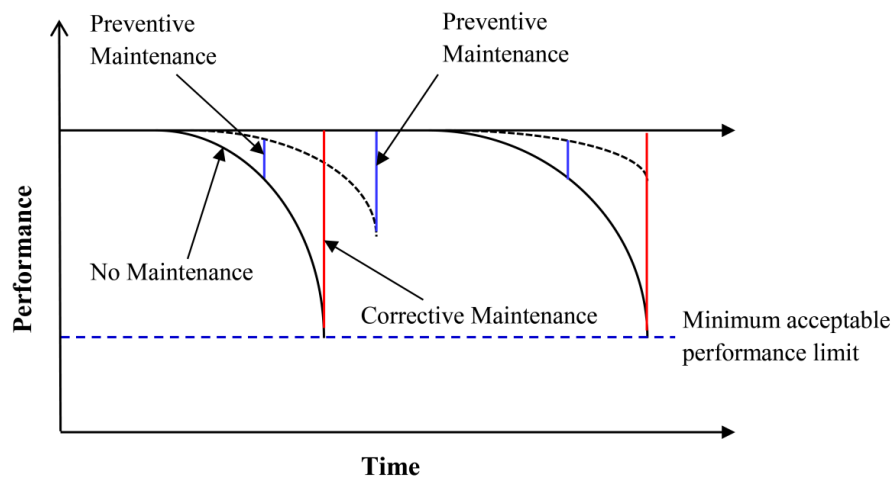


**Figure 6.2** Schematic presentation of lifecycle performance of corroded structures with different maintenance strategy

In order to compare the maintenance costs at present day and in the future, the future cost needs to be determined to its present value by discount factor. By introducing

discount factor  $\alpha$  in above equation (6.9), the expected discounted costs of maintenance over an unbounded horizon per unit time are given by

$$C_d(k) = \frac{\left( \sum_{i=1}^k \alpha^i q_i \right) C_F + \alpha^k \left( 1 - \sum_{i=1}^k q_i \right) C_P}{1 - \left[ \left( \sum_{i=1}^k \alpha^i q_i \right) + \alpha^k \left( 1 - \sum_{i=1}^k q_i \right) \right]} \quad (6.11)$$

where the discount factor  $\alpha$  is given by  $\alpha = (1 + r/100)^{-1}$  in which  $r$  is discount rate per unit time in percentage. The choice of the discount rate is mainly a political decision and it serves as an agreement on comparing investments. In the United Kingdom and the United States, a discount rate of about 4 and 6%, respectively has been used; in the Netherlands, a discount rate of 4% is usually chosen (Van Noortwijk and Frangopol 2004). Finally, the optimal maintenance time interval  $k^*$  without and with discounting can be evaluated by minimising the expected costs per unit time given in equation (6.9) and equation (6.11) respectively. In this thesis only discounted costs of maintenance are evaluated.

## 6.7 Summary for structural reliability analysis and evaluation of optimal repair time

The following are steps for evaluation of structural reliability and probability of failure:

1. At any time  $X_p$  and  $w_{cx}$  are evaluated from Chapter 3 then corresponding  $T_{ubx}$  and  $M_{ux}$  are evaluated from Chapter 4 and 5 respectively.
2. The deteriorate rate  $J_x$  is evaluated for three types of deterioration:

- a. For cover surface cracking,  $J_x = w_{cx}$
  - b. For flexural strength deterioration,  $J_x$  is evaluated from equation (6.2)
  - c. For bond strength deterioration,  $J_x$  is evaluated from equation (6.3)
3. Deterioration limit  $J_L$  is defined as follows:
- a. Crack width limits when  $J_x = w_{cx}$ .
  - b. Flexural strength limits when  $J_x$  is obtained from equation (6.2).
  - c. Bond strength limits when  $J_x$  is obtained from equation (6.3).
4. Finally,  $P_f(t)$  and  $P_s(t)$  are evaluated from equations (6.5) and (6.6) respectively for each type of deterioration (i.e. cover surface cracking, bond strength deterioration and flexural strength deterioration).

The following are steps for evaluation of optimal repair time:

5. Probability of failure per unit time  $q_i$  is evaluated from equation (6.10).
6.  $\alpha$ ,  $C_F$ ,  $C_P$  and  $k$  are defined.
7. Expected discounted costs of maintenance  $C_d(k)$  are evaluated from equation (6.11). Finally, the optimal repair time interval  $k^*$  is evaluated by minimising the  $C_d(k)$  evaluated from equation (6.11).

## 6.8 Numerical example 1

In this section the methodology mentioned in the preceding sections to analyse the whole lifecycle performance analysis of corrosion affected RC structures is applied to a numerical example. A simply supported RC beam of 5.0 m span of a bridge exposed to an aggressive environment is now utilised to demonstrate the applicability of the

proposed method for assessing the time-dependent reliability analysis during its service life and is operated in aggressive environments with mean annual corrosion current per unit length  $i_{corr} = 1 \mu\text{A}/\text{cm}^2$ . The beam is doubly reinforced with the cross-sectional width  $b = 300$  mm and effective depth  $d = 560$  mm. Four steel rebars with diameter  $D_b = 20$  mm are provided as the tensile reinforcement and two rebars of diameter  $D_{sc} = 16$  mm are provided as the compressive steel with clear cover thickness  $C = 40$  mm along with the stirrup of diameter  $D_{st} = 6$  mm at spacing of 100 mm. The concrete has a characteristic compressive strength  $f_{ck} = 40$  MPa, the yield strength of original reinforcing steel  $f_{yk} = 460$  MPa with modulus of elasticity  $E_{st} = 200$  GPa. The characteristic compressive strength of concrete is used for estimating the tensile strength and modulus of elasticity of the concrete from Eurocode 2, (2004). The concrete fracture energy  $G_F = 200$  N/m is adopted and ultimate cohesive crack width  $w_u = 1.48$  mm and critical crack width  $w_{cr} = 0.23$  mm are estimated from CEB-FIP(1990) for given compressive strength and assumed maximum aggregate size of 20 mm. The total four numbers of cracks and the volume ratio of the corrosion products  $\gamma_{vol} = 2.0$  are also adopted here.

During the analysis, deterioration of structural capacity of the aforementioned reinforced concrete beam is evaluated with respect to mass loss (corrosion level) of reinforcing bar and cracking in concrete cover surface by using the proposed approach in Chapters 3, 4 and 5. The gamma process discussed in this chapter is then adopted for stochastic modelling of structural capacity deterioration in terms of cover surface cracking, bond strength and flexural strength deterioration. Then the time-dependent reliability analysis is undertaken to evaluate the probability of failure in serviceability

associated with crack width and failure in ultimate resistance associated with bond strength and load carrying capacity.

6.8.1 Effect of reinforcement corrosion on lifecycle performance

In lifecycle analysis, reduction in rebar due to reinforcement corrosion is the time-dependent in nature. Therefore, in this section in order to study the effect of reduction of rebar due to corrosion on structural reliability, time-dependent reliability analysis is evaluated in terms of probability of failure and corresponding survivability of the corroded RC beam as a function of corrosion level.

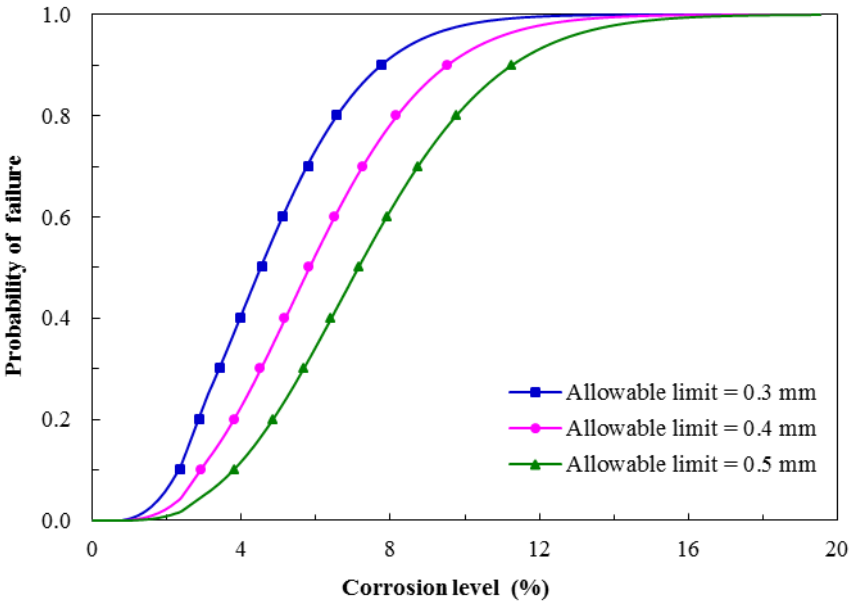
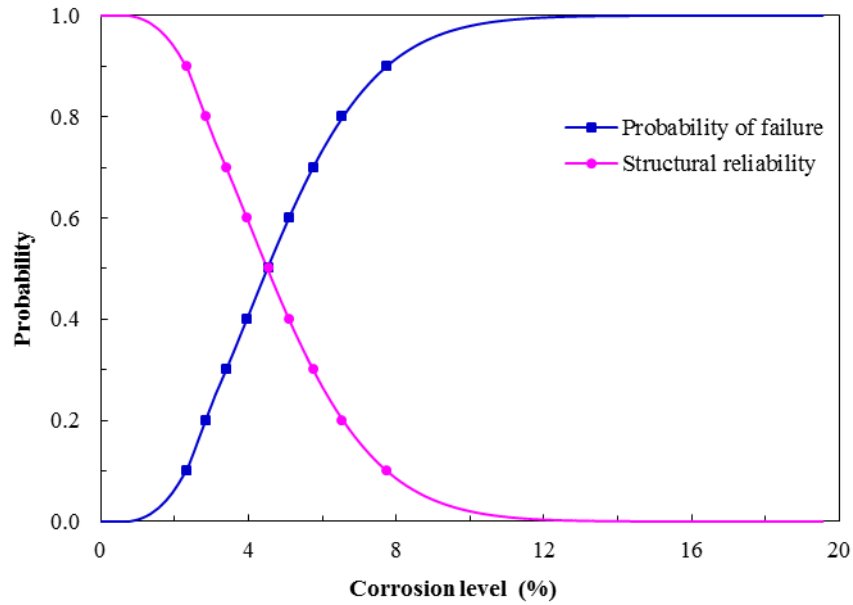


Figure 6.3 Probability of failure versus corrosion level for various allowable crack widths limits

The deterioration of structural performance in terms of serviceability (measured by surface cracking of the concrete cover) is here modelled as gamma process. At first, surface crack width ( $w_{cx}$ ) is considered as an indicator of performance deterioration for



**Figure 6.4** Probability of failure and reliability versus corrosion level for allowable crack width limit of 0.3 mm

the serviceability of the RC structure and adopted to replace  $J_x$  in equation (6.4). The lifetime distribution of probability of failure ( $P_f$ ) of the corroded beam is obtained from equation (6.5) for different acceptable crack width limits,  $J_L = w_L = 0.3, 0.4$  and  $0.5$  mm, respectively. The results are then presented in Figure 6.3 as a function of corrosion level. As expected, the probability of failure associated with cracking of the concrete cover depends on the given acceptable crack width limits, with a higher probability of failure for a lower acceptable crack width limit. The probability of failure increases steadily with time and reaches approximately 50% when corrosion level is approximately between 5% and 8%. Similarly, the lifetime distribution of the probability of failure together with structural reliability is presented in Figure 6.4. Here the structural survivability during the corrosion process is represented by the reliability function as mentioned in equation (6.6) and evaluated by using  $w_L = 0.3$  mm. Here

again, as expected the reliability of the beam during the lifetime continuously decreases as the probability of failure increases.

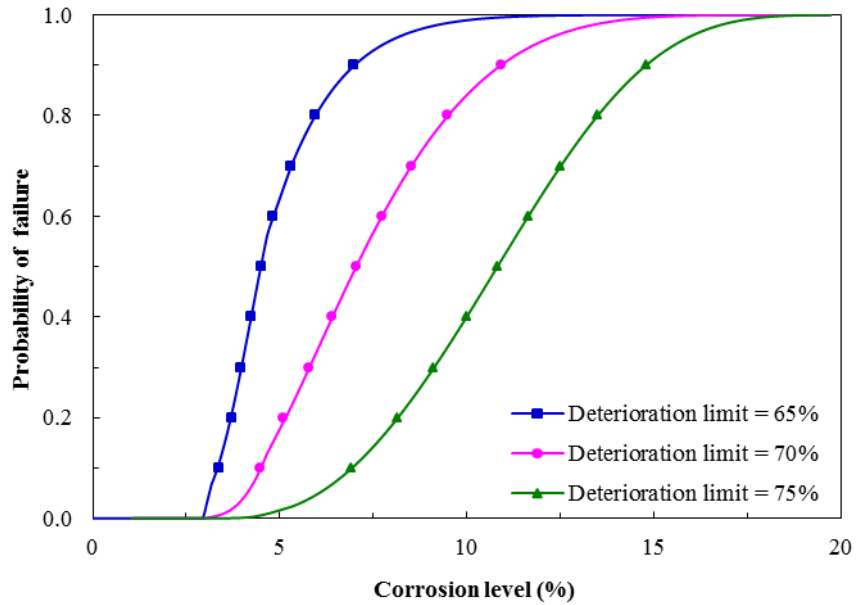


**Figure 6.5** Probability of failure versus corrosion level for various allowable bond strength deterioration limits

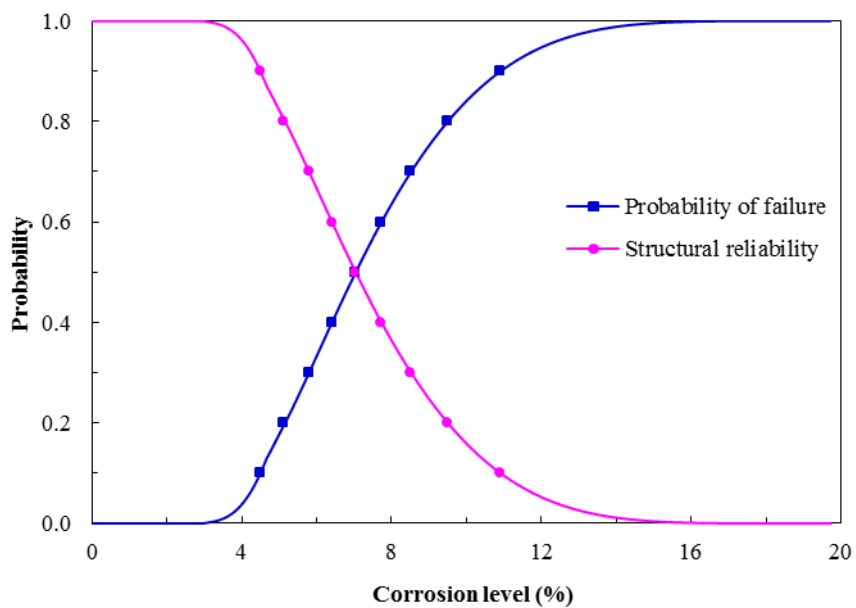


**Figure 6.6** Probability of failure and reliability versus corrosion level for allowable bond strength deterioration limit of 70%

The deterioration of the structural performance in terms of structural capacity (bond strength deterioration) is now indicated by the bond strength. As shown in Figure. 4.13, when surface crack width is about 0.4 mm, the residual bond strength of confined beam has only maintained 65% of its initial (non-corroded stage) bond strength. Therefore to calculate the probability of failure, maximum allowable limits of bond strength deterioration are considered as  $J_L = 65\%$ , 70% and 75%, respectively. The results of probability of failure ( $P_f$ ) are shown in Figure 6.5 for different allowable bond strength deterioration limits. Here again, the probability of failure associated with bond strength deterioration depends on the given allowable bond strength deterioration limits. In all three cases of deterioration limits, the probability of failure increases steadily showing lower probability of failure for the higher allowable deterioration limit at the same level of reinforcement corrosion. In order to evaluate the structural reliability in terms of bond strength deterioration of the corroded RC beam, equation (6.6) is applied for deterioration limit of 70% and presented along with the corresponding probability of failure in Figure 6.6. The Figure 6.6 clearly indicates that an increase in corrosion significantly decreases the reliability of the corroded RC beam.

The lifetime evolution of structural deterioration of corrosion-affected RC structures is here again modelled by the gamma process. In lifecycle modelling of corrosion affected RC structure, the structures are generally assessed on the basis of the ultimate limit state analysis. Therefore, the results for the probability of the RC beam reaching its ultimate limit state is presented in Figure 6.7.

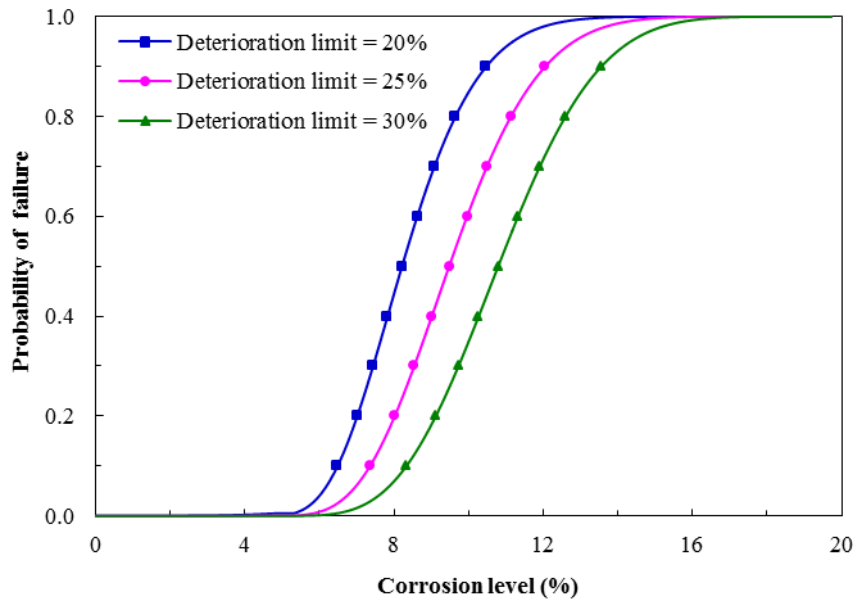


**Figure 6.7** Probability of failure versus corrosion level for various allowable flexural strength deterioration limits

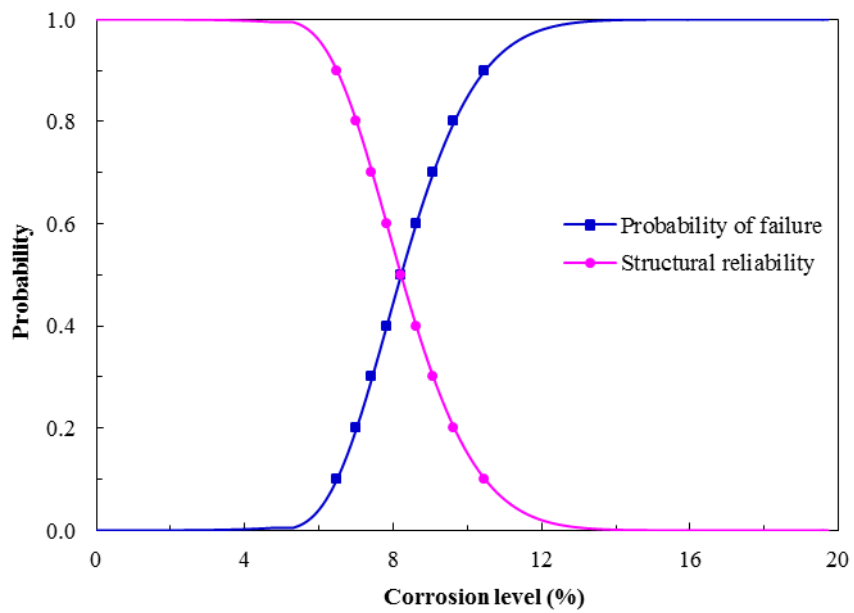


**Figure 6.8** Probability of failure and reliability of lifetime versus corrosion level for allowable flexural strength deterioration limit of 20%

In Figure 6.7, the ultimate limit state is represented by the fact that flexural strength capacity reaches the pre-defined deterioration limit. As shown in Figure 5.11 when surface crack width reaches about 0.4 mm, the residual flexural strength loses about 15% of its original strength for confined beam and about 35% for unconfined beam. Here, to calculate the probability of failure, the maximum allowable limits of flexural strength deterioration are chosen as  $J_L = 20\%$ , 25% and 30%, respectively. The results of probability of failure ( $P_f$ ) of the corroded RC beam are shown in Figure 6.7 for the chosen allowable flexural strength deterioration limits. From the results, the probability of failure associated with flexural strength deterioration depends on the given allowable strength deterioration limits. At the same level of reinforcement corrosion the probability of failure is lower for the higher allowable deterioration limit. The Figure 6.8 shows the trend of structural reliability and corresponding probability of failure of the corroded RC beam at allowable flexural strength deterioration limit of 20%. As expected and observed in Figure 6.8, as the corrosion progresses structural survivability decreases so as the probability of failure increases. This is due to the continuous reduction of flexural strength of RC beam caused by reinforcement corrosion. Results from Figure 6.3 to 6.8 indicate that the survival capacity of corrosion affected structures is more vulnerable in case of serviceability than load carrying capacity (i.e. bond and flexural strength).

#### 6.8.2 *Effect of cover surface cracking on life cycle performance*

Cracking in concrete cover is the time-dependent in nature and is an important parameter which helps in condition monitoring of RC structures. Hence, it is always beneficial to evaluate the effect of concrete cover cracking on the structural reliability

of corrosion damaged RC beams. Therefore in this section, time-dependent reliability analysis is evaluated in terms of probability of failure of the corroded RC structures as a function of cover surface cracking. Furthermore corresponding structural reliability of the RC beam is also presented as a function of cover surface cracking.

The results for the probability of the RC beam reaching its ultimate limit state (bond strength capacity) is shown in Figure 6.9 and corresponding structural reliability is shown in Figure 6.10. In order to perform the time dependent reliability analysis as function of cover surface cracking, the maximum allowable limits of bond strength deterioration as chosen in Figure 6.5 are considered i.e.  $J_L = 65\%$ ,  $70\%$  and  $75\%$ , respectively. Here the ultimate limit state is represented by the fact that bond strength capacity reaches the pre-defined deterioration limit and the results of probability of

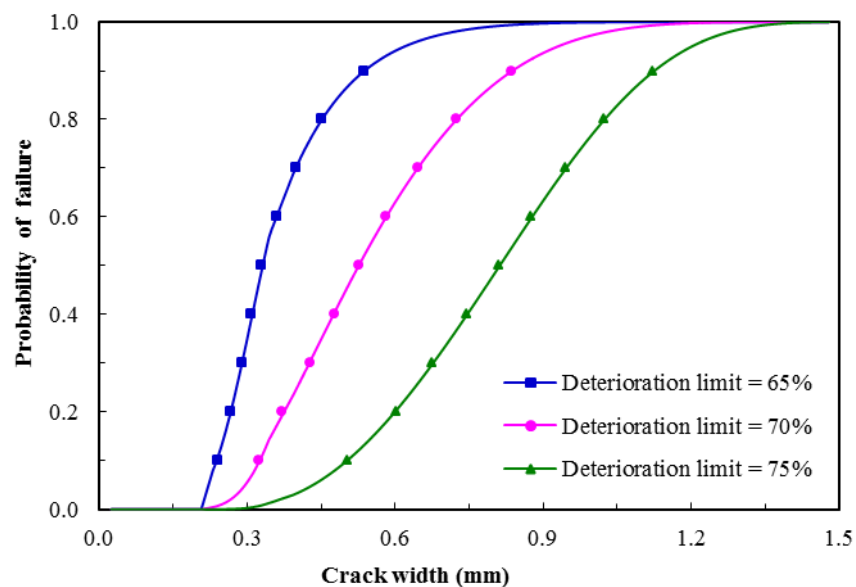


**Figure 6.9** Probability of failure versus cover surface cracking for various allowable bond strength deterioration limits

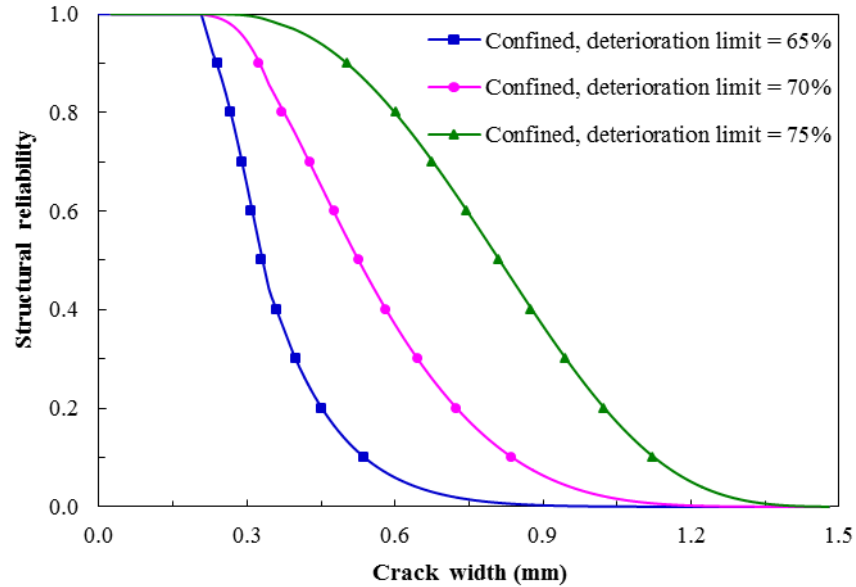


**Figure 6.10** Structural reliability versus cover surface cracking for various allowable bond strength deterioration limits

failure and structural reliability are presented in Figure 6.9 and 6.10 respectively for the chosen allowable bond strength deterioration limits. The probability of failure associated with the bond strength for different allowable limit increases steadily with increase in surface crack width. Here again, as anticipated, the probability of failure and reliability associated with bond strength deterioration depends on the given allowable strength deterioration limit, with higher probability of failure for a lower allowable deterioration limit at any stage of cover surface cracking.

The results for the probability of failure of the corroded RC beam in terms of structural capacity (measure by flexural strength) are shown in Figure 6.11. The lifetime distribution of probability of failure  $P_f$  of the structural strength capacity is obtained for different allowable flexural strength deterioration limit as used in Figure 6.7 i.e. 20%, 25% and 30%. As mentioned earlier, the deterioration of structural performance

in terms of structural capacity is here again modelled as gamma process and evaluated as a function of cover surface cracking. In all three cases of allowable flexural strength deterioration limit, the probability of failure increases steadily with further progress of cracking in the cover surface and reaches 50% when crack width is approximately between 0.6 mm to 0.8 mm.

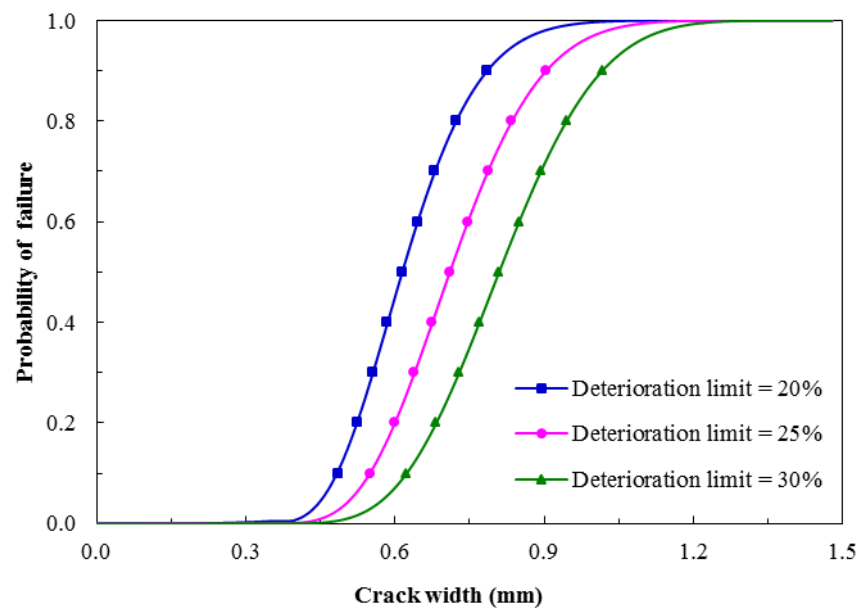


**Figure 6.11** Probability of failure versus cover surface cracking for various allowable flexural strength deterioration limits

Similarly, corresponding structural reliability is evaluated by using equation (6.6) as a function of concrete cover surface cracking and is plotted in Figure 6.12. The results indicate that the structural reliability decreases with increase in cracking process and it depends on the given allowable flexural strength deterioration limits, as expected. It is clear from the results obtained in Figure 6.9 to Figure 6.12 that cracking in concrete cover surface has significant impact on the reliability of the RC beam suffering from reinforcement corrosion.

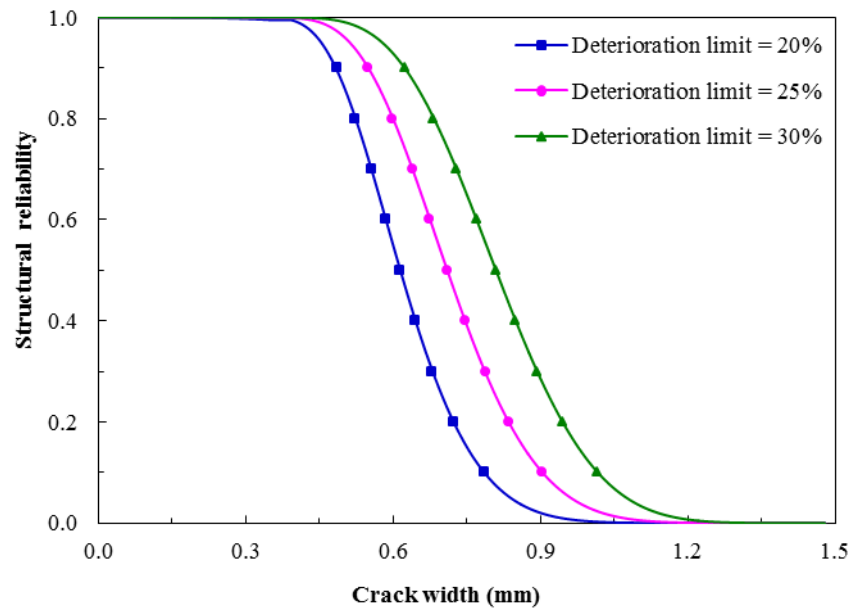


**Figure 6.12** Structural reliability versus cover surface cracking for various allowable flexural strength deterioration limits

### 6.8.3 Effect of stirrups on lifecycle performance

The strength deterioration rate of confined RC element is different from the unconfined one. Therefore, in order to study the effect of stirrup in the lifecycle performance of corroded RC element, a time-dependent reliability analysis of corrosion affected RC beam with and without stirrup with respect to cover surface cracking is presented in this section.

The structural reliability of confined and unconfined concrete in terms of bond strength deterioration is given in Figure 6.13. Here again the different allowable flexural strength deterioration limits (i.e.  $J_L = 65\%$ ;  $70\%$  and  $75\%$ ) as mentioned in Figure 6.9 have been considered during the analysis.

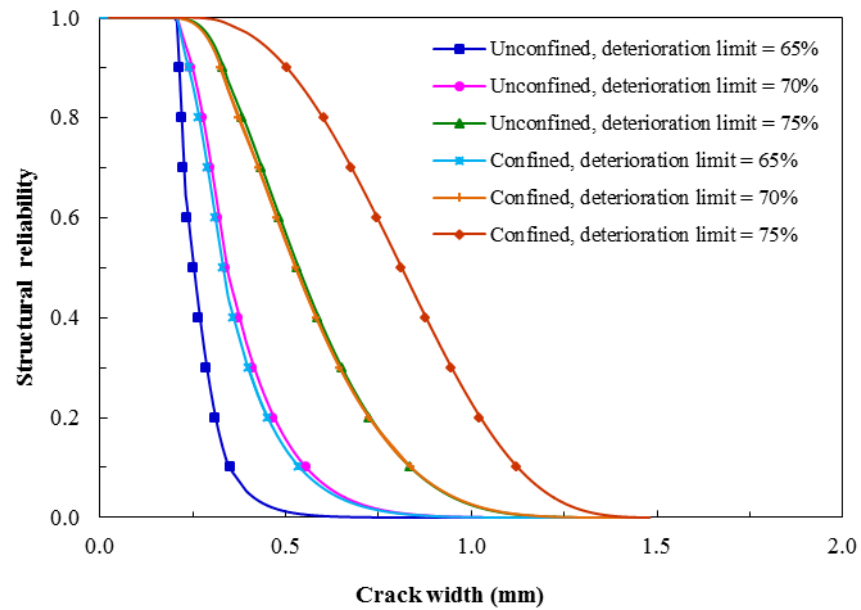


**Figure 6.13** Structural reliability versus cover surface cracking for various allowable bond strength deterioration limits of confined and unconfined beam

From the results in Figure 6.13, the probability of failure associated with bond strength deterioration depends on the given allowable strength deterioration limits for both confined and unconfined concrete. At the same level of reinforcement corrosion the probability of failure is lower for the higher allowable deterioration limits. Moreover, it is clear that unconfined concrete has considerably higher probability of failure than the confined concrete when the same values of the predefined allowable limit and cover surface cracking.

Similarly, the structural reliability of confined and unconfined concrete in terms of flexural strength deterioration is shown in Figure 6.14. Here, different allowable flexural strength deterioration limits, i.e.  $J_L = 20\%$ ;  $25\%$  and  $30\%$ , respectively, as considered in Figure 6.11 have been considered during the analysis. Here again, at any stage of cover cracking structural reliability continuously decreases for both unconfined

and unconfined and confined concrete, showing higher probability of failure for a lower allowable deterioration limit. Furthermore, from the time-dependent reliability analysis shown in Figure 6.13 and Figure 6.14, it is clear that the unconfined concrete has considerably lower structural reliability than the confined concrete when the same predefined allowable limit and concrete cover crack width are considered.

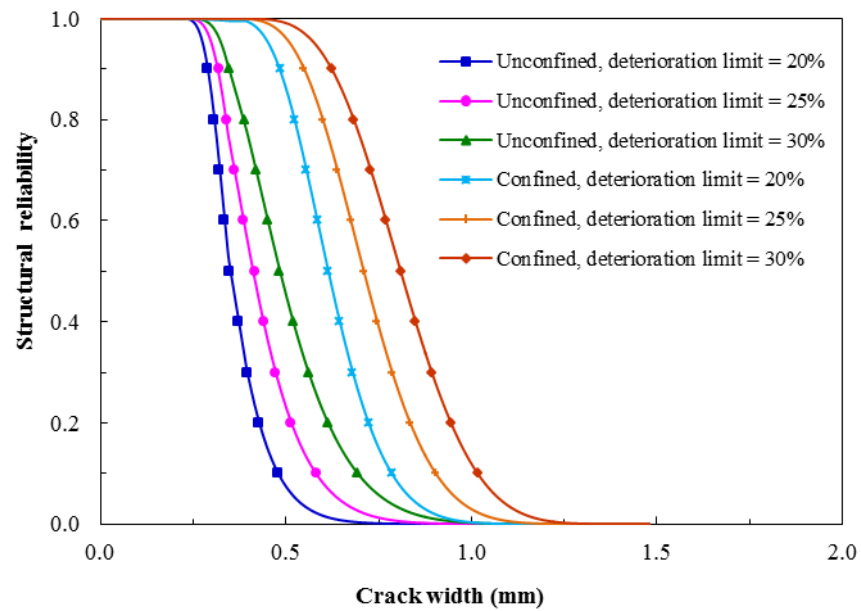


**Figure 6.14** Structural reliability versus cover surface cracking for various allowable flexural strength deterioration limits of confined and unconfined concrete beam

## 6.9 Numerical example 2

In this section the methodology mentioned in the preceding sections to find the optimal repair time is applied to a numerical example for a simply supported RC beam exposed to an aggressive environment and is subjected to mean annual corrosion current per unit length  $i_{corr} = 6 \mu\text{A}/\text{cm}^2$ . The cross-sectional width and effective depth of beam are  $b = 300$  mm and  $d = 560$  mm, respectively. Four steel rebars with diameter  $D_b = 16$

mm are provided as the tensile reinforcement and two rebars of diameter  $D_{sc} = 12$  mm are provided as the compressive steel with clear cover thickness  $C = 40$  mm along with the stirrup of diameter  $D_{st} = 6$  mm at spacing of 100 mm. The volume ratio of rust product is assumed as 2.5. The characteristic compressive strength of concrete is also assumed as  $f_{ck} = 40$  Mpa and corresponding concrete properties such as tensile strength and modulus of elasticity are obtained from EC2 (2004). Four number of cracks are assumed to be formed in the concrete cover and the critical and ultimate cohesive crack width required for this study have been obtained from CEB-FIP (1990) for adopted maximum aggregate size of 16 mm and fracture energy of 190 N/m.

#### 6.9.1 Evaluation of lifetime distribution of time to failure

The results of lifetime distribution of time of failure  $P_f(t)$  evaluated by using equation (6.5) in terms of structural serviceability and load carrying capacity are presented in Figures 6.15 and 6.16, respectively. As mentioned earlier in Section 6.7, the deterioration of structural performance in terms of structural serviceability (measured by the growth of equivalent crack width at the cover surface) and load carrying capacity (flexural strength deterioration) is modelled as gamma process. Finally, by using time-dependent reliability analysis, the corresponding time to failure is evaluated for various limits of deterioration. The time to failure corresponding to corrosion level  $X_p$  can be evaluated from equation (3.2). In Figure 6.15, acceptable crack width limits  $w_L = J_L = 0.3, 0.4$  and  $0.5$  mm, respectively are considered. Similarly, allowable flexural strength deterioration limits of 20%, 25% and 30% are utilized in Figure 6.16.

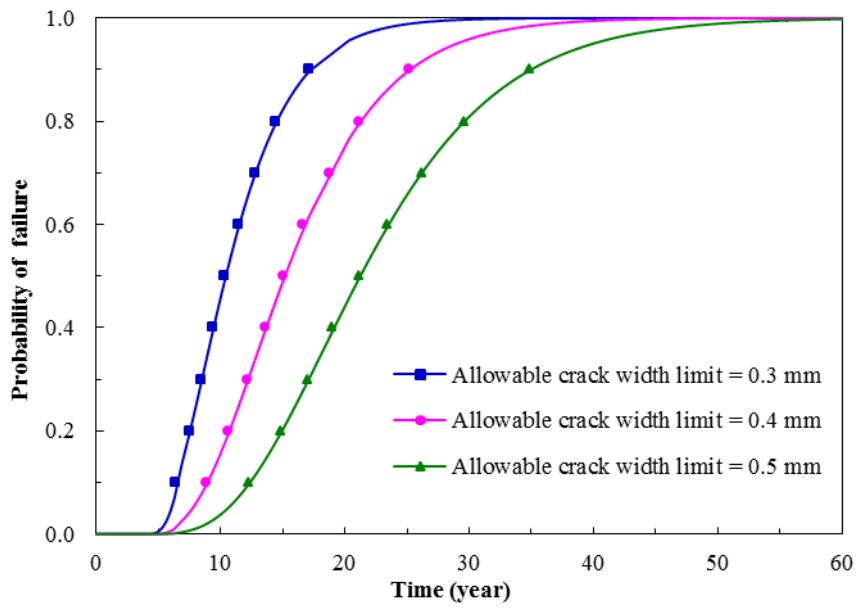


**Figure 6.15** Lifetime distribution of time to failure for various acceptable crack width limits

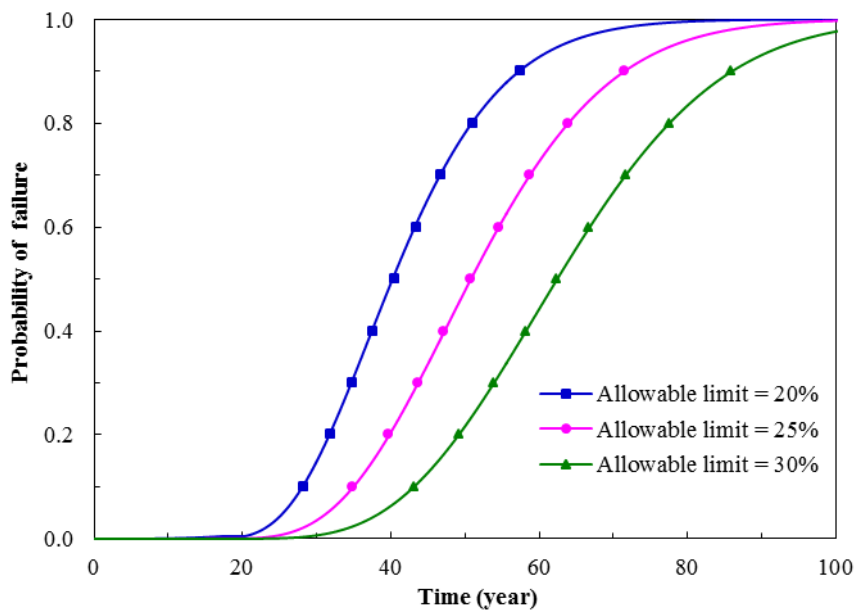


**Figure 6.16** Lifetime distribution of time to failure for various allowable flexural strength deterioration limits

As expected, in both Figures (i.e. Figures 6.15 and 6.16) the probability of failure increases with increase in time, showing higher probability of failure for a lower

deterioration limit. In case of structural serviceability, the corroded beam reaches its 50% probability of failure at the time between 10 and 20 years, while it will be at the age between 40 and 60 years in the case of structural capacity. This means that the corroded RC beam possess higher risk of failure in serviceability limit state rather than in the ultimate limit state.

### 6.9.2 Evaluation of optimal repair time

The optimal repair time associated with corrosion induced cover surface cracking and corresponding flexural strength deterioration is then investigated as shown in Figures 6.17 and Figure 6.18. In order to find an optimal value of the repair time, the cost defined in equation (6.11) is minimised with respect to the number of time interval  $k$ . Only relative costs are needed to be considered in calculations, assuming here the corrective maintenance cost  $C_F = 1.0$  and the preventive  $C_P = 0.1C_F$  is adopted in this study.

Figure 6.17 shows the results for the expected relative costs as a function of repair time for various acceptable limits, where the annual discount rate of 5% is considered. The results show that the optimal repair times are 5 year for  $J_L = 0.3$  mm, 7 year for  $J_L = 0.4$ , and 10 year for  $J_L = 0.5$  mm, respectively. Similarly, the results in Figures 6.18 and 6.19 shows the relative maintenance cost versus repair time for the case of confined and unconfined beam respectively.

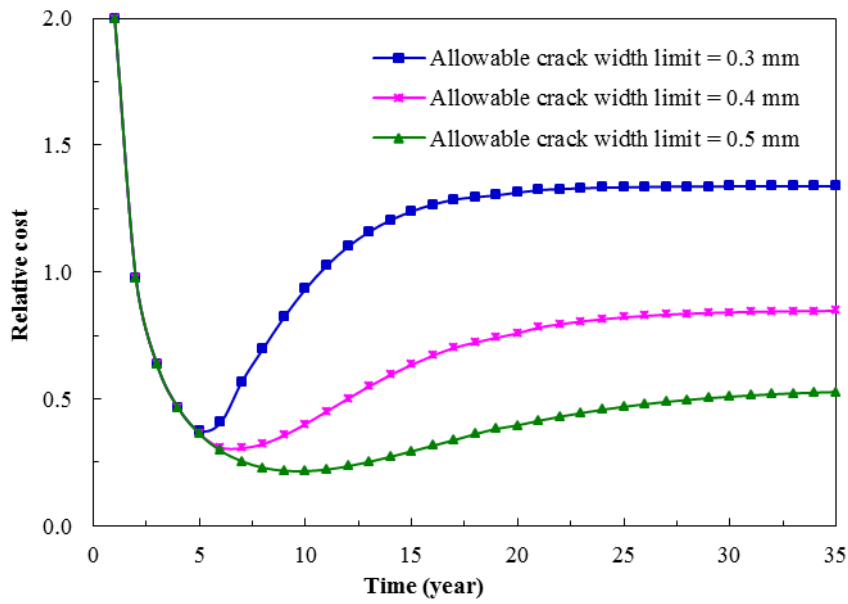


**Figure 6.17** Expected relative costs over repair time interval with discounting of an annual rate of 5% as a function of repair time for for various acceptable crack width limits

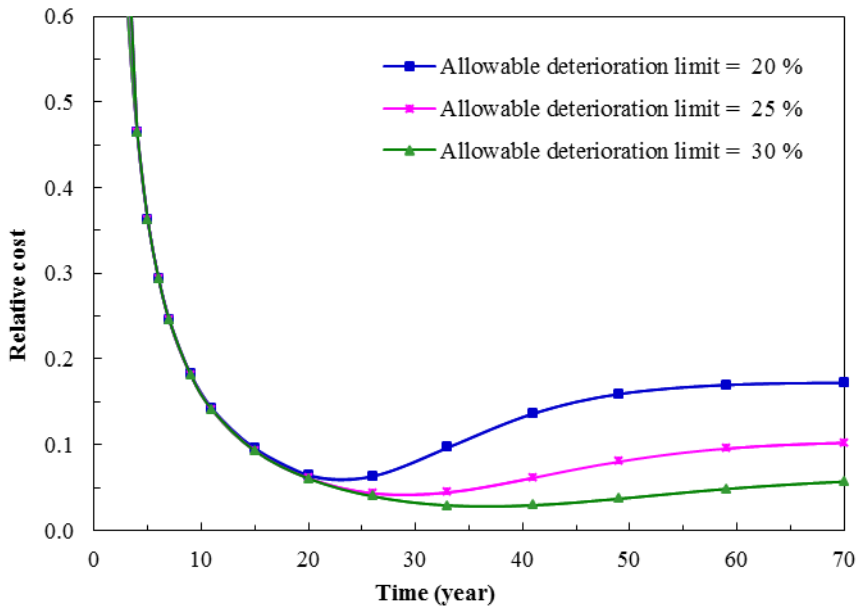


**Figure 6.18** Expected relative costs over repair time interval with discounting of an annual rate of 5% as a function of repair time for various allowable flexural strength deterioration limits of confined beam

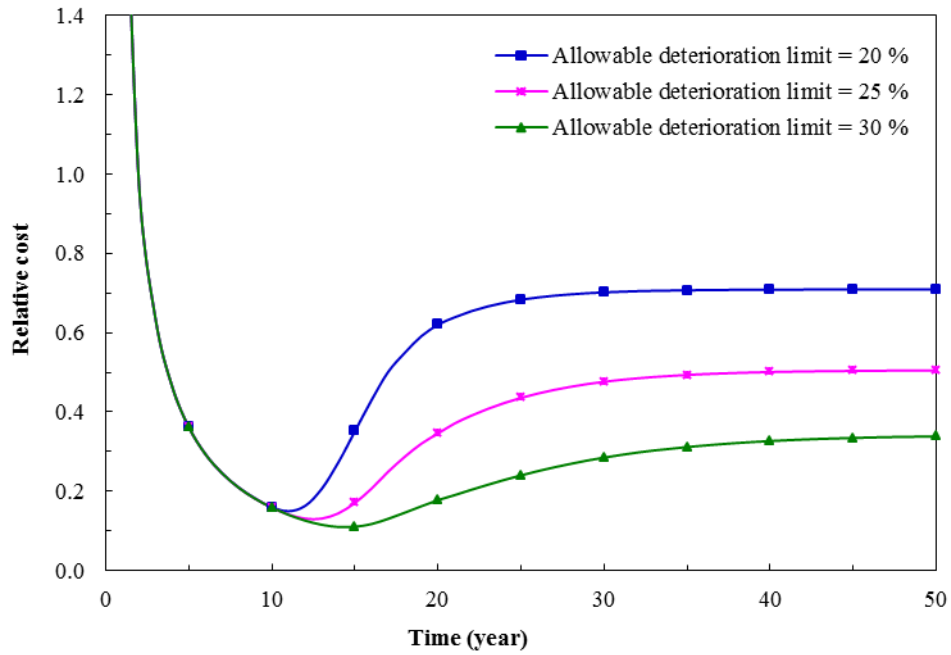


**Figure 6.19** Expected relative costs over repair time interval with discounting of an annual rate of 5% as a function of repair time for various allowable flexural strength deterioration limits of unconfined beam

The results in Figures 6.18 and 6.19 are evaluated for different allowable limits of deterioration (flexural strength) with an annual discounting rate of 5%, which indicates that the optimal repair time increases as the allowable deterioration limit increases, indicating an optimal repair time of 29 years in the case of confined beam and 12 years in case of unconfined beam for the deterioration limit of 25%. This indicates that optimum repair time is considerably sooner in case of confined concrete. Furthermore, the optimal repair time will be sooner if the maintenance strategy is based on serviceability of the structure.

### 6.9.3 Effect of preventive maintenance cost on optimal repair time

Figures 6.20 and 6.21 show the influence of the preventive maintenance cost  $C_P$  on the optimal repair time, where the preventive maintenance cost ranges from  $C_P = 10\%$  of  $C_F$  to  $50\%$  of  $C_F$ . The acceptable crack width limit is set at  $0.3$  mm in Figure 6.20 and allowable flexural strength deterioration limit  $J_L$  is set to  $25\%$  in Figure 6.21. In both cases, it can be seen that the value of the optimal repair time increases when the preventive maintenance cost goes up. For instance, in Figure 6.20 from 5 years for  $C_P = 0.1C_F$  to 11 years for  $C_P = 0.5C_F$ . Similarly in case of Figure 6.21, from 24 years for  $C_P = 0.1C_F$  to 41 years for  $C_P = 0.5C_F$ . The results also show that earlier repairs are necessary to reduce the risk of failure if the preventive maintenance cost is relatively low. When the preventive cost is high, the optimal repair time could be longer.

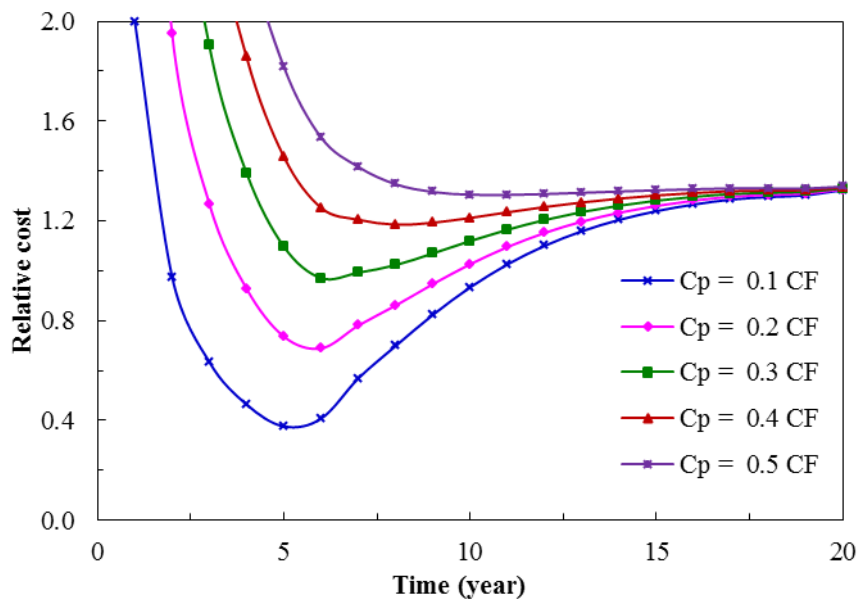


**Figure 6.20** Expected relative costs with discounting and  $J_L = 0.3$  mm as a function of repair time for various preventive maintenance costs  $C_P$

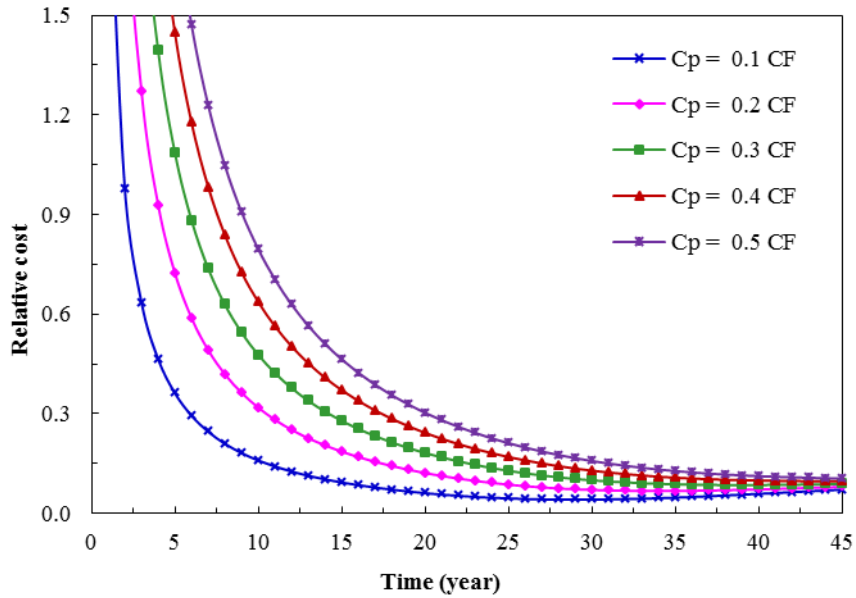


**Figure 6.21** Expected relative costs with discounting and  $J_L = 25\%$  as a function of repair time for various preventive maintenance costs  $C_P$

#### 6.9.4 Effect of cover depth on optimal repair time

The effect of cover depth on optimal repair time of corroded RC beam with respect to cover surface cracking and flexural strength deterioration is presented in Figures 6.22 and 6.23 respectively. In the investigations, various cover depth to rebar diameter ratios: 2, 2.5 and 3 are considered along with the preventive maintenance cost factor  $C_P = 0.1$  and discount factor = 5%. The deterioration limit of 0.3 mm (acceptable crack width limit) is considered in Figure 6.22 and deterioration limit of 25% (flexural strength deterioration limit) is considered in Figure 6.23. As expected, the results indicate that optimal repair time increases in higher cover depth in both cases of analysis. However, the increase in optimal repair time with respect to cover depth is comparably higher in Figure 6.23.

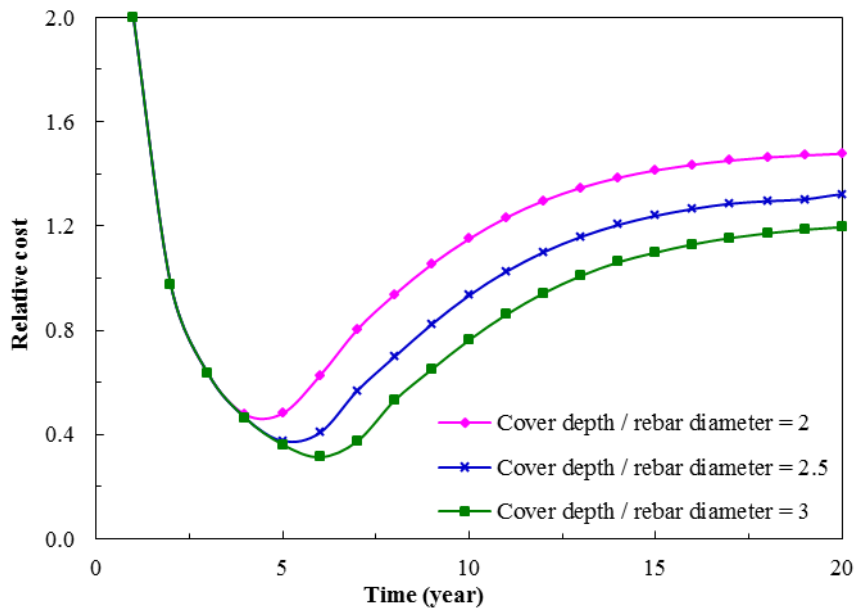


**Figure 6.22** Expected relative costs with discounting as a function of repair time, evaluated for various cover depths with  $J_L = 0.3$  mm

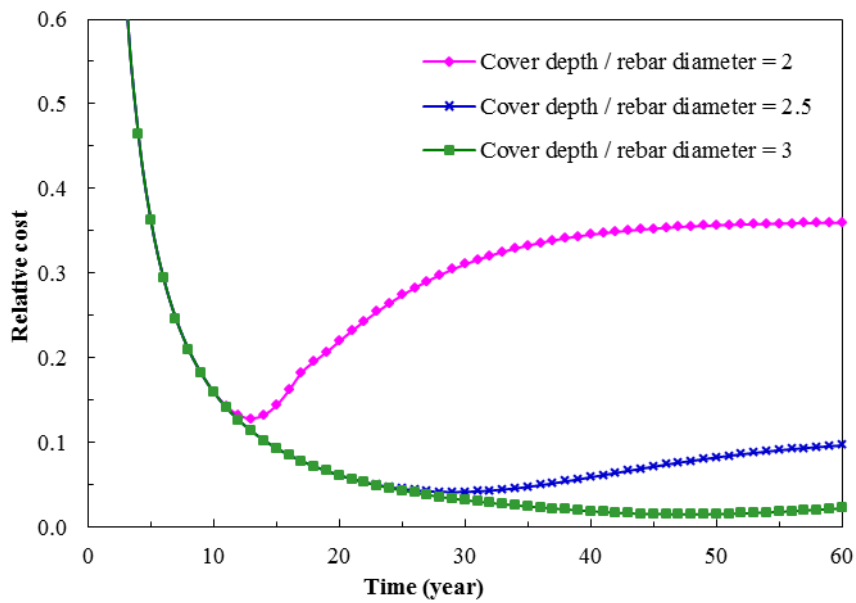


**Figure 6.23** Expected relative costs with discounting as a function of repair time, evaluated for various cover depths with  $J_L = 25\%$

## 6.10 Summary and conclusions

This section presents a novel approach for evaluating the life cycle performance of corrosion affected RC structures. At first, stochastic deterioration modeling and time-dependent reliability analysis of corrosion affected RC beam is discussed analytically. By using the stochastic model based on gamma process, the probability of structural failure associated with the surface crack width and strength deterioration (bond and flexural) over the lifecycle of corrosion affected RC structures have been evaluated. The optimized strategy for the repair time is illustrated on the basis of the minimization of the balance between the risk of failure and the maintenance costs.

On the basis of the results obtained from the numerical example following conclusions are drawn: a) The proposed stochastic deterioration model based on the gamma process can be applied to assess the lifecycle performance with uncertainties, such as cracking and strength deterioration in corroded RC structures; b) The probability of failure of corrosion affected RC structure during their life cycle depends not only on the predefined allowable limit of their deterioration but also on the types of the structure; c) Structural reliability decreases with time due to increase in cover surface cracking and its corresponding strength deterioration; d) The optimal maintenance strategy during the service life of a structure affected by reinforcement corrosion can be determined by optimising the balance between the risk of failure and the maintenance costs; e) The optimal repair time depends on various factors such as allowable deterioration limit, type of the structures and preventive maintenance cost. Thus, the proposed approach is capable of assessing the life cycle performance and determining the optimum repair plan of concrete structures affected by reinforcement corrosion.

## Chapter 7 Conclusions and Suggestions for Future Work

### 7.1 Summary and conclusions

The main aim of this research was to improve the understanding of the structural behaviour of corrosion damaged RC structures with special attention to three topics: 1) corrosion induced concrete cover cracking, 2) bond strength degradation and 3) flexural strength degradation. The research was also aimed to investigate the lifecycle management of corrosion damaged RC structures based on condition-based maintenance model by considering realistic behaviour of corroded rebar and surrounding cracked concrete. In the research, at first, analytical models were developed to study the structural effect of the deterioration caused by reinforcement corrosion. Then the results obtained from the developed analytical investigations were validated with the field and experimental data available. Furthermore, by using the stochastic gamma process on analytical results, lifecycle performance assessment was also investigated by using time-dependent reliability analysis. Finally, the optimal repair planning and maintenance strategies during the lifetime were determined by balancing the cost of maintenance and risk of failure. A full set of conclusions were included at the end of each chapter. The more significant conclusions are now summarised in this chapter.

#### Corrosion induced cover cracking

- \* A new analytical model for predicting the crack growth in concrete cover is developed by considering the realistic properties of corrosion induced cracked concrete such as anisotropic behaviour, residual tensile strength and reduced

tensile stiffness. The proposed model is capable of predicting crack growth in concrete cover with progress of reinforcement corrosion. It has also been found that concrete geometry has significant effect on crack initiation at the concrete cover surface.

#### Corrosion induced bond strength degradation

- \* A novel theoretical approach for evaluating corrosion induced bond strength degradation is proposed by considering three different phases of crack growth in concrete cover: 1) crack initiation, 2) crack propagation and 3) residual life phase. The proposed model is capable of providing reliable results when compared with the experiment and field data available. From the investigation it was found that reduction of rebar and corresponding cracking in the concrete cover surface has significant effect on the residual bond strength. The reduction in residual bond strength is more prominent in unconfined concrete specimen. Increase in cover depth enhances the bond strength at the intact stage. However, at the crack propagation and residual life stages cover depth increase has insignificant impact on residual bond strength.

#### Corrosion induced flexural strength degradation

- \* A new theoretical approach for evaluating the residual flexural strength of corroded RC beam is proposed. The proposed methodology is based on flexural analysis of RC beam that considers the realistic parameters associated with the flexural strength loss such as sectional area loss of rebar and bond strength degradation due to reinforcement corrosion. During the analysis, a new strain compatibility condition caused by the insufficient bond strength is considered

together with the different failure modes. The results from the study confirmed that due to reinforcement corrosion bond strength is comparatively more affected than the flexural strength. Furthermore, the progress of reinforcement corrosion has a substantial effect on the flexural strength of the concrete beams failing in bond. It has also been found that increase in cover depth and providing transverse reinforcement can reduce the rate of flexural strength deterioration of corroded beam failing in bond.

#### Lifecycle management of corrosion damaged RC structures

- \* A new approach has been proposed to investigate the lifecycle management of RC structures suffering from reinforcement corrosion. In lifecycle performance assessment, gamma process was adopted for stochastic deterioration modelling to take uncertainties into account. The time-dependent reliability analysis is then employed to evaluate the probability of failure and reliability of the RC beam in both limit states. A condition-based maintenance model was applied to investigate the optimal repair strategy of corrosion damaged RC beam with consideration of realistic behaviour of damages caused by reinforcement corrosion. The optimal repair planning and maintenance strategies during the lifecycle were determined by balancing the cost for maintenance and the risk of failure. The results from the analysis showed that the proposed stochastic deterioration model based on the gamma process can be applied to assess the lifecycle performance with uncertainties, such as cracking and strength deterioration in corroded RC structures. Furthermore the adopted condition-based maintenance model can also be useful in assessing the optimal repair strategy of corrosion damaged RC structures. As expected, the structural

reliability depends not only on predefined allowable limit of deterioration but also on types of the structure. For instance at the same deterioration limit probability of failure of unconfined beam is higher than confined beam. Likewise, these two factors also influence the lifecycle maintenance cost such as the optimal repair time.

## **7.2 Suggestions for future work**

Following recommendations are suggested for future study:

- \* More experimental and field investigations are required to evaluate nature of corrosion products formed subject to different conditions. The influence of the different parameters such as corrosion product formed in different conditions, rebar type and position, concrete cover thickness, concrete strength and the steel yield strength on the behaviour of reinforced concrete elements subjected to corrosion are also needed to be studied both in the laboratory and in the field. A long-term data collection and study of the deterioration of real concrete structures due to corrosion are also needed. This information will help in developing more effective theoretical model for performance assessment of corrosion damaged RC structures.
  
- \* Further research is needed to consider a non-uniform corrosion induced concrete cracking for both analytical and numerical solutions. Acceleration of reinforcement corrosion due to cover cracking is also need to be studied. In

addition, structural effect caused by reinforcement corrosion occurring in partial length is also required.

- \* The effect of corrosion on stirrups should be studied. Furthermore the effect of corroded stirrups on the concrete crack development and residual strength of corroded RC element should also be studied in future so that load carrying capacity considering bond, flexural and shear failure can be achieved. More studies are also required to investigate on the deflection associated with the reinforcement corrosion.
  
- \* In the real structure, along with the reinforcement corrosion other factors, such as weathering, freeze-thaw, chemical attack, and mechanical overloading can also affect the performance of structures. Further research is needed to address the combined effects of these factors on the performance of the structures.
  
- \* As the allowable deterioration limit significantly influences the probability of failure and the optimal repair time. It is recommended to develop robust assessment criteria to indicate the failure of the structure in both limit states.

## References

- Abdel-Hameed, M. (1975). A gamma wear process. *IEEE Transactions on Reliability*, 24(2), pp. 152-153.
- ACI (1992). Bond Under Cyclic Loads (ACI 408R-92). American Concrete Institute, Farmington Hills.
- ACI (2003). Bond and development of straight reinforcement in tension (ACI 408R-03). American Concrete Institute, Farmington Hills.
- AGA(2015).American Galvanizing Association.<<http://archive.galvanizeit.org/about-hot-dip-galvanizing/how-long-does-hdg-last/in-concrete>>.
- Agrawal, A.K. and Kawaguchi, A. (2009). Bridge element deterioration rates : final report. New York State Department of Transportation, Albany.
- Ahmad, S. (2003). Reinforcement corrosion in concrete structures, its monitoring and service life prediction-a review. *Cement and Concrete Research*, 25(4), pp. 459-471.
- Al-Barqawi, H. and Zayed, T. (2006). Condition rating model for underground infrastructure sustainable water mains. *Journal of Performance of Constructed Facilities, ASCE*, 20(2), pp. 126-135.
- Almusallam, A.A., Al- Ghantani, A.S., Aziz, A.R. and Rasheeduzzafar (1996). Effect of reinforcement corrosion on bond strength. *Construction and Building Materials*, 10(2), pp. 123-129.
- Alonso, C., Andrade, C., Rodriguez, J. and Diez, J.M. (1998). Factors controlling cracking of concrete affected by reinforcement corrosion. *Materials and Structures*, 31(7), pp. 435-441.

Al-Sulaimani, G.J., Kaleemullah, M., Basunbul, I.A. and Rasheeduzzafar (1990). Influence of corrosion and cracking on bond behaviour and strength of reinforced concrete members. *ACI Structural Journal*, 87(2), pp. 220-231.

Amleh, L. and Ghosh, A. (2006). Modeling the effect of corrosion on bond strength at the steel-concrete interface with finite element analysis. *Canadian Journal of Civil Engineering*, 33(6), pp. 673-682.

Andrade, C., Alonso, C. and Molina, F.J. (1993). Cover cracking as a function of rebar corrosion: part I-experimental test. *Materials and Structures*, 26(8), pp. 453- 464.

Ang, A.H.S. and Tang, W.H. (1984). Probability concepts in engineering planning and decision. John Wiley and Sons Inc, New York.

Au, F.T.K. and Du, J.S. (2004). Prediction of ultimate stress in un-bonded prestressed tendons. *Magazine of Concrete Research*, 56(1), pp. 1-11.

Auyeung, Y.B., Balaguru, P. and Chung, L. (2000). Bond behaviour of corroded reinforcement bars. *ACI Materials Journal*, 97(2), pp. 214-221.

Azad, A.K., Ahmad, S. and Al-Gohi, B.H.A. (2010). Flexural strength of corroded reinforced concrete beams. *Magazine of Concrete Research*, 62(6), pp. 405-414.

Azad, A.K., Ahmad, S. and Azher, S.A. (2007). Residual strength of corrosion-damaged reinforced concrete beams. *ACI Materials Journal*, 104(1), pp. 40-47.

Balafas, I. and Burgoyne, C.J. (2010). Environmental Effects on cover cracking due to corrosion. *Cement and Concrete Research*, 40(9), pp. 1429-1440.

Balafas, I. and Burgoyne, C.J. (2011). Modeling the structural effects of rust in concrete cover. *Journal of Engineering Mechanics, ASCE*, 137(3), pp. 175-185.

Banba, S., Abe, T., Nagaoka, K. and Murakami, Y. (2014). Evaluation method for bond-splitting behavior of reinforced concrete with corrosion based on confinement stress of concrete against corrosion expansion. *Journal of Advanced Concrete Technology*, 12(1), pp. 7-23.

Bazant, Z.P. and Planas, J. (1998). Fracture and size effect in concrete and other quasibrittle materials. CRC Press, Florida.

Bazant, Z.P. (1979). Physical model for steel corrosion in concrete sea structures-theory. *Journal of the Structural Division, ASCE*, 105(6), pp. 1137-1153.

Bazant, Z.P. and Oh, B.H. (1983). Crack band theory for fracture of concrete. *Materials and Structures*, 16(3), pp. 155-177.

Bertoa, L., Simioni, P. and Saetta, A. (2008). Numerical modelling of bond behaviour in RC structures affected by reinforcement corrosion. *Engineering Structures*, 30(5), pp. 1375-1385.

Bertolini, L., Elsener, B., Pedferri, P., Redaelli, E. and Polder, R.B. (2004). Corrosion of steel in concrete: prevention, diagnosis, repair. Wiley VCH, Weinheim.

Bhargava, K., Ghosh, A.K., Mori, Y. and Ramanujama, S. (2006). Model for cover cracking due to rebar corrosion in RC structures. *Engineering Structures*, 28(8), pp. 1093-1109.

Bhargava, K., Ghosh, A.K., Mori, Y. and Ramanujam, S. (2007). Corrosion-induced bond strength degradation in reinforced concrete-analytical and empirical models. *Nuclear Engineering and Design*, 237(11), pp. 1140-1157.

Bhargava, K., Mori, Y. and Ghosh, A.K. (2011a). Time-dependent reliability of corrosion-affected RC beams. Part 1: Estimation of time-dependent failure probability. *Nuclear Engineering and Design*, 241(5), pp. 1371-1384.

Bhargava, K., Mori, Y. and Ghosh, A.K. (2011b). Time-dependent reliability of corrosion-affected RC beams. Part 2: Estimation of time-dependent failure probability. *Nuclear Engineering and Design*, 241(5), pp. 1385-1394.

Borgard, B., Warren, C., Somayaji, S. and Heidersbach, R. (1990). Mechanisms of corrosion of steel in concrete. In: N.S. Berker, V. Chaker and D. Whiting, eds. Corrosion rate of steel in concrete. ASTM STP 1065, Philadelphia, pp. 174-188.

Broomfield, J.P. (2007). Corrosion of steel in concrete: understanding, investigation and repair. CRC Press, New York.

Cairns, J. and Abdullah, R.B. (1996). Bond strength of black and epoxy-coated reinforcement-a theoretical approach. *ACI Materials Journal*, 93(4), pp. 362-369.

Cairns, J. and Zhao, Z., (1993). Behaviour of concrete beams with exposed reinforcement. *Proceedings of the ICE - Structures and Buildings*, 99(2), pp. 141-154.

Cairns, J., Du, Y. and Law, D. (2006). Residual bond strength of corroded plain round bars. *Magazine of Concrete Research*, 58(4), pp. 221-231.

Cairns, J., Du, Y. and Law, D. (2008). Structural performance of corrosion-damaged concrete beams. *Magazine of Concrete Research*, 60(5), pp. 359-370.

Castel, A., Francois, R. and Arliguie, G. (2000). Mechanical behaviour of corroded reinforced concrete beams-Part 1: Experimental study of corroded beams. *Materials and Structures*, 33(9), pp. 539-544.

Cattan, J. and Mohammadi, J. (1997). Analysis of bridge condition rating data using neural networks. *Computer-Aided Civil Engineering and Infrastructure Engineering*, 12(6), pp. 419-429.

CEB-FIP (1990). CEB-FIP model code 1990, Design code. Thomas Telford, London.

Chen, D. and Mahadevan, S. (2008). Chloride-induced reinforcement corrosion and concrete cracking simulation. *Cement and Concrete Composites*, 30(3), pp. 227-238.

Chen, H.P. and Alani, A.M. (2012). Reliability and optimised maintenance for sea defences. *Proceedings of the ICE- Maritime Engineering*, 165(2), pp. 51-64.

Chen, H.P. and Alani, A.M. (2013). Optimized maintenance strategy for concrete structures affected by cracking due to reinforcement corrosion. *ACI Structural Journal*, 110(2), pp. 229-238.

Chen, H.P. and Bicanic, N. (2010). Identification of structural damage in buildings using iterative procedure and regularisation method. *Engineering Computations*, 27(8), pp. 930-950.

Chen, H.P. and Nepal, J. (2014). Modelling of flexural strength deterioration in corroded reinforced concrete structures and its stochastic analysis. *Engineering Structures*, (under review).

Chen, H.P. and Nepal, J. (2015a). Analytical Model for residual bond strength of corroded reinforcement in concrete structures. *Journal of Engineering Mechanics, ASCE*, 10.1061/(ASCE)EM.1943-7889.0000997.

Chen, H.P. and Nepal, J. (2015b). Stochastic modelling and lifecycle performance assessment of bond strength of corroded reinforcement in concrete. *Structural Engineering and Mechanics*, 54(2), pp. 319-336.

Chen, H.P. and Nepal, J. (2015c). Analysing the effect of cover cracking on structural reliability of corroded reinforced concrete structures. *Advances in Structural Engineering*, (under review).

Chen, H.P. and Xiao, N. (2012). Analytical solutions for corrosion-induced cohesive concrete cracking. *Journal of Applied Mathematics*, Article ID 769132.

Chernin, L., Val, D.V. and Stewart, M.G. (2012). Prediction of cover crack propagation in RC structures caused by corrosion. *Magazine of Concrete Research*, 62(2), pp. 95-111.

Chernin, L., Val, D.V. and Volokh, K.Y. (2010). Analytical modelling of concrete cover cracking caused by corrosion of reinforcement. *Materials and Structures*, 43(4), pp. 543-556.

Chung, L., Kim, J.H.J. and Yi, S.T. (2008a). Bond strength prediction for reinforced concrete members with highly corroded reinforcing bars. *Cement and Concrete Composites*, 30(7), pp. 603-611.

Chung, L., Najm, H. and Balaguru, P. (2008b). Flexural behavior of concrete slabs with corroded bars. *Cement and Concrete Composites*, 30(3), pp. 184-193.

Comité Euro-international du Béton - Fédération International de la Précontrainte (CEB-FIP) (1990). CEB-FIP Model Code 1990 Design Code. Thomas Telford, London.

Coronelli, D. (2002). Corrosion cracking and bond strength modelling for corroded bars in reinforced concrete. *ACI Structural Journal*, 99(3), pp. 267-276.

Coronelli, D. and Gambarova, G. (2000). A mechanical model for bond strength of corroded reinforcement in concrete., Proceedings of 14<sup>th</sup> Engineering Mechanics Conference (ASCE EM2000), Austin, Texas.

Coronelli, D., Hanjari, K. and Lundgren, K. (2013). Severely corroded RC with cover cracking. *Journal of Structural Engineering, ASCE*, 139(2), pp. 221-232.

Das, P.C. (2000). Reliability based bridge management procedures. In: M.J. Ryall, G.A.R. Parke, and J.E. Harding, Bridge management 4 - inspection, maintenance, assessment and repair. Thomas Telford, London.

Du, Y.G., Clark, L.A. and Chan, A.H.C. (2005). Residual capacity of corroded reinforcing bars. *Magazine of Concrete Research*, 57(3), pp. 135-147.

Duffo G.S., Reinoso, M., Ramos, C.P. and Farina, S.B. (2012). Characterization of steel rebars embedded in a 70-year old concrete structure. *Cement and Concrete Research*, 42(1), pp. 111-117.

DuraCrete (1998). Modeling of Degradation, BRITE-EURAM-Project BE95-1347/R4-5.

DuraCrete (2000). Probabilistic performance based on durability design of concrete structures: Statistical quantification of the variables in the limit state functions, Report : BE 95-1347, pp. 62-63.

EC2 (2004). Eurocode 2: Design of concrete structures - Part 1-1: General rules and rules for buildings (BS EN 1992-1-1:2004). European committee for standardization, Brussels.

Edirisinghe, R., Setunge, S. and Zhang, G. (2013). Application of gamma process for building deterioration prediction. *Journal of Performance of Constructed Facilities*, ASCE, 27(6), pp. 763-777.

Edwards, E. (2012). Corrosion of steel in concrete.

<<http://www.corrosionengineering.co.uk/knowledge-library/corrosion-of-steel-in-concrete>>.

Ehlen, M.A., Thomas, M.D.A. and Bentz, E.C. (2009). Life-365 service life prediction model version 2.0. *ACI Concrete International*, 31(5), pp. 41-46.

EI Maaddawy, T., Soudki, K. and Topper, T. (2005a). Analytical model to predict nonlinear flexural behavior of corroded reinforced concrete beams. *ACI Structural Journal*, 102(4), pp. 550-559.

EI Maaddawy, T. and Soudki, K. (2007). A model for prediction of time from corrosion initiation to corrosion cracking. *Cement and Concrete Composites*, 29(3), pp. 168-175.

EI Maaddawy, T., Soudki, K. and Topper, T. (2005b). Long-term performance of corrosion-damaged reinforced concrete beams. *ACI Structural Journal*, 102(5), pp. 649-656.

El Reedy, M.A. (2008). Steel-reinforced concrete structures: assessment and repair of corrosion. CRC Press, Florida

Elices, M., Guinea, G.V., Gomez, J. and Planas, J. (2002). The cohesive zone model: advantages, limitations and challenges. *Engineering Fracture Mechanics*, 69(2), pp. 137-163.

Ellingwood, B.R and Mori, Y. (1997). Reliability-based service life assessment of concrete structures in nuclear power plants: optimum inspection and repair. *Nuclear Engineering and Design*, 175(3), pp. 247-258.

Ellingwood, B.R. and Mori, Y. (1993). Probabilistic methods for condition assessment and life prediction of concrete structures in nuclear power plants. *Nuclear Engineering and Design*, 142(2-3), pp. 155-166.

Enright, M.P. and Frangopol, D.M. (1998a). Service-life prediction of deteriorating concrete structures. *Journal of Structural Engineering, ASCE*, 124(3), pp. 309-317.

Enright, M.P. and Frangopol, D.M. (1998b). Probabilistic analysis of resistance degradation of reinforced concrete bridge beams under corrosion. *Engineering Structures*, 20(11), pp. 960-971.

Eyre, J.R. and Nokhasteh, M.A. (1992). Strength assessment of corrosion damaged reinforced concrete slabs and beams. *Proceedings of the ICE-Structures and Buildings*, 94(2), pp. 197-203.

Fang, C., Lundgren, K., Chen, L. and Zhu, C. (2004). Corrosion influence on bond in reinforced concrete. *Cement and Concrete Research*, 34(11), pp. 2159-2167.

FESI (2012). FESI NEWS .< <http://www.fesi.org.uk>>.

FHWA (2004). Status of the Nation's Highways, Bridges, and Transit: 2004 Conditions and Performance. <<http://www.fhwa.dot.gov/policy/2004cpr/index.htm>>

Fib Model Code (FIB) (2010). Bond of reinforcement in concrete-state of the art report. Bulletin No.10, TG4/2 (Bond Models), Lausanne, Switzerland.

Fischer, C. (2010). Experimental investigations on the effect of corrosion on bond of deformed bars. Proceedings of the 8<sup>th</sup> fib PhD Symposium, Kgs, Lyngby, Denmark.

Frangopol, D.M. (1997). Application of lifecycle risk-based criteria to bridge assessment and design. In: P.C. Das, ed. Safety of bridges. Thomas Telford , London, pp. 151-157.

Frangopol, D.M. (1999). Lifecycle cost analysis for bridges, Chapter 9, In: D.M. Frangopol, ed. Bridge safety and reliability. ASCE, Reston, Virginia, pp. 210-236.

Frangopol, D.M. (2003). Preventative maintenance strategies for bridge groups-analysis. Final project Report to Highways Agency, London.

Frangopol, D.M. and Das, P.C. (1999). Management of bridge stocks based on future reliability and maintenance costs . In: P.C. Das, D.M. Frangopol and A.S. Nowak, eds. Current and future trends in bridge design, construction, and maintenance. Thomas Telford, London, pp. 45-58.

Frangopol, D.M., Gharaibeh, E.S., Kong, J.S. and Miyake, M. (2000a). Optimal network level bridge maintenance planning based on minimum expected cost. *Journal of Transport Research Board*, 2, pp. 26-33.

Frangopol, D.M., Kong, J.S. and Gharaibeh, E. (2001). Reliability-based lifecycle management of highway bridges. *Journal of Computing in Civil Engineering*, ASCE, 15, pp. 27-34.

Frangopol, D.M., Kong, J.S. and Gharaibeh, E.S. (2000b). Bridge management based on lifetime reliability and whole life costing: the next generation. In: M.J. Ryall, G.A.R. Parke and J.E. Harding, eds. *Bridge management 4*. Thomas Telford, London, pp. 392-399.

Giuriani , E., Plizzari, G. and Schumm, C. (1991). Role of stirrups and residual tensile strength of cracked concrete on bond. *Journal of Structural Engineering*, ASCE, 117(1), pp. 1-18.

Hahn, M., Palmer, R.N. and Merrill, M.S. (1999). Prioritizing sewer line inspection with an expert system. *Proceedings of WRPMD'99: Preparing for the 21st Century*, Tempe, Arizona, United States.

Hillerborg, A., Modeer, M. and Petersson, P.E. (1976). Analysis of crack formation and crack growth in concrete by means of fracture mechanics and finite elements. *Cement and Concrete Research*, 6(6), pp. 773-781.

Hong, H.P. (2000). Assessment of reliability of aging reinforced concrete structures. *Journal of structural Engineering*, ASCE, 126(12), pp. 1458-1465.

Horringmoe, G., Saether, I., Antonsen, R. and Arntsen, B. (2007). Laboratory investigations of steel bar corrosion in concrete background document SB-3.10, Nour Technology.

Jaffer S.S. and Hansson , C.M. (2009). Chloride-induced corrosion products of steel in cracked concrete subjected to different loading conditions. *Cement and Concrete Research*, 39(2), pp. 116-125.

Jirasek, M. and Bazant, Z.P. (2001). In-elastic analysis of structures. John Wiley and Sons, West Sussxex, England.

Khan, I., Francois, R. and Castel, A. (2014). Prediction of reinforcement corrosion using corrosion induced cracks width in corroded reinforced concrete beams. *Cement and Concrete Research*, 56, pp. 84-96.

Kim, D.K., Lee, J.J., Lee, J.H. and Chang, S.K. (2005). Application of Probabilistic Neural Networks for Prediction of Concrete Strength. *Journal of Materials in Civil Engineering, ASCE*, 17(3), pp. 353-362.

Kim, S., Frangopol, D.M. and Soliman, M. (2013). Generalized probabilistic framework for optimum inspection. *Journal of Structural Engineering, ASCE*, 139(3), pp. 435-447.

Kleiner, Y. and Rajani, B. (2001). Comprehensive review of structural deterioration of water mains: statistical models. *Urban Water*, 3(3), pp. 131-150.

Kong, J.S. and Frangopol, D.M. (2003). Lifecycle reliability-based maintenance cost optimization of deteriorating structures with emphasis on bridges. *Journal of Structural Engineering, ASCE*, 129(6), pp. 818-828.

Law, D.W., Tang, D., Molyneaux, T.K.C. and Gravina, R. (2011). Impact of crack width on bond: confined and unconfined rebar. *Materials and Structures*, 44(7), pp. 1287-1296.

Lee, H.S., Noguchi, T. and Tomosawa, F. (2002). Evaluation of the bond properties between concrete and reinforcement as a function of the degree of reinforcement corrosion. *Cement and Concrete Research*, 32(8), pp. 1313-1318.

Li, F. and Yuan, Y. (2013). Effects of corrosion on bond behavior between steel strand and concrete. *Construction and Building Materials*, 38, pp. 413-422.

Liu, M. and Frangopol, D.M. (2005). Time-dependent bridge network reliability: Novel Approach. *Journal of Structural Engineering, ASCE* , 131(2), pp. 329-337.

Liu, Y. and Weyers, R.E. (1998). Modelling the time-to-corrosion cracking in chloride contaminated reinforced concrete structures. *ACI Materials Journal*, 95(6), pp. 675–680.

Lou, Z., Gunaratne, M., Lu, J.J. and Dietrich, B. (2001). Application of neural network model to forecast short-term pavement crack condition: florida case study. *Journal of Infrastructure Systems, ASCE*, 7(4), pp. 166-171.

Lounis, Z., Martin-Perez, B., Daigle, L. and Zhang, J. (2006). Decision Support Tools for Service Life Prediction and Rehabilitation of Concrete Bridge Decks - Final Report, Institute for Research in Construction: National Research Council Canada (B5318.2).

Lundgren, K. (2002). Modelling the effect of corrosion on bond in reinforced concrete. *Magazine of Concrete Research*, 54(3), pp. 165-173.

Makropoulos, C.K., Butler, D. and Maksimovic, C. (2003). Fuzzy Logic Spatial Decision Support System for Urban Water Management. *Journal of Water Resources Planning and Management*, 129(1), pp. 69-77.

Mangat, P.S. and Elgarf, M.S. (1999a). Bond characteristics of corroding reinforcement in concrete beams. *Materials and Structures*, 32(2), pp. 89-97.

Mangat, P.S. and Elgarf, M.S. (1999b). Flexural strength of concrete beams with corroding reinforcement. *ACI Structural Journal*, 96(1), pp. 149-158.

Marcotte, T.D. and Hansson, C.M. (2007). Corrosion products that form on steel within cement paste. *Materials and Structures*, 40(3), pp. 325–340.

Martin-Perez, B. (1999). Service life modelling of R.C. highway structures exposed to chlorides. PhD thesis, University of Toronto.

Melchers, R. (1999). Structural Reliability Analysis, Prediction. 2nd ed. Wiley, Chichester.

Molina, F.J., Alonso, C. and Andrade, C. (1993). Cover cracking as a function of rebar corrosion: part 2-numerical model. *Materials and Structures*, 26(9), pp. 532-548.

Mori, Y. and Ellingwood, B.R. (2006). Reliability assessment of reinforced concrete walls degraded by aggressive operating environments. *Computer-Aided Civil and Infrastructure Engineering*, 21(3), pp. 157-170.

Mosley, B., Bungey, J. and Husle, R. (2007). Reinforced concrete design to Eurocode 2. 6th ed. Palgrave Macmillan, New York.

Mullard, J.A. and Stewart, M.G. (2012). Lifecycle cost assesment of maintenace strategies for RC structuries in chloride environments. *Journal of Bridge Engineering, ASCE*, 17(2), pp. 353-362.

Nepal, J. and Chen, H.P. (2014a). Reliability based Lifecycle Modelling of Reinforced Concrete Structures. *International Journal of life cycle Performance Engineering*, (under review).

Nepal, J. and Chen, H.P. (2014b). Evaluation of residual strength of corrosion damaged reinforced concrete structures. In *Lifecycle of Structural Systems: Design, Assessment, Maintenance and Management*, In eds. H. Furuta, D.M. Frangopol, M. Akiyama, Taylor and Francis, London, UK.

Nepal, J. and Chen, H.P. (2014c). Evaluation of structural behavior of corrosion damaged reinforced concrete bridges. Proceedings of 15<sup>th</sup> European Bridge Conference and Exhibition - Structural Faults and Repair, London, UK.

Nepal, J. and Chen, H.P. (2014d). Residual bond strength behaviour of corroded reinforcement in natural corrosive environment, Young Researchers Forum II: Construction materials, Institute of Concrete Technology, London, UK.

Nepal, J. and Chen, H.P. (2014e). Reliability based structural performance assessment of corrosion damaged RC structures. Young Researchers' Conference, Institution of Structural Engineers, London, UK..

Nepal, J. and Chen, H.P. (2014f). Gamma process modelling for lifecycle performance assessment of corrosion affected concrete structures. World Congress on Advances in Civil, Environmental, and Materials Research, Busan, Korea.

Nepal, J. and Chen, H.P. (2014g). Time-dependent reliability assessment of corrosion affected reinforced concrete structures. 12<sup>th</sup> International Conference on Computational Structures Technology, Naples, Italy.

Nepal, J. and Chen, H.P. (2015a). Risk-based optimum repair planning of corroded reinforced concrete structures. *Structural Monitoring and Maintenance*, 2(2), pp.133-143.

Nepal, J. and Chen, H.P. (2015b). Assessment of concrete damage and strength degradation caused by reinforcement corrosion. *Journal of Physics: Conference Series*, 628(1).

Nepal, J. and Chen, H.P. (2015c). Risk-based life cycle maintenance strategy of corrosion affected RC structures. 7<sup>th</sup> International Society for Structural Health Monitoring of Intelligent Infrastructure, Torino, Italy.

Nepal, J., Chen, H.P. and Alani, A.M. (2013). Analytical modelling of bond strength degradation due to reinforcement corrosion. *Key Engineering Materials*, 569, pp. 1060-1067.

Neves, L.C. and Frangopol, D.M. (2005). Condition, safety, and cost profiles for deteriorating structures with emphasis on bridges. *Reliability Engineering and System Safety*, 89(2), pp. 185-198.

Nielsen, C.V. and Bicanic, N. (2002). Radial fictitious cracking of thick-walled cylinder due to bar pull-out. *Magazine of Concrete Research*, 54(3), pp. 215-221.

Nowak, A.S. and Collins, K.R. (2012). Reliability of structures. CRC Press, Florida.

Otieno, M.B., Beushausen, H.D. and Alexander, G.M. (2011). Modelling corrosion propagation in reinforced concrete structures-A critical review. *Cement and Concrete Composites*, 33(2), pp. 240-245.

Pantazopoulou, S.J. and Papoulia, K.D. (2001). Modeling cover-cracking due to reinforcement corrosion in RC structures. *Journal of Engineering Mechanics, ASCE*, 127(4), pp. 342-351.

Papakonstantinou, K. and Shinozuka, M. (2013). Probabilistic model for steel corrosion in reinforced concrete structures of large dimensions considering crack effects. *Engineering Structures*, 57, pp. 306-326.

Poupard, O., L'Hostis, V., Catinaud, S. and Petre-Lazar, I. (2006). Corrosion damage diagnosis of a reinforced concrete beam after 40 years natural exposure in marine environment. *Cement and Concrete Research*, 36(3), pp. 504-520.

RILEM TC-154-EMC (2004). Electrochemical techniques for measuring metallic corrosion. Test methods for on-site corrosion rate measurement of steel reinforcement in concrete by means of the polarisation resistance method. *Materials and Structures*, 37(273), pp. 623-643.

Rodriguez, J., Ortega, L.M and Casal, J. (1994). Corrosion of reinforcing bars and service life of reinforced concrete structures: corrosion and bond deterioration.

Proceeding of International Conference on Concrete Across Borders, Odense, Denmark.

Rodriguez, J., Ortega, L.M. and Casal, J. (1997). Load carrying capacity of concrete structures with corroded reinforcement. *Construction and Building Materials*, 11(4), pp. 239-248.

Rodriguez, J., Ortega, L.M., Casal, J. and Diez, J.M. (1996). Corrosion of reinforcement and service life of concrete structures. *Durability of Building Materials and Composites*, E & FN Spon, London, pp. 117-126.

Roelfestra, P.E. and Wittmann, F.H. (1986). Numerical method to link strain softening with failure of concrete. In: F.H. Wittmann, ed. *Fracture Toughness and Fracture Energy of Concrete*. Development in Civil Engineering, 18 ed., Elsevier, pp. 163-175.

Roesler, J., Paulino, G.H., Park, K. and Gaedicke, C. (2007). Concrete fracture prediction using bilinear softening. *Cement and Concrete Composites*, 29(4), pp. 300-312.

Saether, I. (2011). Bond deterioration of corroded steel bars in concrete. *Structure and Infrastructure Engineering*, 7(6), pp. 415-429.

Saydam, D. and Frangopol, D.M. (2014). Risk-based maintenance optimization of deteriorating bridges. *Journal of Structural Engineering, ASCE*, 19(3), pp. 252-265.

Saydam, D., Frangopol, D.M and Dong, Y. (2013). Assessment of Risk Using Bridge Element Condition Ratings. *Journal of Infrastructure Systems, ASCE*, 19(3), pp. 252-265.

Shi, X., Xie, N., Fortune, K. and Gong, J. (2012). Durability of steel reinforced concrete in chloride environments: An overview. *Construction and Building Materials*, 30, pp. 125-138.

- Shima, H. (2001). Local bond stress-slip relationship of corroded steel bars embedded in concrete. In: N. Banthia, K. Sakai, and O.E. Gjrrv, eds. Proceedings of the third international conference on concrete under severe conditions. Vancouver, Canada, The University of British Columbia, pp. 454-462.
- Stanish, K., Hooton, R.D. and Pantazopoulou, S.J. (1999). Corrosion effects on bond strength in reinforced concrete. *ACI Structural Journal*, 96(6), pp. 915-921.
- Stewart, M.G. and Rosowsky, D.V. (1998). Time-dependent reliability of deteriorating reinforced concrete bridge decks. *Structural Safety*, 20(1), pp. 91-109.
- Suo, Q. and Stewart, M.G. (2009). Corrosion cracking prediction updating of deteriorating RC structures using inspection information. *Reliability Engineering and System Safety*, 94(8), pp. 1340-1348.
- Tapan, M. and Aboutaha, S.R. (2008). Strength evaluation of deteriorated RC bridge columns. *Journal of Bridge Engineering, ASCE*, 13(3), pp. 226-236.
- Tastani, S.P. and Pantazopoulou, S.J. (2010). Direct tension pullout bond test: experimental results. *Journal of Structural Engineering, ASCE*, 136(6), pp. 731-743.
- Thoft-Christensen, P. (1998). Assessment of the reliability profiles for concrete bridges. *Engineering Structures*, 20(11), pp. 1004-1009.
- Thoft-Christensen, P. and Baker, M.J. (1982). Structural reliability theory, its applications. Springer-Verlag, Berlin.
- Tilly, G.P. and Jacobs, J. (2007). Concrete repairs-performance in service and current practice, IHS BRE Press, Willoughby Road, UK.
- Timoshenko, S.P. and Goodier, J.N. (1970). Theory of Elasticity. 3rd edition. McGraw-Hill, New York.

Torres-Acosta, A.A., Navarro-Gutierrez, S. and Teran-Guillen, J. (2007). Residual flexure capacity of corroded reinforced concrete beams. *Engineering Structures*, 29(6), pp. 1145-1152.

Treece, R.A. and Jirsa, J.O. (1989). Bond strength of epoxy-coated reinforcing bars. *ACI Materials Journals*, 86(2), pp. 167-174.

Usatoday (2006). Overpass falls on cars, killing 5 in Canada. <[http://usatoday30.usatoday.com/news/world/2006-09-30-overpass\\_x.htm](http://usatoday30.usatoday.com/news/world/2006-09-30-overpass_x.htm)>.

Val, D.V. (2005). Effect of different limit states on lifecycle cost of RC structures in corrosive environment. *Journal of Infrastructure Systems, ASCE*, 11(4), pp. 231-240.

Val, D.V. and Stewart, M.G. (2003). Life cycle cost analysis of reinforced concrete structures in marine environments. *Structural Safety*, 25(4), pp. 343-362.

Val, D.V., Leonid, C. and Stewart, M.G. (2009). Experimental and numerical investigation of corrosion-induced cover cracking in reinforced concrete structures. *Journal of Structural Engineering, ASCE*, 135(4), pp. 376-385.

Val, D.V., Stewart, M.G. and Melchers, R.E. (2000). Lifecycle performance of RC bridges:probabilistic approach. *Computer-Aided Civil and Infrastructure Engineering*, 15(1), pp. 14-25.

Val, D.V., Stewart, M.G. and Melchers, R.E. (1998). Effect of reinforcement corrosion on reliability of highway bridges. *Engineering structures*, 20(11), pp. 1010-1019.

Van Noortwijk, J.M. (1998). Optimal replacement decisions for structures under stochastic deterioration. University of Michigan, Ann Arbor.

Van Noortwijk, J.M. (2003). Explicit formulas for the variance of discounted lifecycle cost. *Reliability of Engineering System and Safety*, 80(2), pp. 185-195.

Van Noortwijk, J.M. (2009). A survey of the application of gamma processes in maintenance. *Reliability Engineering and System Safety*, 94(1), pp. 2-21.

Van Noortwijk, J.M. and Frangopol, D.M. (2004). Two probabilistic lifecycle maintenance models for deteriorating civil infrastructures. *Probabilistic Engineering Mechanics*, 19(4), pp. 345-359.

Vidal, T., Castel, A. and Francois, R. (2004). Analyzing crack width to predict corrosion in reinforced concrete. *Cement and Concrete Research*, 34(1), pp. 165-174.

Vu, K., Stewart, M.G. and Mullard, J. (2005). Corrosion-induced cracking: experimental data and predictive models. *ACI Structural Journal*, 102(5), pp. 719-726.

Vu, K.A.T. and Stewart, M.G. (2000). Structural reliability of concrete bridges including improved chloride-induced corrosion models. *Structural Safety*, 22(4), pp. 313-333.

Wang, X.H. and Liu, X.L. (2004). Modelling effects of corrosion on cover cracking and bond in reinforced concrete. *Magazine of Concrete Research*, 56(4), pp. 191-199.

Wang, X.H. and Liu, X.L. (2010). Simplified methodology for the evaluation of residual strength of corroded reinforced concrete beams. *Journal of Performance of Constructed Facilities, ASCE*, 24(2), pp. 108-119.

Webster, M.P. and Clark, L.A. (2000). Structural effect of corrosion-an overview of the mechanism. *Proceedings of Concrete Communication, BCA, Camberley, Birmingham*.

Wellalage, N.K., Zhang, T. and Dwight, R. (2015). Calibrating markov chain-based deterioration models for predicting future conditions of railway bridge elements. *Journal of Bridge Engineering, ASCE*, 20(2), 04014060.

Whitmore, D.W. and Ball, J.C. (2004). Corrosion Management. *ACI Concrete International*, 26(12), pp. 82-85.

Xia, J., Jin, W.L. and Li, L.Y. (2012). Effect of chloride-induced reinforcing steel corrosion on the flexural strength of reinforced concrete beams. *Magazine of Concrete Research*, 64(6), pp. 471-485.

Yang, S.I., Frangopol, D.M. and Neves, L.C. (2006). Optimum maintenance strategy for deteriorating bridge structures based on lifetime functions. *Engineering Structures*, 28(2), pp. 196-206.

Yang, S.Y., Liu, X.L. and Leng, Y.B. (2013). Prediction of flexural deformation of a corroded RC beam with a polynomial tension-stiffening model. *Journal of Structural Engineering, ASCE*, 139(6), pp. 940-948.

Zhang, R., Castel, A. and Francois, R. (2010). Concrete cover cracking with reinforcement corrosion of RC beam during chloride-induced corrosion process. *Cement and Concrete Research*, 40(3), pp. 415-425.

Zhang, S. and Raoof, M. (1995). Prediction of the behaviour of RC beams with exposed reinforcement. *Magazine of Concrete Research*, 47(173), pp. 335-344.

Zhang, W., Song, X., Gu, X. and Li, S. (2012). Tensile and fatigue behavior of corroded rebars. *Construction and Building Materials*, 34, pp. 409-417.

Zhao, Y., Lin, H., Wu, K. and Jin, W. (2013). Bond behaviour of normal/recycled concrete and corroded steel bars. *Construction and Building Materials*, 48, pp. 348-359.

Zhong, J., Gardoni, P. and Rosowsky, D. (2010). Stiffness degradation and time to cracking of cover concrete in reinforced concrete structures subject to corrosion. *Journal of Engineering Mechanics, ASCE*, 136(2), pp. 209-219.

## Appendices

### Appendix A: List of publications

#### 1- Journals:

Chen, H.P. and Nepal, J. (2015). Analytical Model for residual bond strength of corroded reinforcement in concrete structures. *Journal of Engineering Mechanics, ASCE*, 10.1061/(ASCE)EM.1943-7889.0000997.

Chen, H.P. and Nepal, J. (2015). Stochastic modelling and lifecycle performance assessment of bond strength of corroded reinforcement in concrete. *Structural Engineering and Mechanics*, 54(2), pp. 319-336.

Nepal, J. and Chen, H.P. (2015). Risk-based optimum repair planning of corroded reinforced concrete structures. *Structural Monitoring and Maintenance*, 2(2), pp.133-143.

Nepal, J. and Chen, H.P. (2015). Assessment of concrete damage and strength degradation caused by reinforcement corrosion. *Journal of Physics: Conference Series*, 628(1).

Nepal, J., Chen, H.P. and Alani, A.M. (2013). Analytical modelling of bond strength degradation due to reinforcement corrosion. *Key Engineering Materials*, 569, pp. 1060-1067.

Nepal, J. and Chen, H.P. (2014). Reliability based Lifecycle Modelling of Reinforced Concrete Structures. *International Journal of life cycle Performance Engineering*, (under review).

Chen, H.P. and Nepal, J. (2014). Modelling of flexural strength deterioration in corroded reinforced concrete structures and its stochastic analysis. *Engineering Structures*, (under review).

Chen, H.P. and Nepal, J. (2015). Analysing the effect of cover cracking on structural reliability of corroded reinforced concrete structures. *Advances in Structural Engineering*, (under review).

## **2- Book Chapter:**

Nepal, J. and Chen, H.P. (2014). Evaluation of residual strength of corrosion damaged reinforced concrete structures. In *Lifecycle of Structural Systems: Design, Assessment, Maintenance and Management*, In eds. H. Furuta, D.M. Frangopol, M. Akiyama, Taylor and Francis, London.

## **3- Conferences:**

Nepal, J. and Chen, H.P. (2015). Risk-based life cycle maintenance strategy of corrosion affected RC structures. 7<sup>th</sup> International Society for Structural Health Monitoring of Intelligent Infrastructure, Torino, Italy.

Nepal, J. and Chen, H.P. (2014). Evaluation of structural behavior of corrosion damaged reinforced concrete bridges. Proceedings of 15<sup>th</sup> European Bridge Conference and Exhibition - Structural Faults and Repair, London, UK.

Nepal, J. and Chen, H.P. (2014). Residual bond strength behaviour of corroded reinforcement in natural corrosive environment, Young Researchers Forum II: Construction materials, Institute of Concrete Technology, London, UK.

Nepal, J. and Chen, H.P. (2014). Reliability based structural performance assessment of corrosion damaged RC structures. Young Researchers' Conference, Institution of Structural Engineers, London, UK.

Nepal, J. and Chen, H.P. (2014). Gamma process modelling for lifecycle performance assessment of corrosion affected concrete structures. World Congress on Advances in Civil, Environmental, and Materials Research, Busan, Korea.

Nepal, J. and Chen, H.P. (2014). Time-dependent reliability assessment of corrosion affected reinforced concrete structures. 12<sup>th</sup> International Conference on Computational Structures Technology, Naples, Italy.